



POLISH ACADEMY OF SCIENCE  
INSTITUTE OF FUNDAMENTAL  
TECHNOLOGICAL RESEARCH

PhD. Dissertation  
**Semi-Active Control System  
for Trajectory Optimization of a Moving Load  
on an Elastic Continuum**

Dominik PISARSKI

Thesis Advisor: Prof. Czesław I. BAJER

Prepared at DEPARTMENT OF INTELLIGENT TECHNOLOGIES

Warszawa, 2011



## Podziękowania

*Pragnę serdecznie podziękować Panu Profesorowi Czesławowi Bajerowi. Za nieustanne wsparcie i motywację, niezliczone godziny dyskusji, bezcenną radę i wreszcie za naukę nie tylko o Nauce...*

*Za owocne rozmowy i cenne wskazówki dla mojej pracy dziękuję Prof. A. Myślińskiemu, Prof. J. Holnickiemu-Szulc, Dr A. Ossowskiemu, Prof. T. Szolcowi oraz Prof. P. Skudrzykowi.*

*Za wsparcie i życzliwość dziękuję również koleżankom i kolegom z IPPT PAN, AGH i UJ. Szczególne podziękowania kieruję do: K. Łukasiewicz, L. Skudrzyka, P. Surówki, D. Kruszelnickiej, T. Pióro, B. Dyniewiczza, R. Konowrockiego.*

*I wreszcie (last but not least) dziękuję moim Rodzicom i Bratu. Bez Was nie byłoby ani mnie, ani tej pracy. Dedykuję ją dla Was...*



## STRESZCZENIE

W pracy przedstawione zostały wyniki badań półaktywnego układu sterowania do optymalizacji trajektorii przejazdu ruchomych obciążeń po jednowymiarowym sprężystym continuum. Modele matematyczne continuum reprezentowane są przez równania belki Eulera-Bernoulliego oraz struny. W tak przyjętych modelach sformułowane zostało zadanie sterowania optymalnego. Korzystając z zasady maksimum Pontryagina wyprowadzone zostały rozwiązania optymalne – sterowania typu bang-bang. Postać tych rozwiązań jest uwikłana. Konieczne zatem jest użycie metod numerycznych optymalizacji. W tym celu wyprowadzone zostały pochodne funkcji celu. Na przykładzie oscylatora potwierdzona została skuteczność metody parametryzacji czasów przełączeń. Metoda ta została zastosowana do zadania optymalizacji trajektorii przejazdu ruchomej siły po belce. Badania numeryczne pozwoliły ustalić stosowną liczbę przełączeń każdej z funkcji sterujących. Jakość zaproponowanej metody sterowania zweryfikowana została w szerokim zakresie parametrów modelu. Dodatkowo rozważono dwa przypadki specjalne: układ złożony z dwóch belek sprzężonych sterowanymi tłumikami oraz układ z odkształceniem wstępnym. Zaproponowano model reologiczny półaktywnego inteligentnego materiału tłumiącego. Omówiono problemy otwarte oraz wyznaczono kierunki dalszych badań.

## ABSTRACT

The work presents the results of research on semi-active control method for optimization of trajectories of a moving load transversing a one-dimensional elastic continuum. Mathematical models of the continuum are represented by the equation of Euler-Bernoulli beam and string. For such a models the optimal control problem was posed. Based on the Maximum Pontryagin Principle the optimal solutions were derived - controls of bang-bang type. The solutions are given in implicit form. It is therefore necessary to use numerical optimization methods. For this purpose, the functional derivatives were derived. High efficiency of the switching times method was confirmed by numerical example. The method was then applied to the problem of optimal passage of a load on the beam. Numerical studies enabled us to establish an appropriate number of switches for each of the control functions. The quality of the proposed control method was verified for a wide range of model parameters. In addition, two special cases were considered: a system consisting of two beams coupled with controlled dampers and a system with the initial deflection. The idea of smart damping layer was presented. The directions of future works were proposed.



# Contents

<b>1</b>	<b>Introduction</b>	<b>1</b>
1.1	The subject of the Thesis . . . . .	1
1.2	Purposes and scope of the Thesis . . . . .	3
1.3	Review of previous research . . . . .	5
1.4	Main contributions and thesis . . . . .	9
1.5	Structure of the Thesis . . . . .	10
<b>2</b>	<b>Mathematical models of semi-active elastic systems</b>	<b>13</b>
2.1	Introduction . . . . .	13
2.2	Models of semi-active controlled elastic continuum . . . . .	14
2.3	Weak formulation, ODE system representation . . . . .	17
2.4	Approximated solutions . . . . .	19
2.5	Two special cases . . . . .	23
2.5.1	Double beam system . . . . .	24
2.5.2	The initial deflection . . . . .	26
2.6	The method of power series . . . . .	27
2.7	State space representation . . . . .	31
<b>3</b>	<b>Optimization in semi-active control systems</b>	<b>35</b>
3.1	Problem statement . . . . .	36
3.2	Optimal control problem for bilinear systems . . . . .	37
3.3	Existence of solution . . . . .	38
3.4	Necessary conditions for optimal controls . . . . .	39
3.5	Prediction of switchings in optimal controls . . . . .	41

---

3.6	Functional derivative, the method of steepest descent for optimal control problem . . . . .	43
3.7	Numerical example: semi-active controlled oscillator . . . . .	44
3.7.1	Case 1: $t_f = 0.67$ . . . . .	45
3.7.2	Case 2: $t_f = 1$ . . . . .	47
3.8	The method of parameterized switching times . . . . .	48
3.9	Switching times method - numerical examples . . . . .	52
3.9.1	Case 1: $t_f = 0.67$ . . . . .	52
3.9.2	Case 2: $t_f = 1$ . . . . .	54
<b>4</b>	<b>Optimization of moving load trajectories via semi-active control method</b>	<b>57</b>
4.1	Optimal control problem formulation . . . . .	58
4.2	Numerical optimization methods in the semi-active controlled elastic systems	59
4.2.1	The passive cases . . . . .	60
4.2.2	The gradient method . . . . .	60
4.2.3	The switching times method . . . . .	62
4.3	The total number of semi-active dampers . . . . .	67
4.4	The placement of semi-active dampers . . . . .	69
4.5	The velocity of a travelling load . . . . .	70
4.6	Initially deflected beam . . . . .	74
4.6.1	Case 1: The first mode . . . . .	74
4.6.2	Case 2: The third mode added . . . . .	76
4.7	Double beam system . . . . .	78
<b>5</b>	<b>Final remarks, future works</b>	<b>87</b>
5.1	Summary of the work . . . . .	87
5.2	The idea of a smart damping layer . . . . .	88
5.3	Future work . . . . .	90
<b>A</b>	<b>Numerical results</b>	<b>91</b>
<b>B</b>	<b>Matlab codes</b>	<b>97</b>
	<b>Bibliography</b>	<b>105</b>

## 1.1 The subject of the Thesis

Problems of structures subjected to a load travelling with high speed are of a special interest for practising engineers. Both, analytical and numerical solutions are applied to problems with a single or multi-point contact such as: train-track or vehicle-bridge interaction, pantograph collectors in railways, magnetic levitation railways, guideways in robotic technology.

The current trend to lightening structures requires new and more efficient methods to decrease the vibration levels. In large-scale engineering structures like bridges or viaducts that span gaps, beams must resist loads due to heavy and fast vehicles. The construction of new bridges of sufficiently higher load carrying capacity is usually limited by costs. Moreover, static strengthening can be restricted for technological reasons. Existing old weak structures can be reinforced by supplementary supports with magneto or electro-rheological dampers controlled externally (please see the Figures 1.1(a), 1.1(b)).

Pioneering concepts of integration of semi-active control systems within engineering design, transportation and robotics are dated back to 70s. Systems based on the action of electro or magneto-rheological dampers are an attractive alternative to passive and active control systems (force-controlled). When correctly designed algorithms the semi-active control systems can outperform passive damping systems. They can efficiently reduce the undesired vibrations, enable the system to perform craved trajectories or increase their stability. In turn, due to low energy consumptions, they are a strong competitive to force-controlled active systems. Moreover, the poorly designed active control system can supply the energy in antiphase and in the extremal case can damage the structure. Over the years, the semi-active systems have replaced the passive and active, and this is also due to the developing more interesting design solutions for semi-active vibration absorbers. Today, not only rheological fluids, but also cheaper to construct and control pneumatic foams can be used as a medium of such absorbers.

Diversity of actuators opens up new possibilities in the design of control algorithms.

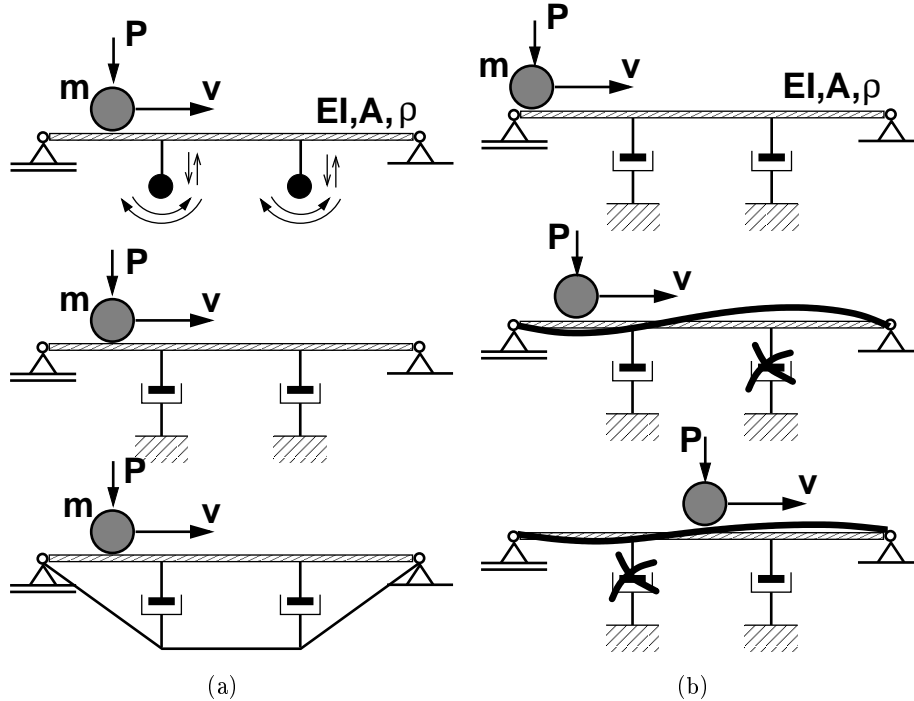


Figure 1.1: The idea of passive (a) and semi-active (b) control of a beam deflection under a travelling load.

Well designed semi-active control system can be an attractive solution for building protection against surrounding infrastructure. In particular for many priceless monuments, located in town centres and exposed to destructive action of the public railway transport (please see the Figure 1.2), only the additional smart damping system can be a successful solution to maintain their viability. The low susceptibility of the material, that the monuments are built of, does not succumb to excessive momentary or long-term deformation. The solution for this problem is a concept of modification of the track structure. Semi-active damping layer incorporated into the track can reduce vibration levels propagating into the ground in more efficient way than the traditional vibroisolation.

To the potential application of semi-active damping methods we can also include the robotic systems, in particular the linear guideways. The straight or precisely controlled trajectory of a moving object is essential in some technological processes such as cutting (flame, plasma, laser, textile, waterjet, glass cutting) or bonding (glueing, welding, soldering). Other especially suited areas of application for linear guideway systems are large format plotters and scanners for various industries as well as devices in medical and semiconductor technologies. New solutions can accelerate procedures and decrease the mass and size of guideways supporting carriages.



Figure 1.2: Areas of potential application of semi-active damping systems.

## 1.2 Purposes and scope of the Thesis

The primary purpose of this research is **to design safety and efficient semi-active control method for straight line passage of a moving load when transversing the one-dimensional continuum**. By the efficient control method we mean one that provides better values for appropriate cost functional than any of the passive cases. On the other hand we make the following requirements: the designed control system should be simple in practical realization and it must stay stable in the case of errors or disturbances.

When the proper strategy of control is assumed the efficient computational methods are required. Thus, the aim is **to elaborate numerical procedures that enable us to obtain the trajectories for optimal controls**. For the procedure two conditions must be met: low computational cost and high accuracy of results.

The final purposes of the research are **to analyze the solutions of optimal controls and to propose practical realization**. The analysis must be performed in a way that shows the efficiency of the proposed method for a wide spectrum of system parameters. Moreover, the advantages and disadvantages of the control strategy should be emphasized.

**The scope** of the Thesis includes the following:

- literature review to settle the problem among the existing studies,
- the introduction to the mathematical model together with the appropriate assumptions,

- investigation on the phenomenon accompanying the passage of a single moving force on a semi-active controlled beam or string,
- elaboration of the method for obtaining the trajectories of single moving force on a semi-active controlled beam or string,
- investigation on the accuracy of approximated trajectories of a travelling force,
- mathematical formulation of the optimal control problem,
- investigation on the problem of existence of the optimal control problem,
- implementation of the first order optimality condition,
- investigation on the numerical methods for solving the optimal control problem,
- design of the safety switching control method with reduced number of switchings,
- analysis of the optimal control solutions for a wide range of speed of the travel,
- extensions of the system to the following: initially deflected beam, double beam system,
- **practical realization proposal.**

The problems of optimization in the semi-active multidimensional control systems have been poorly investigated so far. For this reason the following dissertation is cognitive and it is limited to the most fundamental issues only. The following problems are **not of the scope** of the Thesis and they may be dedicated to the future works:

- the extensions of mathematical model of span: the Euler-Bernoulli beam with the internal damping, Timoshenko beam,
- the extensions of travelling load: inertial effects of the travelling particle, multiple moving load,
- further optimization: the optimal placements for semi-active dampers, optimization of the curves of the initial deflection, optimization of the quotient of bending stiffness in the case of double beam system,
- the theory of stability of the multidimensional semi-active switching system.

### 1.3 Review of previous research

Literature on the issues of moving load and the control methods that should be mentioned here is extremely rich and it would be the huge challenge to create the full list. Therefore, the author of the Thesis should decide to shorten this list and present only the most significant works from the point of view of the dissertation topic items. The list is divided into three parts. In the first part the issues of moving loads on the continuum is presented. The second part is devoted to the most significant approaches on control methods adopted to mechanical systems. Finally, the contributions published by the author of the Thesis are discussed in brief. Some of the important works are also cited during the following chapters.

The systematic study of the behavior of vibrating elastic bodies goes back to Jacob Bernoulli. He established the governing differential equation for the deflection curves of elastic bars [Komkov 1972]. He published the results in his masterwork [Bernoulli 1696]. The first who got interest in two-dimensional systems was probably Leonard Euler. He studied and extended the Bernoulli's results. He investigated vibrations of a perfectly elastic membrane. For details please see [Timoshenko 1954]. The differential equations of vibrating thin plates can be traced to Kirchhoff (see [Timoshenko 1954]).

Today, the simple distributed parameter systems describe many mechatronic systems with applications in manufacturing, space, robotics and power transmission. The equation of Euler-Bernoulli model can accurately model the longitudinal and transverse boom vibration coupled with the payload and bus rigid body motion [Rahn 2001]. The same model is used to describe a simply-supported beam traversed by a vehicle [Fryba 1972], [Y. B. Yang 2004].

The travelling load is modeled as one of two types: non-inertial (massless) or inertial. The analysis of the moving massless force is relatively simple and is treated in numerous papers, e. g. [Olsson 1991]. We include to this group all the papers devoted to the travelling oscillator, i.e. a mass particle joined to the base with a spring [Bergman 1997]. The inertial force moving over the structure is rarely reported in literature [Bolotin 1950]. The closed solution exists in the case of a mass moving on a massless string [Stokes 1883], [Fryba 1972]. Otherwise the final results are obtained numerically, although the solution is preceded by complex analytical calculations. New and important feature of discontinuity of the inertial particle trajectory is exhibited in [B. Dyniewicz 2009]. In numerous references authors treat the problem in a very low range of the mass speed. In this case results are sufficient, even if the inertial term contributing to moving mass is not correctly treated by the time integration method. Simply, the moving mass influence in the case of low speed is minor comparing with static displacements. In the following papers [C.I. Bajer 2008], [C.I. Bajer 2009b], [C.I. Bajer 2009a] authors presented and discussed a method for determining matrices responsible for the description of the moving mass on a continuum. They

implemented the space-time finite element method by using linear interpolation. A good number of important contributions were also done for the wheel-rail contact problems. The interesting results may be found for example in the paper [A. Myslinski 2011]. The authors considered the wheel-rail contact problem including friction, frictional heat generation as well as heat transfer across the contact surface and wear. The numerical results indicated showed that the elastic graded layer can reduce the values of the normal contact stress and the maximal temperature in the contact zone. The application of the coating material can efficiently decrease the contact pressure and the rolling contact fatigue. Optimization of the rail profile or material properties with combination of coating approach is required to reduce generated temperatures. Optimization results concerning contact issues are presented in the work [Myslinski 2008].

The idea of the track shape control was previously considered in literature. Pawel Flont and Jan Holnicki-Szulc developed the approach that uses active smart sleepers. These smart sleepers are equipped with actuators that enable the track to shift up and down. The results are presented in details in the paper [P. Flont 1997]. The objective was to minimize the track deflection measure. By means of numerical simulation the authors evidenced over 80 percent reduction of this measure.

There are still many open problems associated with optimal control methods of semi-active systems – mainly because of their nonlinearities (bilinear products are incorporated). The following paragraphs details the basic control algorithms for semi-active control methods used in mechanical systems. More of them are experience-based techniques. The trajectories of such controls are piecewise constant and the switching rules are based on the current state of a system.

One of the first concept of the semi-active control in mechanical systems was proposed by Karnopp, Crosby and Harwood. In the work ([D. Karnopp 1974]) they presented the idea of active suppression of the oscillator with one degree of freedom, moving over uneven ground. The algorithm developed by the authors – Skyhook – is today one of the most widely used in suspension control systems for vehicles. The idea was designed to improve comfort of passengers. One of the most popular issue, in which the Skyhook is applied, is called moving oscillator problem. The extensive results are demonstrated in the following papers [D. Giraldo 2002], [Y. Chen 2002]. In some recent works the variable dampers are incorporated also for seismic isolation. This approach is presented in the papers [A. Ruangrassamee 2003], [K. Yoshida 2000]. In [Z. Fulin 2002], the authors propose to control both parameters: stiffness and damping. The control function led to maximum dissipation of energy. In general, a decrease in vibration amplitude was to be achieved.

The problem of reducing the beam vibrations via active control methods is also widely considered in literature. For details see for example [T. Frischgesel 1998]. An active constrained layer is applied in the approach presented in the work [Baz 1997]. A beam subjected to a harmonic load was also controlled by an active method in [Pietrzakowski 2001].

The analysis in the frequency domain allowed the authors to reduce the maximum amplitudes. The actively controlled string system was considered in [C. A. Tan 2000]. The problem of optimal design of structures with active support is analyzed in the paper [D. Bojczuk 2005]. The approach presented by the authors provides a useful tool for the determination of the number, positions and generalized forces of actuators. They considered two different cases with fixed and varying load, respectively. They concluded that application of the active support changes essentially the structure response and enables significant increase of structure stiffness or decrease of maximal deflection.

Semi-active systems have also found numerous applications in structures subjected to seismic excitation. The works that should be mentioned here are: [Soong 2005], [K. Yoshida 2000]. The task for semi-active control system is to stabilize system when lost the equilibrium state. Solutions are obtained by minimization of the cost functional determined on the infinite time interval. This refers to the Linear Quadratic Regulation method (LQR). It should be mentioned here the lack of mathematical precision in formulating and solving the minimization task in that way. The LQR method can not be directly used in the case of bilinear systems. The problem lies within the directions of damping forces acting on the structure. These directions strictly depend on the velocities of the vibration. Thus, for some time intervals there is no possibility to generate the desired controls that result from the LQR. In terms of mechanical systems the LQR method is dedicated to active control systems and can not be directly used in case of parametric control problems. However, R. Mohler developed the iterative method which is analogous to the LQR, but applied for bilinear systems. This method is presented in details in his work [Mohler 1973]. Another approach is to derive the switching rules using Lyapunov stability theory. Methods based on the so-called optimal Lyapunov functions ([Ossowski 2003]) deserve a special attention here. The switched input trajectories can drive the system to the equilibrium point. The trajectories of the system in those cases are the exponentials with the maximum rate of convergence.

Problems of vibration control are also widely considered in the robotic systems. Technological processes aided manipulators require high accuracy, without sacrificing production rate. The large inertia of the effectors and the object of manipulation may cause significant errors in the desired trajectory. Active control methods implemented in the feedback loop, allows us to compensate these errors. The application of PD regulators were proposed, among others, by Choura and Yigit in the paper [S. Choura 2001]. The method based on the concept of "H-infinity" and fuzzy logic was presented by Yang and Kim [H. W. Park 1999]. Kang and Mills used the piezoelectric layers as sensors and actuators [B. Kang 2005].

Most of the active and semi-active methods that have been developed lead to feedback controls determined by state-space measures. In the case of a continuous system, such an approach is typically complex due to observer design. The alternative method

is pre-computed open loop control. This is particularly useful in problems with a well-defined excitation. In linear mechanical systems, semi-active control methods usually result in switching operations, where the parameters to be controlled (damping, stiffness) are switched between two or more values. The switching conditions are based on state or time events. Optimally switched linear systems are widely considered in literature. Interesting results may be found for example in the paper [T. Das 2006].

Intensive researches on the semi-active control of systems represented by Partial Differential Equations (PDE) have opened a lot of unsolved problems. One of them occurs if the cost functional is limited to a fixed period of time. The switching scheme for control is given in implicit form and it depends on state and adjoint state variables. Solving the Two-Point Boundary Value Problem is time consuming and in general difficult to solve in the case of multidimensional problem. Another unsolvable problem that occurs in the case of systems described by PDE is a stability of switched system. The asymptotic stability of a switched system can be proved in the simplest cases only. The extensive research on these problems was treated in terms of the Lie algebra and it was done by D. Liberzon et al. in the following works [D. Liberzon 1999], [D. Liberzon 2006].

The early idea of the semi-active control of one-dimensional continuum under a travelling load was presented in [R. Bogacz 2000]. The extension of the idea was reported in the work [D. Pisarski 2010b]. The span was supported by a set of dampers placed on the rigid base. Open loop control of damping parameters allowed us to actively reduce the deflection of a string or a beam supporting the travelling load. The control of beam vibrations exhibited a significantly higher control efficiency than in the case of a string.

The idea of straight-line passage is based on the principle of a two-sided lever. The first part of the beam which is subjected to a moving load is supported by semi-active damper placed on the rigid base (please see the Figure 1.1(b)). The first damper is active while the second is passive. At this stage, a part of the beam is turned around its center of gravity, levering the right hand part with a passive damper attached. The temporal increment of displacements on the right hand part of the beam enables us to exploit it during the second stage of passage.

Technical difficulties with the rigid support of the bottom parts of our dampers require new, more practical solutions. Dampers are supported with an elastic string or bar system. However, the elastic support reduces the efficiency of the performance and also involves technological problems.

In the paper [D. Pisarski 2011b], a new and significantly more efficient idea presented in the Figure 1.3(a) is considered. The main stiff simply-supported beam is covered by a supplementary beam, joined to the main beam by a set of controlled dampers. This upper beam can be assumed as a simply supported as well, since this type of boundary condition can be implemented in a natural way. Such a modification does not require the rigid base and it can be easily incorporated into existent guideways (Figure 1.3(b)). We

assume the upper beam as significantly less rigid than the main lower beam. We must emphasize here that the desired dynamic effect is obtained from the relative velocity of both lower and upper beams. Let us consider the second stage of the motion depicted in Figure 1.3(a). The upper beam subjected to a force  $P$  is deflected. At the same time, the velocity of the lower beam allows to lever the joining damper and effectively supports the upper beam. The relative velocity of both lower and upper beam enable us to design the efficient control for the straight line passage. The dynamic response of a double-beam system traversed by a constant moving load was studied in [Abu-Hilal 2006]. The authors explored the effects of the moving speed of the load and the damping and stiffness of the viscoelastic layer on the deflections of the beams.

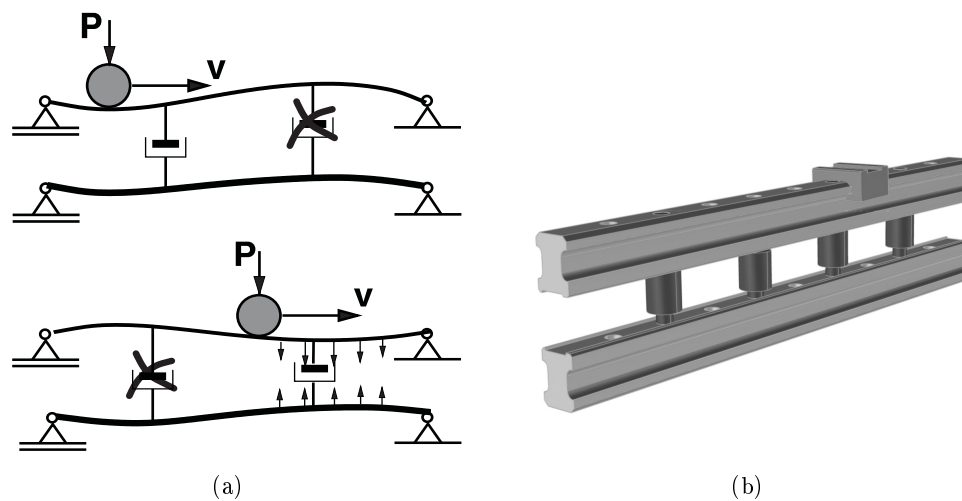


Figure 1.3: Semi-active linear guideway: (a) principle of acting, (b) real view.

Some additional results can be found in the following papers: [D. Pisarski 2009b], [D. Pisarski 2009a], [D. Pisarski 2010a], [D. Pisarski 2011a].

## 1.4 Main contributions and thesis

In the Thesis the author considers the continuum (beam or string) that after spatial discretization counts up to several dozen degrees of freedom. The cost functional is defined in the finite time interval that equals to the time of the travel of the vehicle over the limited fragment of track. In the considered problem the state equation as well as the objective functional are nonlinear. Among the existing solutions there is no control method that solves this multidimensional optimal control problem. There is therefore a need to develop one. The first solutions were proposed by the author of the Thesis in the paper [D. Pisarski 2010b]. In this development the control method was based on the

observation of the system dynamics. Then the parameterization of the control function was involved. The optimal control problem was transformed into the non-linear mathematical programming problem. This allowed to create a map of switching controls for various system parameters, especially the travel speed of load. Next, the appropriate gradient methods were developed. The switching times method derived by using the fundamentals of the calculus of variation exhibited high performance for the posed problem. With the best knowledge of the author, the presented semi-active control method is a new and unique solution over the world.

Below the main theses of the dissertation is listed:

*In the problem of straight line passage of the moving load upon the elastic continuum, for a wide range of system parameters there exists at least one semi-active switching control method such that it outperforms the passive damping. (Theorem\* 3.4 has been formulated and proved to provide the sufficient condition for existence of this switching control.) The near optimal solution requires a finite number of switchings for every control.*

*Total number of semi-active dampers significantly affects the quality of the switching control method. Dense distribution of controlled dampers gives an excellent opportunity to realize precisely straight passage of a moving load.*

*The velocity of a moving load significantly affects the behaviour of the semi-active control system. The proposed switching control method exhibits the best efficiency in the case of high speed passage. There exist the regularity in the structure of switching control functions.*

The main contributions have been published in the following journal papers:

1. D. Pisarski, Cz. I. Bajer: Semi-Active Control of 1D Continuum Vibrations Under a Travelling Load. Journal of Sound and Vibration, vol. 329, no. 2, pages 140-149, 2010.
2. D. Pisarski, Cz. I. Bajer: Smart Suspension System for Linear Guideways. Journal of Intelligent and Robotic Systems, vol. 62, no. 3-4, pages 451-466, 2011.

## 1.5 Structure of the Thesis

The structure of this dissertation is as follows:

### **Chapter 2. Mathematical models of semi-active controlled elastic systems**

In this part the description of physical objects together with their mathematical representation is provided. The aim is to specify the systems that are used in further optimization problems.

An outline of this chapter is as the follows. In the first section we consider the mathematical representation of semi-active controlled one-dimensional elastic bodies. Some of

up to date solutions are presented. In the next section we perform the space discretization of governing equation and derive the system of ordinary differential equation as a new representation of the system. In the following section we investigate the approximated, finite dimensional models. Next, we expand the model with two additional special cases. Further, the method of power series is presented and its accuracy is verified by means of numerical examples. Finally the state space representation of the model is presented.

### **Chapter 3. Optimization in semi-active control systems**

In this chapter we consider the optimal control techniques in application to multidimensional bilinear systems (as the mathematical representation of the semi-active mechanical systems). We investigate two different numerical optimization methods: the gradient method and the switching times method. The main purpose for this part is to provide the mathematical formulation and test numerical methods for the posed optimal control problem.

The chapter is organized as follows. In the first section the generalized optimal control problem is stated. Then, we consider optimal control for bilinear systems. Next, short divagation on the existence is provided. In the following sections the necessary optimal conditions are given including the derivation on functional derivatives. Further, the switching times method is presented. Finally, we provide simple numerical examples to verify the efficiency of the proposed methods.

### **Chapter 4. Numerical optimization of moving load trajectories**

In this chapter the problems of optimal passages of moving load are solved. The special attention is paid to the following issues: what is the structure of optimal control functions and what is the impact of parameters of the system on this structure.

In the first section of this chapter the optimal control problem for the straight line passage of a moving load is formulated. Then, the two different numerical methods are applied to solve the posed optimization problem. A short divagation on the relevant number of switchings in the switching times method is also provided. Next, in order to demonstrate how different parameters of the system effect on quality of the proposed control methods, a number of numerical examples is given. Finally, two extensions of the system are considered: the initially deflected beam and the linear guideway composed of two parallel beams.

### **Chapter 5. Final remarks, future works**

The chapter summarizes the results of the work. The idea of smart damping layer is presented. Finally, the directions for further work are recommended.



## Mathematical models of semi-active elastic systems

### Contents

- 2.1 Introduction**
- 2.2 Models of semi-active controlled elastic continuum**
- 2.3 Weak formulation, ODE system representation**
- 2.4 Approximated solutions**
- 2.5 Two special cases**
- 2.6 The method of power series**
- 2.7 State space representation**

### 2.1 Introduction

The primary purpose of this chapter is to provide the governing equations of one-dimensional bodies subjected to a travelling load and controlled by a set of semi-active dampers. We pay attention to two special models of continuum: the Euler-Bernoulli beam and a string. Presented material gives the necessary background for the control problems discussed later in this work.

An outline of the chapter is as the following. The first section is devoted to mathematical representation of semi-active controlled one-dimensional elastic bodies. Some of up to date solutions are provided. In the next section we perform the space discretization of governing equation and derive the system of ordinary differential equation as a new representation of the system. In the following section we investigate the approximated finite dimensional models. Next, we expand the model with two additional special cases.

Further, the method of power series is presented and its accuracy is verified by means of numerical example. Finally the state space representation of the model is presented.

## 2.2 Models of semi-active controlled elastic continuum

In this section we focus on the mathematical representation of semi-active controlled one-dimensional elastic continuum, when subjected to a moving load. Physical properties of the model are provided. Also the additional assumptions are listed. Next, we write the governing equations under these assumptions. Finally, some of the up to date solutions of similar problems are mentioned.

In this dissertation our interest of elastic bodies is limited to beams and strings as the most appropriate and also the easiest in analysis representation of spans and cables, respectively. Among all types of natural vibrations exhibited by an excited one - dimensional elastic continuum we consider only transverse vibrations, as a consequence of nature of the moving load excitation. For the continuum we assume that it is homogenous and isotropic. Moreover, it holds Hooke's law [Symon 1971]. We assume also that the displacements are sufficiently small such that the response to dynamic excitations always preserves the linear-elastic behavior.

One of the mathematical model of a beam that meets all of these statements is Euler-Bernoulli beam. The full derivation of equation of motion as well as the detailed discussion on the Euler-Bernoulli beam model can be found for example in [Timoshenko 1954]. The semi-active controlled system in which the Euler-Bernoulli equation represents a span is shown in the Figure 2.1. The parameters of a beam are  $EI$ ,  $\mu$  and  $l$  that stand for bending stiffness, constant mass density per unit length and total length of the beam, respectively. The boundary conditions for the beam is specified by simple supports at its ends. The transverse deflection of the beam is measured in the direction of vector  $\vec{W}$ . The dynamics of the beam is described by  $w(x, t)$  - the distribution of the deflection in the space-time domain.

The beam is excited by concentrated force passing the beam at the constant velocity  $v > 0$ . The magnitude of the excitation  $P < 0$  is presumed to be constant. This is under the assumption that the mass accompanying the travelling load is small compared with the mass of the beam, so the inertial forces can be neglected.

We adopt the damping coefficients of the viscous supports as the controls. By  $u_i(t)$  we denote the  $i$ -th control as the function of time. The  $a_i$  is the  $i$ -th fixed point of a damper. By  $m$  we denote the total number of viscous supports. The reactions of dampers are assumed to be proportional to the velocity of displacements in given points.

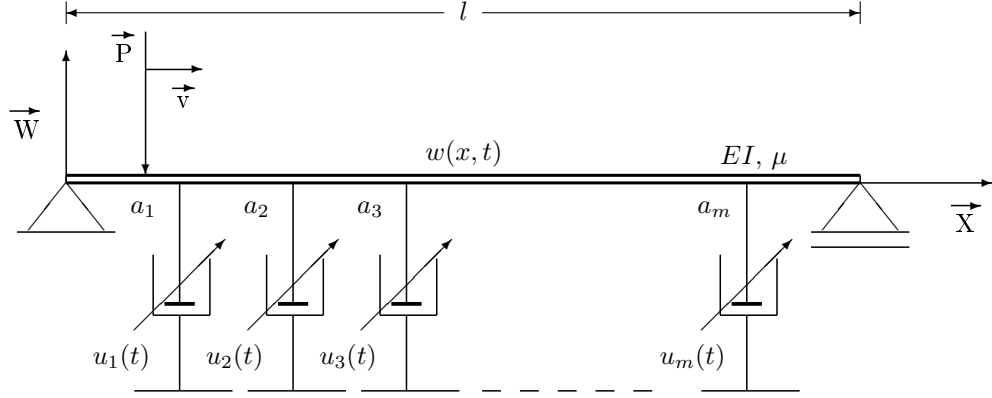


Figure 2.1: Euler-Bernoulli beam system supported by active viscous dampers.

The initial state of the system, in our case the state before the traveling load meets the beam, is set zero values, i. e.  $w(x, t = 0) = 0$ ,  $\dot{w}(x, t = 0) = 0$  for all  $x \in [0, l]$ .

The standard approach to specify the distribution of concentrated moving force as well as the reaction of the dampers is based on the idea of using the Dirac delta function  $\delta(\cdot)$  [Dirac 1958]. This approach is widely regarded in the positions [Fryba 1972], [Fryba 1993] in application to structures subjected to moving loads.

Under all of the formulated assumptions we can write the governing equation. Together with the initial and boundary conditions the equation of motion for the system depicted in the Figure 2.1 is of the form

$$\begin{cases} EI \frac{\partial^4 w(x, t)}{\partial x^4} + \mu \frac{\partial^2 w(x, t)}{\partial t^2} = - \sum_{i=1}^m u_i(t) \frac{\partial w(x, t)}{\partial t} \delta(x - a_i) + P \delta(x - vt), \\ w(x = 0, t) = 0, \quad w(x = l, t) = 0, \quad \left( \frac{\partial^2 w(x, t)}{\partial x^2} \right)_{|x=0} = 0, \quad \left( \frac{\partial^2 w(x, t)}{\partial x^2} \right)_{|x=l} = 0, \\ w(x, t = 0) = 0, \quad \dot{w}(x, t = 0) = 0. \end{cases} \quad (2.1)$$

Equation 2.1 is the fourth order, nonlinear, partial differential equation (PDE). The non-linearity is caused by the presence of bilinear forms – products of controls and velocities  $u_i(t)$  ( $\partial w(x, t) / \partial t$ ). The group of PDE containing such a kind of products is called bilinear PDEs and is widely regarded as one of the most applicable set of nonlinear differential equations. For more details please see the next chapter.

Let us now consider the analogous system to 2.1, but instead of the Euler-Bernoulli beam we now put stretched string as shown in the Figure 2.2.

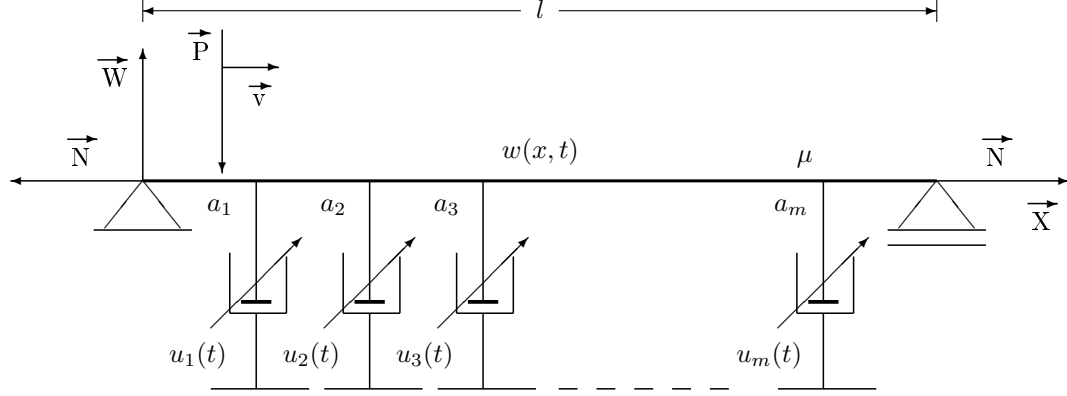


Figure 2.2: String system supported by active viscous dampers.

For such a system we can write equation of motion of the form

$$\begin{cases} -N \frac{\partial^2 w(x, t)}{\partial x^2} + \mu \frac{\partial^2 w(x, t)}{\partial t^2} = - \sum_{i=1}^m u_i(t) \frac{\partial w(x, t)}{\partial t} \delta(x - a_i) + P \delta(x - vt), \\ w(x = 0, t) = 0, \quad w(x = l, t) = 0, \\ w(x, t = 0) = 0, \quad \dot{w}(x, t = 0) = 0. \end{cases} \quad (2.2)$$

Here,  $N$  denotes the stretching force. For derivation and more details concerning the string equation please see [Evans 1998]. Equation 2.2 is the hyperbolic partial differential equation. Its wave-like solution exhibits quite different properties from the solution of Euler-Bernoulli beam. The impact of these properties on the control capabilities is discussed later in this work.

To solve any of the formulated problems 2.1, 2.2, the use of numerical methods is necessary. Even if the control is set to be a constant function, there exists no analytical method to obtain the exact, closed form solution. From the mathematical point of view, the presence of dampers or springs fixed to the beam, results directly in coupling of infinite dimensional system of ordinary differential equations. The structure of these systems, resulting from 2.1 and 2.2, is presented and investigated in the following sections of this dissertation.

The effects of a moving load on an elastic solids are widely studied by L. Fryba. In the work [Fryba 1972], he presents analytical methods for solving one, two and three-dimensional bodies under a travelling load where none of the mentioned coupling is present. As the tools for deriving the solutions he uses the Fourier expansions and the Laplace transform. The dynamic response of a double-beam system traversed by a constant moving load is studied in the paper [Hilal 2006]. The author considers two simply supported parallel prismatic beams, one upon the other and connected continuously by a viscoelastic layer. Such a defined system also gives the opportunity to derive the analytical solution. The decoupling of the system is proceeded under the assumption that the beams must be identical. The similar approach is presented in the work [H. V. Vu 2000], where the authors present the method of solving vibration of a double-beam system subject to a harmonic excitation.

### 2.3 Weak formulation, ODE system representation

In this section we perform the space discretization in order to transform the system described by PDE into the infinite dimensional system of ODEs. We use Sine functions as the orthogonal basis. With such a basis the weak formulation is introduced. Using the fundamental properties of orthogonal functions we derive the resulting system of ODEs.

We consider again the system 2.1 given of the form

$$EI \frac{\partial^4 w(x, t)}{\partial x^4} + \mu \frac{\partial^2 w(x, t)}{\partial t^2} = - \sum_{i=1}^m u_i(t) \frac{\partial w(x, t)}{\partial t} \delta(x - a_i) + P \delta(x - vt), \quad (2.3)$$

with boundary and initial conditions

$$\begin{aligned} w(0, t) = 0, \quad w(l, t) = 0, \quad \left( \frac{\partial^2 w(x, t)}{\partial x^2} \right)_{|x=0} = 0, \quad \left( \frac{\partial^2 w(x, t)}{\partial x^2} \right)_{|x=l} = 0, \\ w(x, 0) = 0, \quad \dot{w}(x, 0) = 0. \end{aligned} \quad (2.4)$$

We apply Fourier expansions for  $w(x, t)$  as follows

$$w(x, t) = \frac{2}{l} \sum_{j=1}^{\infty} V(j, t) \sin \frac{j\pi x}{l}. \quad (2.5)$$

Here,  $\sin \frac{j\pi x}{l} =: \theta_j(x)$  are eigenfunctions respecting boundary conditions 2.4 and  $V(j, t)$  are functions to be determined. The pair  $w(x, t)$ ,  $V(j, t)$  satisfies the relation:

$$V(j, t) = \int_0^l w(x, t) \theta_j(x) dx. \quad (2.6)$$

Inserting Equation 2.5 into 2.3 we obtain

$$EI \frac{\partial^4}{\partial x^4} \left[ \frac{2}{l} \sum_{j=1}^{\infty} V(j, t) \theta_j(x) \right] + \mu \frac{\partial^2}{\partial t^2} \left[ \frac{2}{l} \sum_{j=1}^{\infty} V(j, t) \theta_j(x) \right] = P \delta(x - vt) +$$

$$- \sum_{i=1}^m u_i(t) \frac{\partial}{\partial t} \left[ \frac{2}{l} \sum_{j=1}^{\infty} V(j, t) \theta_j(x) \right] \delta(x - a_i). \quad (2.7)$$

Then, each term of Equation 2.3 is multiplied by  $\sin \frac{k\pi x}{l} =: \theta_k(x)$  and then integrated with respect to  $x$  in the interval  $[0, l]$ . This results in the weak formulation given of the form

$$EI \left( \frac{j\pi}{l} \right)^4 \frac{2}{l} \sum_{j=1}^{\infty} V(j, t) \int_0^l \theta_j(x) \theta_k(x) dx + \mu \frac{2}{l} \sum_{j=1}^{\infty} \ddot{V}(j, t) \int_0^l \theta_j(x) \theta_k(x) dx =$$

$$P \int_0^l \theta_k(x) \delta(x - vt) dx - \sum_{i=1}^m u_i(t) \frac{2}{l} \sum_{j=1}^{\infty} \dot{V}(j, t) \int_0^l \theta_j(x) \theta_k(x) \delta(x - a_i) dx. \quad (2.8)$$

Equation 2.8 must hold for every  $k = 1, 2, \dots$ . Now, we can use the orthogonality conditions for the eigenfunctions  $\theta_j(x), \theta_k(x)$

$$\int_0^l \theta_j(x) \theta_k(x) dx = \frac{l}{2} \delta_{j,k}, \quad (2.9)$$

where  $\delta_{j,k}$  is the Kronecker delta. Now, we remind the sifting property the of Dirac delta function which states that the product of any well-behaved function and the Dirac delta yields the function evaluated where the Dirac delta is singular

$$\int_0^l \Theta(x) \delta(x - x_0) dx = \begin{cases} \Theta(x_0) & \text{if } 0 < x_0 < l, \\ 0 & \text{if } (0, l) \text{ does not contain } x_0. \end{cases} \quad (2.10)$$

Thus, the terms of Eqn. 2.8 where Dirac delta is incorporated can be computed as below

$$\int_0^l \theta_j(x) \theta_k(x) \delta(x - a_i) dx = \theta_j(a_i) \theta_k(a_i),$$

$$\int_0^l \theta_k(x) \delta(x - vt) dx = \theta_k(vt). \quad (2.11)$$

Eq. 2.8 can be written as

$$\mu \sum_{j=1}^{\infty} \ddot{V}(j, t) \delta_{j,k} + \frac{2}{l} \sum_{i=1}^m u_i(t) \sum_{j=1}^{\infty} \dot{V}(j, t) \theta_j(a_i) \theta_k(a_i) + EI \sum_{j=1}^{\infty} \left( \frac{j\pi}{l} \right)^4 V(j, t) \delta_{j,k} =$$

$$P \theta_k(vt), \quad k = 1, 2, \dots \quad (2.12)$$

Finally we rewrite PDE 2.3 as a system of ODEs

$$\mu \ddot{V}(k, t) + \frac{2}{l} \sum_{i=1}^m \sum_{j=1}^{\infty} u_i(t) \dot{V}(j, t) \sin \frac{j\pi a_i}{l} \sin \frac{k\pi a_i}{l} + EI \frac{k^4 \pi^4}{l^4} V(k, t) = P \sin \frac{k\pi vt}{l},$$

$$k = 1, 2, \dots$$
(2.13)

In a similar way we can proceed the weak formulation and write the ODEs representation for the string system 2.2.

$$\mu \ddot{V}(k, t) + \frac{2}{l} \sum_{i=1}^m \sum_{j=1}^{\infty} u_i(t) \dot{V}(j, t) \sin \frac{j\pi a_i}{l} \sin \frac{k\pi a_i}{l} + N \frac{k^2 \pi^2}{l^2} V(k, t) = P \sin \frac{k\pi vt}{l},$$

$$k = 1, 2, \dots$$
(2.14)

In the next sections of this work we consider only approximate solutions of 2.13, 2.14 by using finite-dimensional modal space, i. e.  $j, k = 1, 2, \dots, N < \infty$ . Reduction of the infinite dimensional continuum model to a finite dimensional ( $N^{th}$  order) discrete model means that an infinite number of motion components are neglected. If the order  $N$  is chosen too small, it can result in spillover instability that occurs when the controller, designed for the finite dimensional system, senses and actuates higher order modes, driving them unstable. This phenomenon is investigated in the paper [Balas 1978]. On the other hand, if  $N$  is chosen too high then the design of high order compensator is difficult and costly to implement. The control design based on distributed parameter models eliminates control spillover instabilities. Unfortunately, only few control methods for distributed parameters systems have been developed [Rahn 2001] (e.g. Lyapunov techniques [J. L. Junkis 1993] and semigroup theory [R. F. Curtain 1995]). In this dissertation for control design we use the finite dimensional models.

## 2.4 Approximated solutions

The aim of this section is to establish appropriate values for the number of terms in Fourier series (modes)  $N$  that one should take into account when solves the systems 2.1, 2.2. By appropriate we mean such that provides good accuracy. On the other hand, this number should be not too large, to make the control design feasible. Due to high complexity of the considered systems the analysis is performed by means of numerical results. Four representative examples demonstrate the convergence of the solutions while the number of respected modes gradually increases. In these examples we consider Euler-Bernoulli beam system as well as string system, each steered by constant and switching control.

In the first example we consider the Euler-Bernoulli beam system described by Eqn. 2.1. We assume the following values for constants:  $\mu = 69.8$ ,  $EI = 2.9 \cdot 10^7$ ,  $l = 10$ ,

$P = -20000$ ,  $v = 0.9\pi\sqrt{(EI/\mu)/l}$ . Five dampers are located in the positions:  $a_i = i/6 \cdot l$ ,  $i = 1, 2, \dots, 5$ . For all of the following examples the integration of system 2.13 is performed by the common fourth-order Runge-Kutta method (RK4, [D. Kincaid 2002]). The computations are executed in the time interval  $[0, l/v]$  represented in the form of 1000 discrete-time samples. In this case all controls are assumed to be constant functions  $u_i(t) = 5 \cdot 10^5$ ,  $i = 1, 2, \dots, 5$ ,  $t \in [0, l/v]$ .

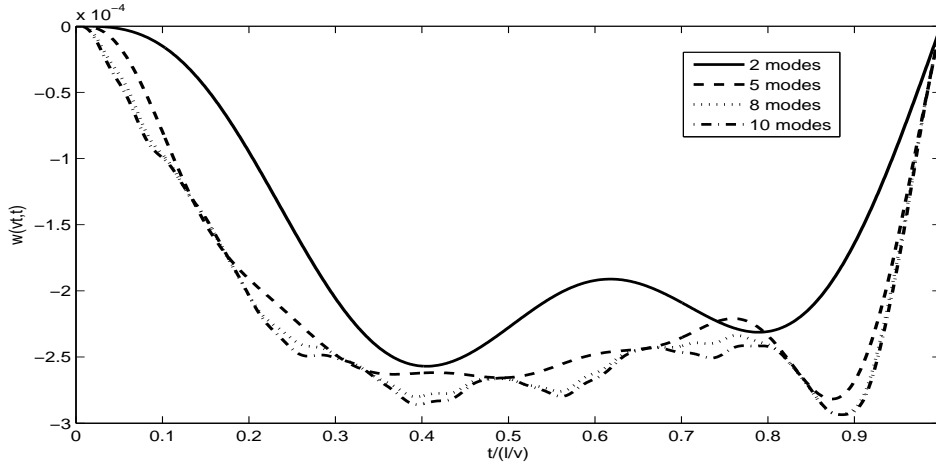


Figure 2.3: Solutions computed for different number of terms in Fourier series – constant control applied.

The Figure 2.3 displays the trajectories  $w(vt, t)$  as functions of time. These trajectories correspond to deflection of a moving load during its travel over the Euler-Bernoulli beam. The solutions are computed for different number of terms in the Fourier series. In order to highlight the convergence of solutions the zoom image is presented in the Figure 2.4. The growing number of modes successively increases the number of details in the trajectory. However, its qualitative properties are retained.

In the next example we consider the same system, however now we substitute the switching controls instead of constants. We assume one switching for every control as follows

$$u_i(t) = \begin{cases} 5 \cdot 10^1 & \text{if } t \in [0, \tau_i), \\ 5 \cdot 10^5 & \text{if } t \in [\tau_i, l/v], \end{cases} \quad (2.15)$$

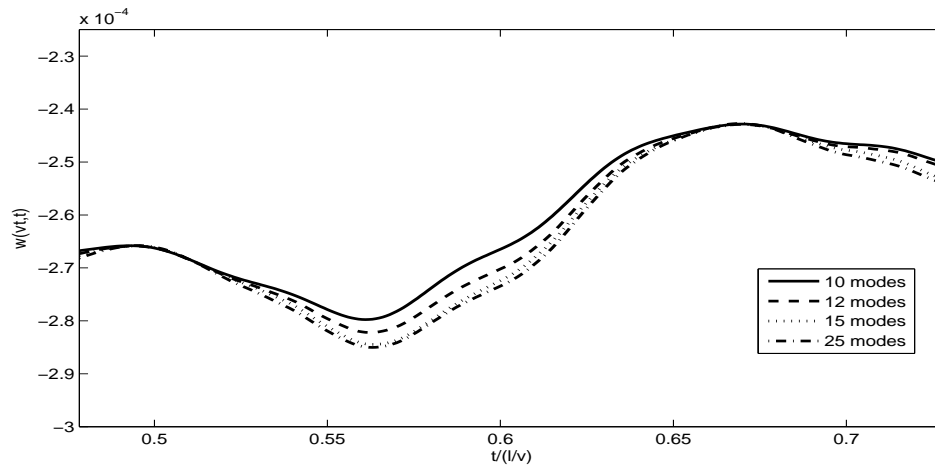


Figure 2.4: Solutions computed for different number of terms in Fourier series – constant control applied.

where  $\tau = [0.1, 0.3, 0.5, 0.6, 0.7](l/v)$ . The corresponding solutions are plotted in the Figure 2.5.

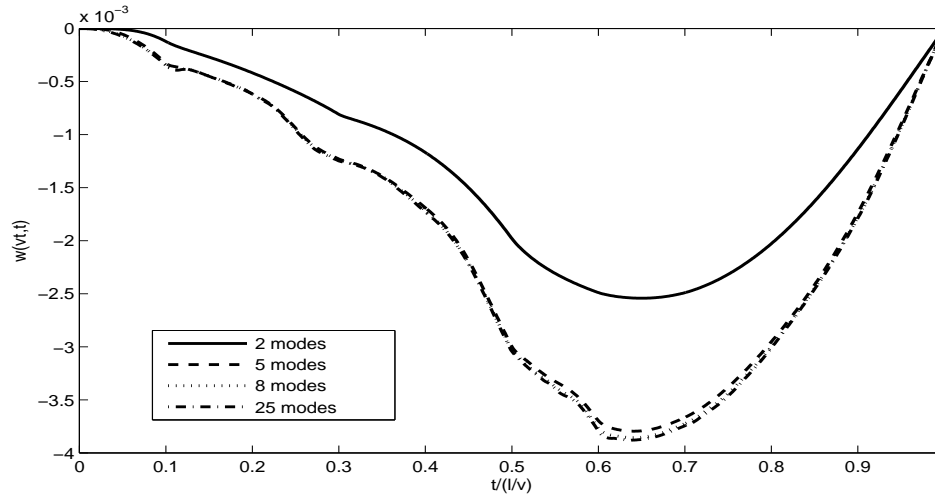


Figure 2.5: Solutions computed for different number of terms in Fourier series – switching control applied.

In this example we can also notice that the trajectories converge. The rate of convergence becomes negligibly small for larger number of modes.

From the standpoint of accuracy of solutions we can accept  $N=10$  as the appropriate

number of modes for each of presented examples. Consequently, we can assume the size of state vector as  $2N=20$ . For such a system we are able to solve the optimal control problem within a reasonable time.

We have to notice that in some cases the number  $N$  may differ slightly depending on the parameters of the system. However, in the case of the Euler-Bernoulli beam system, in which the high level of damping is applied, we can expect the fast convergence of solutions. This may not be the rule for the string system as it is shown in the following cases.

In the next two examples we consider the semi-active string system given by Equation 2.2. The following values are set for constants: mass density  $\mu = 10$ , tensile force  $N = 10^4$ , length  $l = 10$ , point force  $P = -100$ , velocity  $v = 0.5 \pi \sqrt{N/\mu}$ . The placement of the dampers remains unchanged. In the first case we assume that the system is driven by constant controls  $u_i(t) = 5 \cdot 10^2$ ,  $i = 1, 2, \dots, 5$ ,  $t \in [0, l/v]$ . The trajectories of the moving load, computed with the participation of various number of modes are presented in the Figure 2.6.

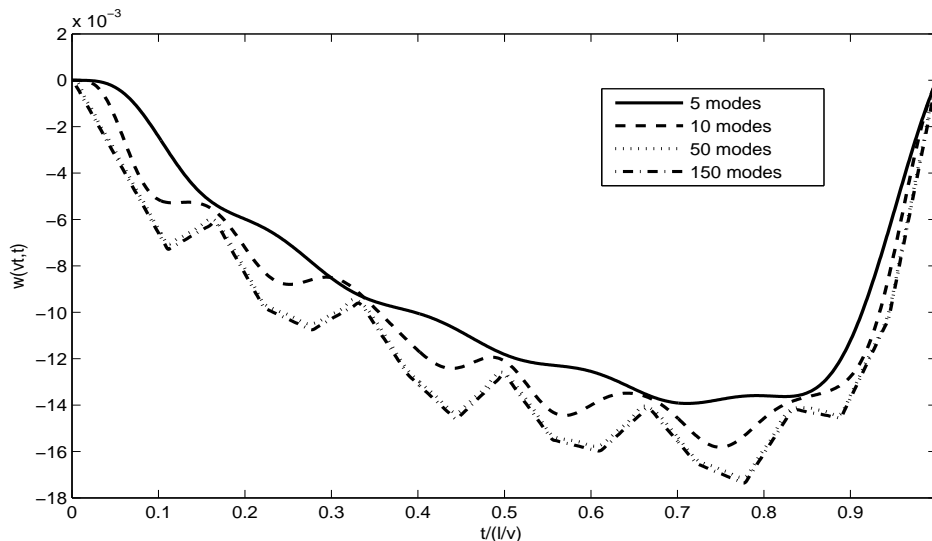


Figure 2.6: Solutions computed for different number of terms in Fourier series – no control applied.

Unlike for the Euler-Bernoulli beam in the case of string system we can not obtain a good approximation if only  $N=10$  modes are taken into account. Waves generated by the concentrated moving force are characterized by the sharp shapes. Moreover, the natural frequencies of string are proportional to  $k^2$  (see Equation 2.14) and this value differs from the analogous value of simply supported beam which is proportional to  $k^4$  (see Equation 2.13). Respecting these two facts we deduce, that the minimum number of modes in the

string system should be at least several times greater than in case of the beam.

In the next example we use the following switching controls

$$u_i(t) = \begin{cases} 5 \cdot 10^{-2} & \text{if } t \in [0, \tau_i), \\ 5 \cdot 10^2 & \text{if } t \in [\tau_i, l/v]. \end{cases} \quad (2.16)$$

Here, the switching times vector is  $\tau = [0.1, 0.3, 0.5, 0.6, 0.7](l/v)$ . The results are presented in the Figure 2.7.

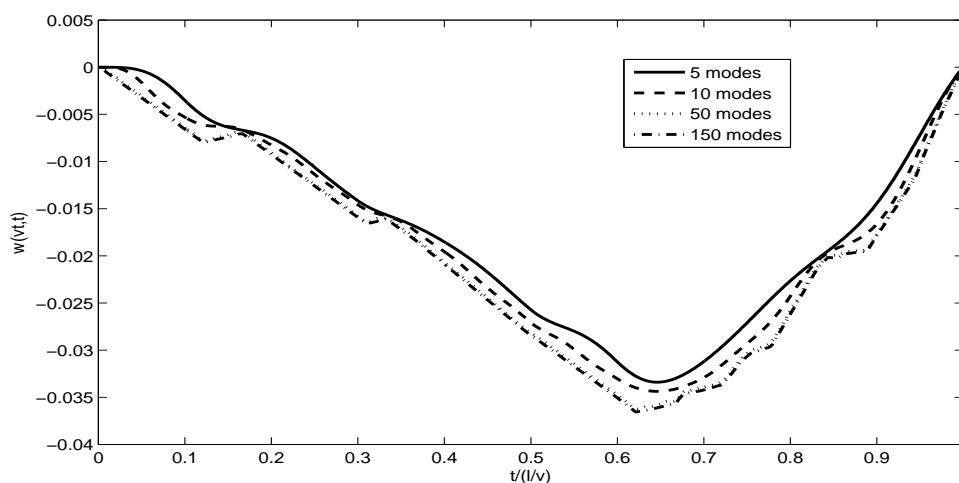


Figure 2.7: Solutions computed for different number of terms in Fourier series – switching control applied.

The last two examples show that in the case of a string system we need to take into account at least  $N=50$  modes for the approximation of hyperbolic partial differential equation – Equation 2.2. The computational cost for such a system increases rapidly when optimal control problem is solved.

## 2.5 Two special cases

In this section two extensions of previously presented model is considered. The first one is a natural extension of a simple supported beam by adding an additional parallel span. The second one is the beam holding the nonzero initial deflection. Both models are used in control design demonstrated in the Chapter 4.

### 2.5.1 Double beam system

Let us consider the system shown in the Figure 2.8. Two parallel Euler-Bernoulli beams are coupled by a set of controlled dampers. For such a system, we can write the equation of motion together with the boundary and initial conditions as follows

$$\left\{ \begin{array}{l} EI_1 \frac{\partial^4 w_1(x, t)}{\partial x^4} + \mu_1 \frac{\partial^2 w_1(x, t)}{\partial t^2} = - \sum_{i=1}^m u_i(t) \left[ \frac{\partial w_1(x, t)}{\partial t} - \frac{\partial w_2(x, t)}{\partial t} \right] \delta(x - a_i) + \\ + P \delta(x - vt), \\ EI_2 \frac{\partial^4 w_2(x, t)}{\partial x^4} + \mu_2 \frac{\partial^2 w_2(x, t)}{\partial t^2} = - \sum_{i=1}^m u_i(t) \left[ \frac{\partial w_2(x, t)}{\partial t} - \frac{\partial w_1(x, t)}{\partial t} \right] \delta(x - a_i), \\ w_1(x = 0, t) = 0, \quad w_1(x = l, t) = 0, \quad \left( \frac{\partial^2 w_1(x, t)}{\partial x^2} \right)_{|x=0} = 0, \quad \left( \frac{\partial^2 w_1(x, t)}{\partial x^2} \right)_{|x=l} = 0, \\ w_2(x = 0, t) = 0, \quad w_2(x = l, t) = 0, \quad \left( \frac{\partial^2 w_2(x, t)}{\partial x^2} \right)_{|x=0} = 0, \quad \left( \frac{\partial^2 w_2(x, t)}{\partial x^2} \right)_{|x=l} = 0, \\ w_1(x, t = 0) = 0, \quad \dot{w}_1(x, t = 0) = 0, \quad w_2(x, t = 0) = 0, \quad \dot{w}_2(x, t = 0) = 0. \end{array} \right. \quad (2.17)$$

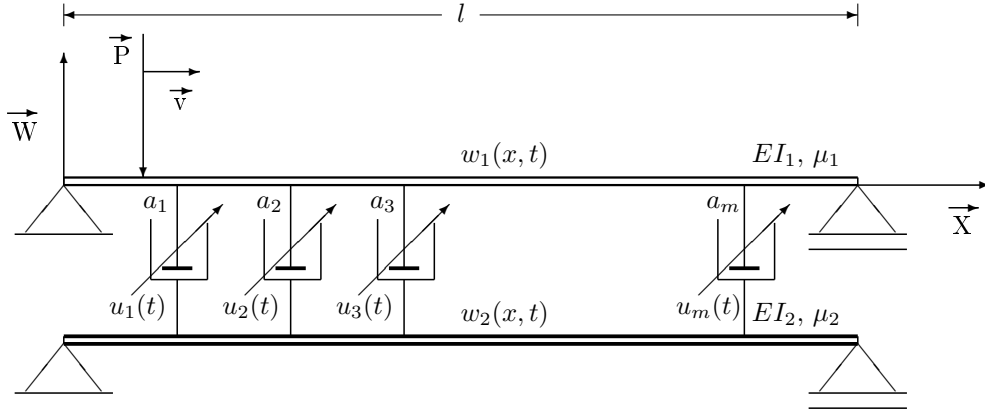


Figure 2.8: Double Euler - Bernoulli beam system coupled with active viscous dampers.

The procedure of transformation 2.17 into the system of ODEs is analogous to the presented in section 2.3. We apply Fourier expansions for  $w_1(x, t)$  and  $w_2(x, t)$  as the

following

$$w_1(x, t) = \frac{2}{l} \sum_{j=1}^{\infty} V_1(j, t) \sin \frac{j\pi x}{l}, \quad w_2(x, t) = \frac{2}{l} \sum_{j=1}^{\infty} V_2(j, t) \sin \frac{j\pi x}{l}. \quad (2.18)$$

Pairs  $w_1(x, t)$ ,  $V_1(j, t)$  and  $w_2(x, t)$ ,  $V_2(j, t)$  satisfy relations

$$V_1(j, t) = \int_0^l w_1(x, t) \theta_j(x) dx, \quad V_2(j, t) = \int_0^l w_2(x, t) \theta_j(x) dx. \quad (2.19)$$

The weak formulation now is of the form

$$\begin{aligned} & EI_1 \left( \frac{j\pi}{l} \right)^4 \left[ \frac{2}{l} \sum_{j=1}^{\infty} V_1(j, t) \int_0^l \theta_j(x) \theta_k(x) dx \right] + \mu_1 \left[ \frac{2}{l} \sum_{j=1}^{\infty} \ddot{V}_1(j, t) \int_0^l \theta_j(x) \theta_k(x) dx \right] = \\ & - \sum_{i=1}^m u_i(t) \left[ \frac{2}{l} \sum_{j=1}^{\infty} [\dot{V}_1(j, t) - \dot{V}_2(j, t)] \int_0^l \theta_j(x) \theta_k(x) \delta(x - a_i) dx \right] + \\ & + P \int_0^l \theta_k(x) \delta(x - vt) dx, \\ & EI_2 \left( \frac{j\pi}{l} \right)^4 \left[ \frac{2}{l} \sum_{j=1}^{\infty} V_2(j, t) \int_0^l \theta_j(x) \theta_k(x) dx \right] + \mu_2 \left[ \frac{2}{l} \sum_{j=1}^{\infty} \ddot{V}_2(j, t) \int_0^l \theta_j(x) \theta_k(x) dx \right] = \\ & - \sum_{i=1}^m u_i(t) \left[ \frac{2}{l} \sum_{j=1}^{\infty} [\dot{V}_2(j, t) - \dot{V}_1(j, t)] \int_0^l \theta_j(x) \theta_k(x) \delta(x - a_i) dx \right], \quad k = 1, 2, \dots \end{aligned} \quad (2.20)$$

Using the orthogonality conditions for eigenfunctions we get

$$\begin{aligned} & \mu_1 \sum_{j=1}^{\infty} \ddot{V}_1(j, t) \delta_{j,k} + \frac{2}{l} \sum_{i=1}^m u_i(t) \sum_{j=1}^{\infty} [\dot{V}_1(j, t) - \dot{V}_2(j, t)] \theta_j(a_i) \theta_k(a_i) + \\ & EI_1 \sum_{j=1}^{\infty} \left( \frac{j\pi}{l} \right)^4 V_1(j, t) \delta_{j,k} = P \theta_k(vt), \\ & \mu_2 \sum_{j=1}^{\infty} \ddot{V}_2(j, t) \delta_{j,k} + \frac{2}{l} \sum_{i=1}^m u_i(t) \sum_{j=1}^{\infty} [\dot{V}_2(j, t) - \dot{V}_1(j, t)] \theta_j(a_i) \theta_k(a_i) + \\ & EI_2 \sum_{j=1}^{\infty} \left( \frac{j\pi}{l} \right)^4 V_2(j, t) \delta_{j,k} = 0, \quad k = 1, 2, \dots \end{aligned} \quad (2.21)$$

Finally we rewrite the ODEs representation for the system 2.17

$$\begin{aligned}
\mu_1 \ddot{V}_1(k, t) + \frac{2}{l} \sum_{i=1}^m \sum_{j=1}^{\infty} u_i(t) \left[ \dot{V}_1(j, t) - \dot{V}_2(j, t) \right] \sin \frac{j\pi a_i}{l} \sin \frac{k\pi a_i}{l} + EI_1 \frac{k^4 \pi^4}{l^4} V_1(k, t) = \\
P \sin \frac{k\pi vt}{l}, \\
\mu_2 \ddot{V}_2(k, t) + \frac{2}{l} \sum_{i=1}^m \sum_{j=1}^{\infty} u_i(t) \left[ \dot{V}_2(j, t) - \dot{V}_1(j, t) \right] \sin \frac{j\pi a_i}{l} \sin \frac{k\pi a_i}{l} + EI_2 \frac{k^4 \pi^4}{l^4} V_2(k, t) = \\
0, \quad k = 1, 2, \dots
\end{aligned} \tag{2.22}$$

### 2.5.2 The initial deflection

We consider the initially deflected system exposed in the Figure 2.9.

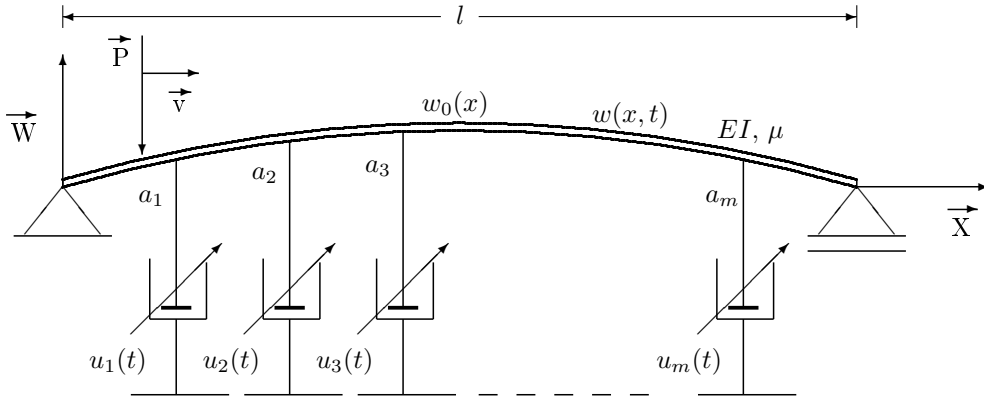


Figure 2.9: Initially deflected Euler-Bernoulli beam system supported by active viscous dampers.

Let us assume  $w_0(x)$  to be the initial deflection of the beam written in the coordinate system spanned by vectors  $\vec{X}$  and  $\vec{W}$ . We notice that  $w_0(x)$  characterizes the shape of the beam in which the system exhibits the lack of elastic forces. Thus, we can write the equation of motion as follows

$$EI \frac{\partial^4 (w(x, t) - w_0(x))}{\partial x^4} + \mu \frac{\partial^2 w(x, t)}{\partial t^2} = - \sum_{i=1}^m u_i(t) \frac{\partial w(x, t)}{\partial t} \delta(x - a_i) + P \delta(x - vt). \tag{2.23}$$

Now, the boundary and initial conditions are of the form

$$\begin{aligned} w(x=0, t) = 0, \quad w(x=l, t) = 0, \quad \left( \frac{\partial^2 w(x, t)}{\partial x^2} \right)_{|x=0} = 0, \quad \left( \frac{\partial^2 w(x, t)}{\partial x^2} \right)_{|x=l} = 0, \\ w(x, t=0) = w_0(x), \quad \dot{w}(x, t=0) = 0. \end{aligned} \quad (2.24)$$

By introducing the substitution  $w(x, t) - w_0(x) = \bar{w}(x, t)$  we can write the system 2.23 in the standard form

$$\left\{ \begin{aligned} EI \frac{\partial^4 \bar{w}(x, t)}{\partial x^4} + \mu \frac{\partial^2 \bar{w}(x, t)}{\partial t^2} &= - \sum_{i=1}^m u_i(t) \frac{\partial \bar{w}(x, t)}{\partial t} \delta(x - a_i) + P \delta(x - vt), \\ \bar{w}(x=0, t) = 0, \quad \bar{w}(x=l, t) = 0, \quad \left( \frac{\partial^2 \bar{w}(x, t)}{\partial x^2} \right)_{|x=0} &= 0, \quad \left( \frac{\partial^2 \bar{w}(x, t)}{\partial x^2} \right)_{|x=l} = 0, \\ \bar{w}(x, t=0) = 0, \quad \dot{\bar{w}}(x, t=0) = 0. \end{aligned} \right. \quad (2.25)$$

We assumed that:  $w_0(0) = w_0(l) = 0$ .

## 2.6 The method of power series

In this section we present the method of power series applied to the previously considered models. This method can be an attractive alternative for the standard numerical procedures as Euler's or Runge-Kutta's. The structure of the systems (2.13, 2.14) let us to derive the solutions as a function of time by means of pow. That may be helpful in the analysis. Moreover, time derivatives result immediately from the power series.

The presented solution is given in an arbitrary time interval. The time marching scheme allows us to perform the solution in successive layers with initial conditions taken from the end of previous stages. The accuracy of the solutions is examined by means of numerical examples. The derivation is carried on for semi-active string system (2.2), but the technique is not specific for any kind of previously regarded systems and it can be applied for the Euler-Bernoulli beam system as well.

Let us consider again the governing equation

$$\begin{aligned} \mu \ddot{V}(k, t) + \frac{2}{l} \sum_{i=1}^m \sum_{j=1}^{\infty} u_i(t) \dot{V}(j, t) \sin \frac{j\pi a_i}{l} \sin \frac{k\pi a_i}{l} + N \frac{k^2 \pi^2}{l^2} V(k, t) = P \sin \frac{k\pi vt}{l}, \\ k = 1, 2, \dots \end{aligned} \quad (2.26)$$

We assume that the controls  $u_i(t)$  are piecewise constant functions as defined below and

shown in the Figure 2.10

$$u_i(t): \left[0, \frac{l}{v}\right] \rightarrow [u_{min}, u_{max}], \quad u_i(t) = \begin{cases} u_{ip}, & \forall t \in (t_{p-1}, t_p], \quad p = 1, 2, \dots, s \\ 0, & t = 0 \end{cases} \quad (2.27)$$

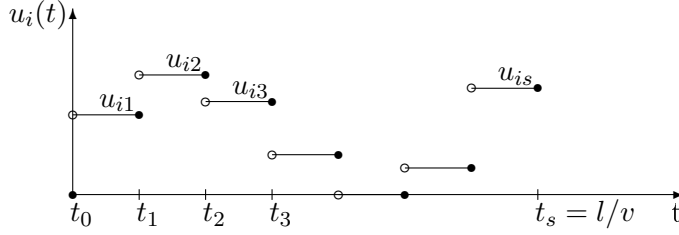


Figure 2.10: Piecewise constant damping function.

Introducing the following notations

$$\frac{\pi v}{l} = \omega, \quad \sin \frac{j\pi a_i}{l} \sin \frac{k\pi a_i}{l} = \alpha_{ijk}$$

Equation 2.26 in the time interval  $t \in (t_{p-1}, t_p]$  is simplified into the form

$$\mu \ddot{V}(k, t) + \frac{2}{l} \sum_{i=1}^m \sum_{j=1}^{\infty} u_{ip} \dot{V}(j, t) \alpha_{ijk} + N \frac{k^2 \pi^2}{l^2} V(k, t) = P \sin(k\omega t), \quad k = 1, 2, \dots, \quad (2.28)$$

where  $u_{ip}$  denotes the magnitude of suspension of  $i^{th}$  damper on  $p^{th}$  time interval.

Equation 2.28 is linear and describes the nonhomogeneous system with constant coefficients. The solution being looked for, is the general solution, where integration constants can be simply represented by initials  $C1_k = V(k, 0)$ ,  $C2_k = \dot{V}(k, 0)$ . It is an easy way to combine the interval solutions to a global one. Denoting  $t_{p-1}$  by  $\tau$ , the power series solution for  $t \in (t_{p-1}, t_p]$  is supposed to take a form

$$V(k, t) = \sum_{n=0}^{\infty} d_n(k) (t - \tau)^n, \quad (2.29)$$

where  $d_n(k)$  are unknown sequences. Thus

$$\dot{V}(k, t) = \sum_{n=0}^{\infty} n d_n(k) (t - \tau)^{n-1}, \quad \ddot{V}(k, t) = \sum_{n=0}^{\infty} (n-1) n d_n(k) (t - \tau)^{n-2} \quad (2.30)$$

and Equation 2.28 can be written as

$$\begin{aligned} & \mu \sum_{n=0}^{\infty} (n-1) n d_n(k) (t - \tau)^{n-2} + \frac{2}{l} \sum_{i=1}^m \sum_{j=1}^{\infty} \sum_{n=0}^{\infty} u_{ip} \alpha_{ijk} n d_n(j) (t - \tau)^{n-1} + \\ & + N \frac{k^2 \pi^2}{l^2} \sum_{n=0}^{\infty} d_n(k) (t - \tau)^n = P \sin(k\omega t), \quad k = 1, 2, \dots \end{aligned} \quad (2.31)$$

Representation of  $\sin(k\omega t)$  in the power series is

$$\begin{aligned} \sin(k\omega t) &= \sin(k\omega(t - \tau + \tau)) = \sin(k\omega(t - \tau)) \cos(k\omega\tau) + \cos(k\omega(t - \tau)) \sin(k\omega\tau) = \\ &= \cos(k\omega\tau) \sum_{n=0}^{\infty} \frac{(-1)^n (k\omega)^{2n+1} (t - \tau)^{2n+1}}{(2n+1)!} + \sin(k\omega\tau) \sum_{n=0}^{\infty} \frac{(-1)^n (k\omega)^{2n} (t - \tau)^{2n}}{(2n)!}. \end{aligned} \quad (2.32)$$

Then we have

$$\begin{aligned} &\mu \sum_{n=0}^{\infty} (n+1)(n+2)d_{n+2}(k)(t - \tau)^n + \\ &+ \frac{2}{l} \sum_{i=1}^m \sum_{j=1}^{\infty} \sum_{n=0}^{\infty} u_{ip} \alpha_{ijk} (n+1)d_{n+1}(j)(t - \tau)^n + N \frac{k^2 \pi^2}{l^2} \sum_{n=0}^{\infty} d_n(k)(t - \tau)^n = \\ &P \cos(k\omega\tau) \sum_{n=0}^{\infty} \frac{(-1)^n (k\omega)^{2n+1} (t - \tau)^{2n+1}}{(2n+1)!} + P \sin(k\omega\tau) \sum_{n=0}^{\infty} \frac{(-1)^n (k\omega)^{2n} (t - \tau)^{2n}}{(2n)!}, \\ &k = 1, 2, \dots \end{aligned} \quad (2.33)$$

It is commonly known that for every sequence  $\gamma_n$ , the following equation is satisfied

$$\sum_{n=0}^{\infty} \gamma_n (t - \tau)^n = \sum_{n=0}^{\infty} \gamma_{2n} (t - \tau)^{2n} + \sum_{n=0}^{\infty} \gamma_{2n+1} (t - \tau)^{2n+1}. \quad (2.34)$$

Finally Eqn. 2.33 is rewritten as

$$\begin{aligned} &\mu \sum_{n=0}^{\infty} (2n+1)(2n+2)d_{2n+2}(k)(t - \tau)^{2n} + N \frac{k^2 \pi^2}{l^2} \sum_{n=0}^{\infty} d_{2n}(k)(t - \tau)^{2n} + \\ &+ \frac{2}{l} \sum_{i=1}^m \sum_{j=1}^{\infty} u_{ip} \alpha_{ijk} \sum_{n=0}^{\infty} (2n+1)d_{2n+1}(j)(t - \tau)^{2n} + \\ &+ \mu \sum_{n=0}^{\infty} (2n+2)(2n+3)d_{2n+3}(k)(t - \tau)^{2n+1} + N \frac{k^2 \pi^2}{l^2} \sum_{n=0}^{\infty} d_{2n}(k)(t - \tau)^{2n} + \\ &+ \frac{2}{l} \sum_{i=1}^m \sum_{j=1}^{\infty} u_{ip} \alpha_{ijk} \sum_{n=0}^{\infty} (2n+2)d_{2n+2}(j)(t - \tau)^{2n+1} = \\ &P \cos(k\omega\tau) \sum_{n=0}^{\infty} \frac{(-1)^n (k\omega)^{2n+1} (t - \tau)^{2n+1}}{(2n+1)!} + P \sin(k\omega\tau) \sum_{n=0}^{\infty} \frac{(-1)^n (k\omega)^{2n} (t - \tau)^{2n}}{(2n)!}, \\ &k = 1, 2, \dots \end{aligned} \quad (2.35)$$

Comparing equivalent terms, we obtain the system of recurrence equations

$$\begin{aligned} \mu(2n+1)(2n+2)d_{2n+2}(k) &= -\frac{2}{l} \sum_{i=1}^m \sum_{j=1}^{\infty} u_{ip} \alpha_{ijk} (2n+1) d_{2n+1}(j) + \\ &- N \frac{k^2 \pi^2}{l^2} d_{2n}(k) + P \sin(k\omega\tau) \frac{(-1)^n (k\omega)^{2n}}{(2n)!}, \\ \mu(2n+2)(2n+3)d_{2n+3}(k) &= -\frac{2}{l} \sum_{i=1}^m \sum_{j=1}^{\infty} u_{ip} \alpha_{ijk} (2n+2) d_{2n+2}(j) + \\ &- N \frac{k^2 \pi^2}{l^2} d_{2n+1}(k) + P \cos(k\omega\tau) \frac{(-1)^n (k\omega)^{2n+1}}{(2n+1)!}, \quad k = 1, 2, \dots \end{aligned} \quad (2.36)$$

and  $d_0(k) = V(k, \tau)$ ,  $d_1(k) = \dot{V}(k, \tau)$ .

Numerical results for convergence rate of the obtained solution are now presented. In the analysis 60 modes, 40 terms in the power series and following data were assumed: mass density  $\mu = 1$ , string length  $l = 1$ , tensile force  $N = 0.5$ , point force  $P = 0.1$ , velocity  $v = 0.2\sqrt{N/\mu}$ , total number of dampers  $m = 1$ , position of damper  $a_1 = 0.5l$ . Suspension magnitude is assumed to be constant and it equals 1 ( $u_{1p} = 1, \forall p = 1, \dots, s$ ).

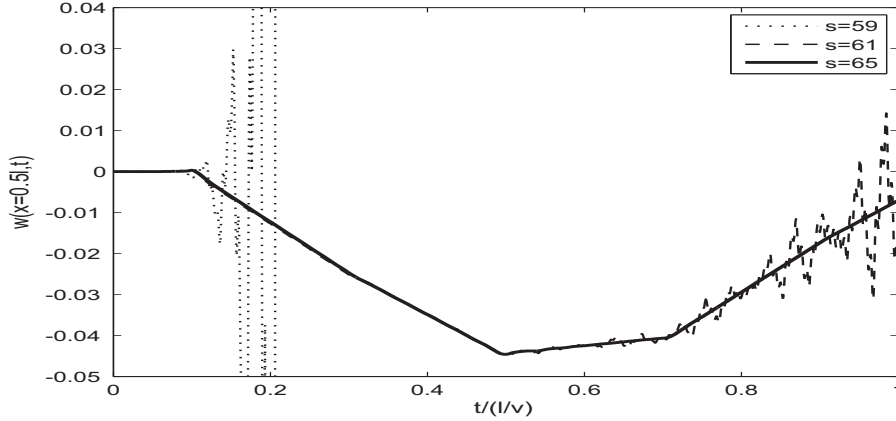


Figure 2.11: Solutions computed for different number of time intervals.

The Figure 2.11 presents solution at  $x = l/2$ . Curves are plotted for various number of intervals  $s = 59, 61$  and  $65$ . For lower number of time intervals and greater time increment the solution in this case diverges.

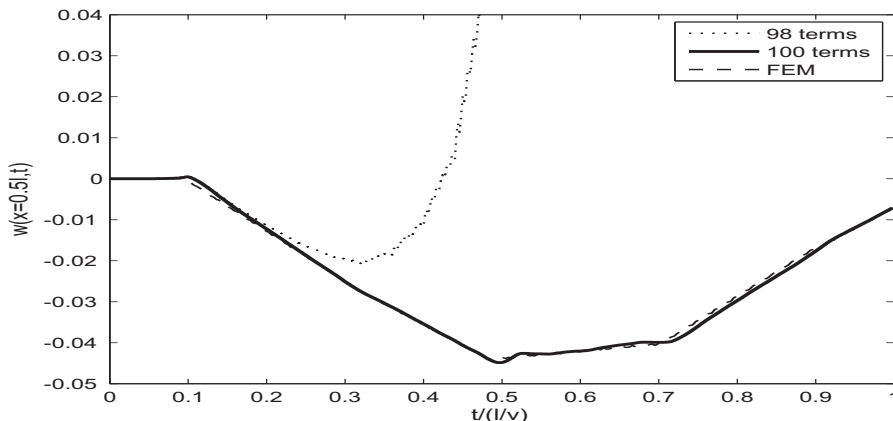


Figure 2.12: Solutions computed for different number of terms in power series, FEM comparison.

To extend the radius of convergence, more terms in power series have to be taken into account. The Figure 2.12 shows the previous solution for  $s = 25$  and 98, 100 terms in power series. Dashed line represents solution obtained by the finite element method.

## 2.7 State space representation

In this section we introduce the state space representation of models described throughout this chapter. This representation, known as a minimum set of variables, that fully describes the system, is a convenient form for specifying and solving the control problems that are addressed later in this dissertation.

For any of the previously regarded model we can write the equation of motion of the following form

$$\dot{\mathbf{y}} = \mathbf{A}\mathbf{y} + \sum_{i=1}^m u_i \mathbf{B}_i \mathbf{y} + \mathbf{f}(\mathbf{y}), \quad (2.37)$$

where  $\mathbf{y} = \mathbf{y}(t) : [0, t_f] \rightarrow \mathbb{R}^{\tilde{n}+1}$  is the state vector. We set time as the last term in the state vector.  $\mathbf{A}$  and  $\mathbf{B}_i$  are constant value matrices. The excitation vector  $\mathbf{f}$  is represented as a function of state variables. The autonomous form of 2.37 is for the convenience of applying first-order necessary optimality conditions.

Below we present the state space representation of the system given by Eqn. 2.13, where  $N$  modes are taken into consideration. The state vector is then given as follows

$$y_{2k-1}(t) = V(k, t), \quad y_{2k}(t) = \dot{V}(k, t), \quad k = 1, 2, \dots, \tilde{n}/2, \quad y_{\tilde{n}+1}(t) = t. \quad (2.38)$$

Here  $\tilde{n} = 2N$ . The components of the matrix  $\mathbf{A} = [\bar{a}_{i,j}]_{(\tilde{n}+1) \times (\tilde{n}+1)}$  are as follows

$$\bar{a}_{i,j} = \begin{cases} 1, & (i,j) = (2k-1, 2k), k = 1, 2, \dots, \tilde{n}/2, \\ -\frac{EI}{\mu} \frac{(j/2)^4 \pi^4}{l^4}, & (i,j) = (2k, 2k-1), k = 1, 2, \dots, \tilde{n}/2, \\ 0, & \text{else.} \end{cases} \quad (2.39)$$

The terms of matrices  $\mathbf{B}_i = [\bar{b}_{j,k}^i]_{(\tilde{n}+1) \times (\tilde{n}+1)}$  are listed below

$$\bar{b}_{j,k}^i = \begin{cases} -\frac{2}{\mu l} \sin \frac{(j/2)\pi a_i}{l} \sin \frac{(k/2)\pi a_i}{l}, & (j,k) = (2l, 2l'), l, l' = 1, 2, \dots, \tilde{n}/2, \\ 0, & \text{else.} \end{cases} \quad (2.40)$$

Finally, we have excitation vector  $\mathbf{f} = \mathbf{f}(\mathbf{y}) : \mathbb{R}^{\tilde{n}+1}$  with its components given of the form

$$f_i = \begin{cases} \frac{P}{\mu} \sin \frac{(i/2)\pi y_{\tilde{n}+1}}{l}, & i = 2k, k = 1, 2, \dots, \tilde{n}/2, \\ 1, & i = 2\tilde{n} + 1, \\ 0, & \text{else.} \end{cases} \quad (2.41)$$

---

This chapter has been devoted to the mathematical representation of one-dimensional semi-active controlled body. The approximated solutions have been investigated and the relevant number of terms in the Fourier series has been established. Model based on a string requires at least  $N=50$  modes for good approximation. For the Euler-Bernoulli beam system the minimum number of terms in the Fourier series that one should take in to account is  $N=10$ . For the sake of control design the state space representation has been derived. The power series method for solving the bilinear PDE has been proposed.

---



## Optimization in semi-active control systems

### Contents

- 3.1 Problem statement**
- 3.2 Optimal control problem for bilinear systems**
- 3.3 Existence of solution**
- 3.4 Necessary conditions for optimal controls**
- 3.5 Prediction of switchings in optimal controls**
- 3.6 Functional derivative, the method of steepest descent for optimal control problem**
- 3.7 Numerical example: semi-active controlled oscillator**
- 3.8 The method of parameterized switching times**
- 3.9 Switching times method - numerical examples**

Optimal control is the standard method for solving dynamic optimization problems. The study of this issue-oriented branch of mathematics goes back to 1950s. In that time two important advances were made. One was Dynamic Programming, founded by Richard Bellman [Bellman 1957]. Dynamic Programming is a procedure that reduces the search for an optimal control function to finding the solution of a partial differential equation (the Hamilton - Jacobi - Bellman Equation) [Vinter 2000]. The other was the the Maximum Principle [L. S. Pontryagin 1962], a set of necessary conditions for a control function to be optimal. Based on these theories numerous computational technics were developed in the 1960s and 1970s [A. E. Bryson 1962]. With the exception of simplest cases, however, it is impossible to express controls in an explicit feedback form.

In this chapter we consider the optimal control techniques in application to multidimensional bilinear systems. We show the most efficient computational methods. Furthermore, the difficulties are exposed.

The chapter is organized as following. In the first section the generalized optimal control problem is stated. Then, we consider optimal control for bilinear systems. A short divagation on the existence is then provided. In the following sections the necessary optimal conditions are given including the derivation on functional derivatives. Further, the switching method is considered. Finally, we provide simple numerical examples to verify the efficiency of the proposed methods.

### 3.1 Problem statement

This section is devoted to generalized optimal control problem. The intention is to provide basic definitions and assumptions that are used in further investigations.

We consider a control system of the form

$$\dot{\mathbf{y}} = \mathbf{f}(\mathbf{y}, \mathbf{u}), \quad \mathbf{y} \in Y, \quad \mathbf{u} \in U, \quad (3.1)$$

where  $Y$  is an open domain in  $\mathbb{R}^n$  and  $U$  an arbitrary subset of  $\mathbb{R}^m$ . The following assumptions are made for the function  $\mathbf{f}(\mathbf{y}, \mathbf{u})$

$$\begin{aligned} (\mathbf{y}, \mathbf{u}) \rightarrow \mathbf{f}(\mathbf{y}, \mathbf{u}) & \text{ is a continuous mapping for } \mathbf{y} \in Y, \quad \mathbf{u} \in U, \\ (\mathbf{y}, \mathbf{u}) \rightarrow \frac{\partial \mathbf{f}(\mathbf{y}, \mathbf{u})}{\partial \mathbf{y}} & \text{ is a continuous mapping for } \mathbf{y} \in Y, \quad \mathbf{u} \in U, \\ \mathbf{y} \rightarrow \mathbf{f}(\mathbf{y}, \mathbf{u}) & \text{ is a smooth vector field on } Y \text{ for any fixed } \mathbf{u} \in U. \end{aligned} \quad (3.2)$$

Next, we define a set of admissible control  $\mathbb{U}$  as the set of measurable functions with values in  $U$ :

$$\mathbb{U} = \{\mathbf{u} : t \rightarrow \mathbf{u}(t) \in U, \mathbf{u} \text{ is measurable}\}. \quad (3.3)$$

Under these assumptions the Cauchy problem:

$$\dot{\mathbf{y}} = \mathbf{f}(\mathbf{y}, \mathbf{u}), \quad \mathbf{y}(0) = \mathbf{y}_0 \quad (3.4)$$

has a unique solution (Carathéodory's existence theorem [Coddington 1955], [Rudin 1987]).

In order to evaluate the quality of a control we introduce the cost functional

$$J = \int_0^{t_f} f_0(\mathbf{y}, \mathbf{u}) dt + g(\mathbf{y}(t_f)), \quad (3.5)$$

where  $f_0$  and  $g$  are the specified scalar functions,  $f_0 : Y \times U \rightarrow \mathbb{R}$ ,  $g : Y \rightarrow \mathbb{R}$ , called running payoff and terminal payoff, respectively. Here  $t_f$  stands for the final time. We study the following optimal control problem.

*Minimize the functional  $J$  among all admissible controls  $\mathbf{u} = \mathbf{u}(t)$ ,  $t \in [0, t_f]$ , where the corresponding trajectory  $\mathbf{y}(t)$  is a solution of Cauchy problem 3.4.*

The solution  $\mathbf{u}$  of this problem is called the optimal control and the corresponding curve  $\mathbf{y}$  is the optimal trajectory. The final state  $\mathbf{y}(t_f)$  can be specified or free. In our investigations we consider only fixed time problems, i. e.  $t_f = \text{constant} > 0$ .

### 3.2 Optimal control problem for bilinear systems

There is a special group of control systems which are linear in both state space and control functions. This group is called bilinear systems and it is in the special interest of this work due to the fact they represent the mathematical models for semi-active controlled systems. One of the pioneers, that worked on the topic of control of bilinear systems, is R. R. Mohler. He began and promoted the application of optimal control methods to bilinear systems, beginning with his study of nuclear power plants in the 1960s. His work is reported in his books [Mohler 1970], [Mohler 1973], [Mohler 1991], which cite case studies by Mohler and many others in physiology, ecology, and engineering [Elliott 2009]. The survey on optimal control of bilinear models of pest population control was presented by Lee [Lee 1978].

In mechanical systems the bilinear terms occur as the products of the state vector and variable stiffness functions or of the most common form i. e. velocity vector and variable damping functions.

In this thesis we consider the bilinear control systems formulated as following

$$\dot{\mathbf{y}}(t) = \mathbf{f}(\mathbf{y}, \mathbf{u}) = \mathbf{A}\mathbf{y}(t) + \sum_{i=1}^m u_i(t)\mathbf{B}_i\mathbf{y}(t) + \tilde{\mathbf{f}}(\mathbf{y}). \quad (3.6)$$

Here  $\mathbf{A}$  and  $\mathbf{B}_i$ ,  $i = 1, 2, \dots, m$  are constant matrices. The excitation vector  $\tilde{\mathbf{f}}(\mathbf{y})$  denotes external forces acting on the system. The control functions  $u_i$  stand for variable parameters of mechanical system. For the practical reason these variables are bounded to the specified interval so the co-domain of input vector is limited to hypercube as follows

$$\mathbf{u}(t) \in \Omega = [u_{min}, u_{max}]^m = \{\boldsymbol{\omega} \in \mathbb{R}^m : u_{min} \leq \omega_i \leq u_{max}, i = 1, \dots, m\}. \quad (3.7)$$

Again, the objective functional to be minimized is

$$J = \int_0^{t_f} f_0(\mathbf{y}, \mathbf{u}) dt. \quad (3.8)$$

In many applications, it is desired to find the control that steers the system 3.6 from an initial state  $\mathbf{y}(0) = \mathbf{y}_0$  to some terminal state  $\mathbf{y}(t_f) = \mathbf{y}_f$  so as to minimize 3.8 with an admissible control 3.7. In general this problem may have not a solution due to lack of controllability, especially in the case of bilinear systems driven by constrained controls.

The widespread Linear Quadratic Regulator approach can be applied for bilinear systems. By introducing a quadratic performance index

$$J = \frac{1}{2} \int_0^{t_f} (\mathbf{y}^T \mathbf{Q} \mathbf{y} + r u^2) dt + \frac{1}{2} \mathbf{y}^T(t_f) \mathbf{P}_f \mathbf{y}(t_f), \quad (3.9)$$

it can be shown, that for the system

$$\dot{\mathbf{y}}(t) = \mathbf{A}\mathbf{y}(t) + \mathbf{B}u(t)\mathbf{y}(t) + \mathbf{b}u(t) \quad (3.10)$$

there exists an optimal feedback controller and it can be computed as a limit of a sequence

$$u^{k+1}(t) = r^{-1} \left[ \mathbf{B}\mathbf{y}^{k+1}(t) + \mathbf{b} \right]^T \mathbf{K}^{k+1}(t) \mathbf{y}^{k+1}(t). \quad (3.11)$$

where  $\mathbf{K}^{k+1}$  is the solution of the differential Riccati equation. For details see [Hofer 1988]. A key reason for using feedback is to reduce the effects of uncertainty which may appear in different forms as disturbances or imperfections in models. However, the iterative method that produces the feedback control 3.11 requires a fast computing controller. Moreover, the method is limited to particular form of objective functional 3.9.

For more general problems we try to derive the optimal controls by applying the first order necessary conditions for optimality. This approach is presented in the following sections.

### 3.3 Existence of solution

In this section we discuss in brief the sufficient conditions for the existence of an optimal control for the problem

$$\begin{aligned} \text{Minimize } J &= \int_0^{t_f} f_0(\mathbf{y}, \mathbf{u}) dt, \\ \text{subject to } \dot{\mathbf{y}}(t) &= \mathbf{f}(\mathbf{y}, \mathbf{u}) = \mathbf{A}\mathbf{y}(t) + \sum_{i=1}^m u_i(t)\mathbf{B}_i\mathbf{y}(t) + \tilde{\mathbf{f}}(\mathbf{y}), \quad \mathbf{y}(0) = \mathbf{0}, \\ \mathbf{u}(t) \in \Omega &= [u_{min}, u_{max}]^m = \{\boldsymbol{\omega} \in \mathbb{R}^m : u_{min} \leq \omega_i \leq u_{max}, i = 1, \dots, m\}. \end{aligned} \quad (3.12)$$

The aim is to present a theorem that asserts the existence of at least one optimal control, that is, the existence of function  $\mathbf{u}^* \in \Omega$  for which  $J(\mathbf{u}^*) \leq J(\mathbf{u})$  for all  $\mathbf{u} \in \Omega$ .

The existence theory is in essence a study of a continuous or semi-continuous function  $J(\mathbf{u})$  on a compact set  $\Omega$ . We introduce the target  $\mathbb{T}(t)$  and the set of successful controls that steer the system to this target

$$\Delta = \{\mathbf{u} \in \Omega \mid \exists t_1 \geq 0 \text{ such that } \mathbf{y}(t_1, \mathbf{y}_0, \mathbf{u}) \in \mathbb{T}(t_1)\}. \quad (3.13)$$

Let  $\Delta(T)$  be a class of all admissible controls which steer  $\mathbf{y}_0$  to the target in time  $t_1$ ,  $0 \leq t_1 \leq T$ . We assume that successful responses on  $[0, T]$  satisfy an a priori bound

$$|\mathbf{y}(t, \mathbf{y}_0, \mathbf{u})| \leq \alpha \text{ for all } \mathbf{u} \in \Omega, \quad 0 \leq t \leq t_1, \quad (3.14)$$

where  $\alpha = \alpha(T)$  is constant. Then, the following theorem can be formulated

**Theorem 3.1.** (*[J. Macki 1982]*) Consider the problem 3.12 on a fixed interval  $[0, t_f]$ , with  $\mathbf{y}(0)$  given,  $\mathbb{T}(t) \equiv \mathbf{0}$  and  $\mathbf{f}(\mathbf{y}, \mathbf{u})$ ,  $f_0(\mathbf{y}, \mathbf{u})$  continuous. Assume that  $\Delta(T) \neq \emptyset$ , and that a successful response satisfies an a priori bound 3.14. If, in addition, the set of points  $\hat{f}(\mathbf{y}, \Omega) = \{(f_0(\mathbf{y}, \mathbf{v}), \mathbf{f}^T(\mathbf{y}, \mathbf{v}))^T \mid \mathbf{v} \in \Omega\}$  is a convex set in  $\mathbb{R}^{n+1}$ , then there exists an optimal control.

Theorem 3.1 covers the case when  $\mathbf{f}$  and  $f_0$  are both linear in the control. Indeed, if

$$\mathbf{f} = \mathbf{A}(\mathbf{y})\mathbf{u} + \mathbf{g}(\mathbf{y}), \quad f_0 = \mathbf{a}(\mathbf{y})^T \mathbf{u} + g_0(\mathbf{y}), \quad (3.15)$$

with  $\mathbf{A}$  an  $n \times m$  matrix,  $\mathbf{g}$  an  $n$  - vector,  $\mathbf{a}$  an  $m$  - vector and  $g_0$  real - valued, then

$$\hat{f}(\mathbf{y}, \Omega) = \{(\mathbf{a}^T \mathbf{v} + g_0, \mathbf{A}\mathbf{v} + \mathbf{g}) \mid \mathbf{v} \in \Omega\} \quad (3.16)$$

is convex.

In some special cases the strong convexity condition is not necessary. If we restrict our controls to take their values in certain special subsets of  $\Omega$ , then it is possible to choose these subsets so they are compact in stronger topologies. Let us assume that controls are piecewise constant with at most  $r$  points of discontinuity. Then it can be shown that the set of these control is compact in  $L^1$  norm and the following theorem can be formulated

**Theorem 3.2.** (*[J. Macki 1982]*) Let  $[0, t_f]$  be a fixed interval. Suppose that controls are piecewise constant with at most  $r$  points of discontinuity and assume  $\Delta(T) \neq \emptyset$ . Assume that  $\mathbf{f}(\mathbf{y}, \mathbf{u})$ ,  $f_0(\mathbf{y}, \mathbf{u})$  are continuous and that successful responses satisfy an a priori bound 3.14. Then there exists an optimal control.

For proofs and details see [Lee 1978], [J. Macki 1982].

### 3.4 Necessary conditions for optimal controls

This section is devoted to the most important necessary condition which an optimal control must satisfy - the Pontryagin Maximum Principle (PMP). The sufficient condition, which guarantees the existence of at least one optimal control, is not useful and does not help us find the minimum. On the other hand, the necessary condition gives us a concrete method for finding these points.

In order to formulate the PMP we introduce the control theory Hamiltonian of the form

$$H(\mathbf{y}, \mathbf{p}, \mathbf{u}) = \mathbf{p}^T \dot{\mathbf{y}} - f_0. \quad (3.17)$$

We consider the autonomous problem defined by 3.1, 3.3, 3.5. Then we can write the following theorem.

**Theorem 3.3.** (*Pontryagin Maximum Principle, L. S. Pontryagin, 1962*).

Assume  $\mathbf{u}^*$  is optimal control and  $\mathbf{y}^*$  is the corresponding trajectory. Then there exists a function  $\mathbf{p}^* : [0, t_f] \rightarrow \mathbb{R}^n$  such that

$$\dot{\mathbf{y}}^*(t) = \nabla_{\mathbf{p}} H(\mathbf{y}^*(t), \mathbf{p}^*(t), \mathbf{u}^*(t)), \quad (3.18)$$

$$\dot{\mathbf{p}}^*(t) = -\nabla_{\mathbf{y}} H(\mathbf{y}^*(t), \mathbf{p}^*(t), \mathbf{u}^*(t)), \quad (3.19)$$

and

$$H(\mathbf{y}^*(t), \mathbf{p}^*(t), \mathbf{u}^*(t)) = \max_{a \in U} H(\mathbf{y}^*(t), \mathbf{p}^*(t), a), \quad t \in [0, t_f]. \quad (3.20)$$

In addition,

$$\text{the mapping } t \rightarrow H(\mathbf{y}^*(t), \mathbf{p}^*(t), \mathbf{u}^*(t)) \text{ is constant.} \quad (3.21)$$

Finally, we have the terminal condition

$$\mathbf{p}^*(t_f) = \nabla g(\mathbf{y}^*(t_f)). \quad (3.22)$$

For proofs see for example [Evans 2000], [J. Macki 1982], [M. Athans 2007].

Next, we discuss the impact of the PMP when applied to the following bilinear control problem.

$$\begin{aligned} \text{Minimize } J &= \int_0^{t_f} f_0(\mathbf{y}) dt, \\ \text{subject to } \dot{\mathbf{y}}(t) &= \mathbf{A}\mathbf{y}(t) + \sum_{i=1}^m u_i(t) \mathbf{B}_i \mathbf{y}(t) + \tilde{\mathbf{f}}(\mathbf{y}), \quad \mathbf{y}(0) = \mathbf{0}, \end{aligned} \quad (3.23)$$

where  $\mathbf{u}(t) \in \Omega = [u_{min}, u_{max}]^m = \{\boldsymbol{\omega} \in \mathbb{R}^m : u_{min} \leq \omega_i \leq u_{max}, i = 1, \dots, m\}$ ,

moreover  $t_f$  is fixed,  $\mathbf{y}(t_f)$  is free.

While the objective functional is given as independent of control in explicit form, we can easily derive the optimal controls. Hamiltonian for the problem 3.12 is of the following form:

$$H(\mathbf{y}, \mathbf{p}, \mathbf{u}) = \mathbf{p}^T(t) \left( \mathbf{A}\mathbf{y}(t) + \sum_{i=1}^m u_i(t) \mathbf{B}_i \mathbf{y}(t) + \tilde{\mathbf{f}}(\mathbf{y}) \right) - f_0(\mathbf{y}). \quad (3.24)$$

Thus, as a result of PMP optimal control functions are bang - bang type

$$u_i^*(t) = \begin{cases} u_{max}, & \mathbf{p}^T(t) \mathbf{B}_i \mathbf{y}(t) > 0 \\ u_{min}, & \mathbf{p}^T(t) \mathbf{B}_i \mathbf{y}(t) < 0 \end{cases}, \quad (3.25)$$

where

$$\dot{\mathbf{p}}(t) = -\frac{\partial H}{\partial \mathbf{y}}, \quad \mathbf{p}(t_f) = \mathbf{0}. \quad (3.26)$$

**Remark:** We do not consider singular cases by assuming that the set of instants  $t$  such that  $\mathbf{p}^T(t) \mathbf{B}_i \mathbf{y}(t) = 0$  is a null set.

The implicit form for controls 4.5 requires solving of two point boundary value problem (TPBVP). There are two popular classes of numerical methods for solving two point boundary value problems. The first class consist of shooting methods that appear in many variants. The second class is represented by relaxation methods. In one variant of shooting methods we set unknown initial conditions as parameters to be determined, then solve the multidimensional root - finding problem so to achieve the desired values at the other boundary. As another variant of the shooting method, we guess unknown free parameters at both ends of the domain, integrate the equations to a common midpoint, and seek to adjust the guessed parameters so that the solution joins smoothly at the fitting point [W. H. Press 1992]. Relaxation methods implement another approach. The domain is represented as a set of points creating mesh. The differential equations are transformed into the finite difference equations. We start with a trial solution that consists of values for the dependent variables at each mesh point, neither satisfying the desired finite-difference equations, nor necessarily even satisfying the required boundary conditions. The iteration which in this case is called the relaxation, consists of adjusting all the values on the mesh to bring them into successively closer agreement with the finite-difference equations together with the boundary conditions. In many cases shooting and relaxation methods are applied together, where the shooting is always the first. All of the methods exhibit good performance in the case of low dimensional problems excluding solutions that are unsmooth or highly oscillatory.

### 3.5 Prediction of switchings in optimal controls

In general for multidimensional problem it is difficult to predict the structure of the solutions of 4.5. We are not able to predict whether the switchings occur, i.e. if there exists an instant  $t$  such as the term  $(\mathbf{p}^T(t) \mathbf{B}_i \mathbf{y}(t))$  changes its sign. In mechanical systems, where the damping coefficient is the parameter to be controlled and the objective is to dissipate the energy in the optimal sense, in some cases we can suspect that the best performance is exhibited by the the system steered by a constant maximum value control. So when can we expect the optimal switching control? To answer to this question let us consider the system 3.6 with  $m = 1$  for simplicity, that is

$$\dot{\mathbf{y}} = \mathbf{A}\mathbf{y} + u\mathbf{B}\mathbf{y} + \tilde{\mathbf{f}}(\mathbf{y}), \quad (3.27)$$

with the adjoint system

$$\dot{\mathbf{p}} = -\frac{\partial H(\mathbf{y}, \mathbf{p}, u)}{\partial \mathbf{y}}. \quad (3.28)$$

The following theorem is proposed by the author of this dissertation and it is the sufficient condition for existence of the control  $u^* \neq u_{max}$  that results in more beneficial value of objective functional described in 3.23.

**Theorem\* 3.4.** Let  $\mathbf{y}_{u_{max}}(t)$  and  $\mathbf{p}_{u_{max}}(t)$  be the solutions of the state 3.27 and the adjoint state 3.28 equations when the following constant control function is given  $u(t) = u_{max}$ . If there exists an interval  $[t_1, t_2] \subseteq [0, t_f]$  such that for all  $t \in [t_1, t_2]$  we have  $(\mathbf{p}_{u_{max}}^T(t) \mathbf{B} \mathbf{y}_{u_{max}}(t)) < 0$ , then there also exists a control  $u^* \in \Omega$ ,  $u^* \neq u_{max}$  such that  $J(u^*) < J(u_{max})$ .

*Proof.* Let  $u^* = u_{max} + \delta u$ . Then we can write the differential of the cost functional in the following form

$$J(u_{max} + \delta u) - J(u_{max}) = \delta J(u_{max})(\delta u) + r_J(u_{max}, \delta u), \quad (3.29)$$

where  $\delta J(u_{max})(\delta u)$  is first variation of the functional  $J(u_{max})$  and  $r_J(u_{max}, \delta u) = o(\delta u)$ , i.e.  $r_J(u_{max}, \delta u)/\|\delta u\| \rightarrow 0$  as  $\|\delta u\| \rightarrow 0$ . For a sufficiently small  $\delta u$  the sign of the right hand side of Eq.(3.29) depends on the sign of the variation. Therefore, we need to prove that  $\delta J(u_{max})(\delta u) < 0$ .

$$J = \int_0^{t_f} [f_0(\mathbf{y}) + \mathbf{p}^T (\dot{\mathbf{y}} - \mathbf{f})] dt, \quad (3.30)$$

where  $\mathbf{p} = \mathbf{p}(t) : [0, t_f] \rightarrow \mathbb{R}^n$  is the adjoint state. We introduce Hamiltonian of the standard form

$$H : \mathbb{R}^n \times \mathbb{R}^n \times \Omega \rightarrow \mathbb{R}, \quad H(\mathbf{y}, \mathbf{p}, u) = \mathbf{p}^T \mathbf{f} - f_0(\mathbf{y}), \quad (3.31)$$

$$J = \int_0^{t_f} (\mathbf{p}^T \dot{\mathbf{y}} - H) dt. \quad (3.32)$$

Infinitesimal change  $\delta u$  causes variations of the functions  $\delta \mathbf{y}(t)$ ,  $\delta \dot{\mathbf{y}}(t)$ ,  $\delta \mathbf{p}(t)$ . This results in the following variation of cost functional

$$\delta J(u)(\delta u) = \int_0^{t_f} \left\{ -\frac{\partial H}{\partial u} \delta u - \left( \frac{\partial H}{\partial \mathbf{y}} \right)^T \delta \mathbf{y} + \mathbf{p}^T \delta \dot{\mathbf{y}} + \left( \dot{\mathbf{y}} - \frac{\partial H}{\partial \mathbf{p}} \right)^T \delta \mathbf{p} \right\} dt. \quad (3.33)$$

To fulfill Eq. 3.49 the last term must be equal to zero:  $(\dot{\mathbf{y}} - \mathbf{f})^T \delta \mathbf{p} = 0$ . Now, under the assumption  $\delta \dot{\mathbf{y}} = \frac{d}{dt}(\delta \mathbf{y})$ , the integration by parts yields

$$\delta J(u)(\delta u) = \int_0^{t_f} -\frac{\partial H}{\partial u} \delta u dt - \int_0^{t_f} \left( \dot{\mathbf{p}} + \frac{\partial H}{\partial \mathbf{y}} \right)^T \delta \mathbf{y} dt + [\mathbf{p}^T \delta \mathbf{y}]_0^{t_f}. \quad (3.34)$$

The second and last term vanishes by setting

$$\dot{\mathbf{p}} = -\frac{\partial H}{\partial \mathbf{y}}, \quad \mathbf{p}(t_f) = \mathbf{0} \quad (3.35)$$

and respecting the initial boundary condition  $\delta \mathbf{y}(0) = \mathbf{0}$ . Then

$$H = \mathbf{p}^T (\mathbf{A} \mathbf{y} + u \mathbf{B} \mathbf{y} + \tilde{\mathbf{f}}(\mathbf{y})) - f_0, \quad (3.36)$$

$$\delta J(u)(\delta u) = - \int_0^{t_f} (\mathbf{p}^T \mathbf{B} \mathbf{y}) \delta u dt. \quad (3.37)$$

Next, we set the variation of control as following

$$\delta u = \begin{cases} 0, & t \in [0, t_1) \\ \varepsilon < 0, & t \in [t_1, t_2] \\ 0, & t \in (t_2, t_f]. \end{cases} \quad (3.38)$$

Then  $u^* \in \Omega$ . For such a control we conclude that

$$\forall t \in [t_1, t_2] \mathbf{p}_{u_{max}}^T(t) \mathbf{B} \mathbf{y}_{u_{max}}(t) < 0 \implies \delta J(u_{max})(\delta u) = - \int_{t_1}^{t_2} (\mathbf{p}_{u_{max}}^T(t) \mathbf{B} \mathbf{y}_{u_{max}}(t)) \varepsilon dt < 0. \quad (3.39)$$

□

The theorem 3.4 can be easily generalized to the system 3.6.

### 3.6 Functional derivative, the method of steepest descent for optimal control problem

In this section we present the numerical treatment for the optimal control problem 3.23. First we introduce the definition of the functional derivative, then the optimization procedure based on the method of steepest descent is developed.

The functional derivative is a generalization of the gradient. It carries information on how a functional changes, when the function changes by a small amount. By the definition, the functional derivative  $\delta J/\delta \mathbf{u}$  is a distribution such that the following equality holds

$$\lim_{\varepsilon \rightarrow 0} \frac{J(\mathbf{u} + \varepsilon \mathbf{h}) - J(\mathbf{u})}{\varepsilon} = \int_{\Gamma} \left( \frac{\delta J(\mathbf{u})}{\delta \mathbf{u}(t)} \right)^T \mathbf{h}(t) dt, \quad t \in \Gamma, \quad (3.40)$$

where  $\mathbf{h} = \mathbf{h}(t) : \Gamma \rightarrow \mathbb{R}^m$  is an arbitrary function. Now, we go back to the proof for the theorem 3.4, where the formula for the first variation is derived. Directly we conclude that the functional derivative is of the form

$$\frac{\delta J}{\delta \mathbf{u}} = - \frac{\partial H}{\partial \mathbf{u}}. \quad (3.41)$$

The formula 3.41 allows us to apply a first-order optimization algorithm. The gradient descent (or the steepest descent) is one of the most popular method for finding a minimum of a function (or functional). In this method one takes steps proportional to the negative of the gradient (or of the approximate gradient) of the function at the current point. For more details see for example [Snyman 2005].

Numerical computations, based on the method of steepest descent, in application to the problem 3.23 can be performed by proceeding the following steps:

- Step 1.** Guess initial control  $\mathbf{u}_0$ , set  $k \leftarrow 0$ .
- Step 2.** Solve the state equation by substituting  $\mathbf{u} = \mathbf{u}_k$ .
- Step 3.** Calculate Hamiltonian  $H(\mathbf{y}, \mathbf{p}, \mathbf{u}) = \mathbf{p}^T \dot{\mathbf{y}} - f_0$ , then solve the adjoint state by backward integration.
- Step 4.** Compute descent direction  $\mathbf{d}_k = -\frac{\delta J}{\delta \mathbf{u}} = \frac{\partial H}{\partial \mathbf{u}}$ . If  $\mathbf{d}_k = 0$ , then stop.
- Step 5.** Choose step size  $\lambda_k$  such that  $\mathbf{u}_{k+1} = \mathbf{u}_k + \lambda_k \mathbf{d}_k$  respects the constraints i.e.  $\mathbf{u}_{k+1} \in [u_{min}, u_{max}]^m$ . Optionally perform the line search by solving  $\lambda_k = \arg \min_{\lambda_k > 0} J(\mathbf{u}_k + \lambda_k \mathbf{d}_k)$ .
- Step 6.** Set  $\mathbf{u}_{k+1}(t) \leftarrow \mathbf{u}_k(t) + \lambda_k \mathbf{d}_k(t)$ ,  $k \leftarrow k + 1$ . If stop condition does not hold then go to the Step 2.

### 3.7 Numerical example: semi-active controlled oscillator

In this section we examine the gradient descent method for one of the most common semi-active optimal control problem. The object under control is the driven oscillator. As the parameter to be controlled we take the damping coefficient. The goal is to test the efficiency of the gradient descent method in the case of parametric control of the oscillating system and also to provide the comparative results for another method that will be proposed in next section.

We consider the following optimization problem:

$$\text{Minimize } J = \int_0^{t_f} \left\{ (y_1)^2 + (y_2)^2 \right\} dt$$

subject to the system

$$\begin{aligned} \dot{y}_1 &= y_2 \\ \dot{y}_2 &= -ky_1 - uy_2 + P \sin(\omega y_3) \\ \dot{y}_3 &= 1. \end{aligned}$$

$$\text{Here, } u(t) \in [u_{min}, u_{max}]$$

$$\text{and } y(t) = [y_1(t), y_2(t), y_3(t)] \subset \mathbb{R}^3, \quad y(0) = [1, -1, 0]^T, \quad t_f \text{ is fixed.} \quad (3.42)$$

The parameters are set to the following values

$$k = 1, \quad P = 5, \quad \omega = 5, \quad u_{min} = 10^{-5}, \quad u_{max} = 3.$$

For the sake of application of PMP in the standard way, the system is given in autonomous form, where the last component of the vector state represents time. Here  $f_0$  is chosen as simple quadratic form and its value is related to the total energy of the system. So, the

desired goal of the variable damping control is to provide a minimum of the integrand of the energy of the system under excitation in the specified time interval  $[0, t_f]$ . The computations are carried out for two cases, each with the different final time  $t_f = 0.67$  and  $t_f = 1$ , respectively.

The Hamiltonian for the problem 3.42 is of the form

$$H(\mathbf{y}, \mathbf{p}, u) = \begin{bmatrix} p_1 \\ p_2 \\ p_3 \end{bmatrix}^T \begin{bmatrix} y_2 \\ -ky_1 - uy_2 + P \sin(\omega y_3) \\ 1 \end{bmatrix} - (y_1)^2 - (y_2)^2. \quad (3.43)$$

Here, the adjoint system is described by the equations

$$\begin{aligned} \dot{p}_1 &= kp_2 + 2y_1 \\ \dot{p}_2 &= -p_1 + up_2 + 2y_2 \\ \dot{p}_3 &= -\omega P p_2 \cos(\omega y_3) \end{aligned} \quad (3.44)$$

and it fulfills the terminal condition  $\mathbf{p}(t_f) = \mathbf{0}$ . From PMP we immediately get the optimal control

$$u^*(t) = \begin{cases} u_{max}, & p_2 y_2 < 0 \\ u_{min}, & p_2 y_2 > 0 \end{cases}. \quad (3.45)$$

**Corollary:** The switchings occur whenever  $p_2$  or  $y_2$  change their signs. The number of switchings and instants of switchings can not be predicted by means of the solution 3.45.

Numerical treatment of the problem 3.42 is based on the procedure presented in section 3.6. Here, the descent direction is

$$d_k = -\frac{\delta J}{\delta u} = \frac{\partial H}{\partial u} = -p_2 y_2. \quad (3.46)$$

The step size is assumed to be constant for every iteration and  $\lambda_k = 1$ . The computations are terminated after performing  $k = 500$  iterations. The discrete time interval  $[0, t_f]$  is split into 500 equal subintervals. We assume the constant control for any of these subintervals. The initial control is assumed to be the constant function, set to the maximum value for all subintervals  $u_0(t) = u_{max}, \forall t \in [0, t_f]$ .

### 3.7.1 Case 1: $t_f = 0.67$

In the first case the time interval, after a few attempts, is taken to be  $[0, t_f] = [0, 0.67]$ , so to capture at least one switching in the optimal control function. The Figure 3.1 displays the trajectory of this control.

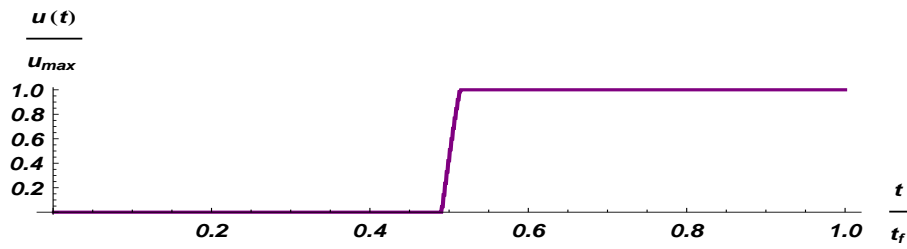


Figure 3.1: Optimized control function – the gradient method.

The clearly visible point of switching appears as the slope part of the trajectory (in the case of more precise computation the angle of slope approaches  $90^\circ$ ). The switching occurs in the instant when the trajectory of velocity changes the sign:  $y_2(t_{switch}) = 0$ . It is depicted in the Figure 3.2.

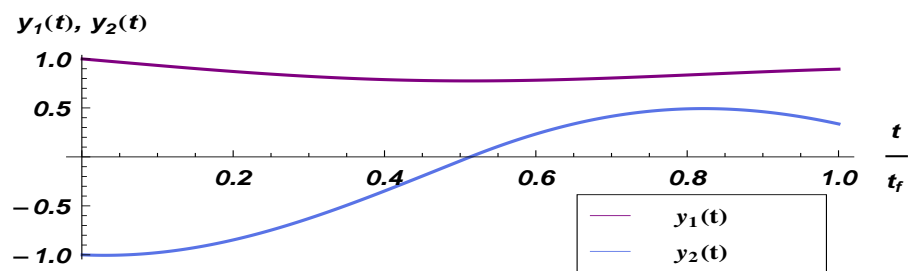


Figure 3.2: Trajectories of the optimized state.

On the other hand the trajectory of  $p_2$  (3.3) does not meet the abscissa (apart from the final zero condition). This results in only one switching during the time interval  $(0, t_f)$ .

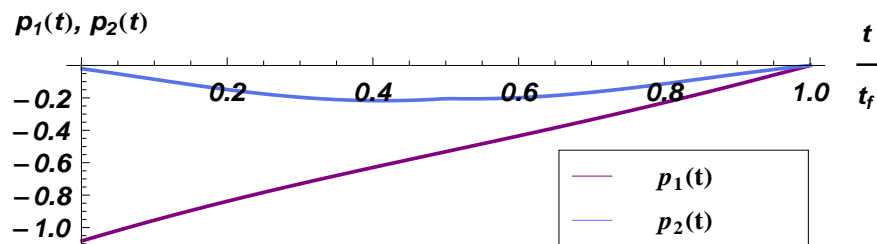


Figure 3.3: Trajectories of the optimized adjoint state.

The values of objective functional in every iteration are plotted in the Figure 3.4.

We remind that in the beginning of iterative procedure the initial control was set as  $u(t) = u_{max}$ . So, we can clearly observe the improvement from constant maximum value control by replacing it with switching one.

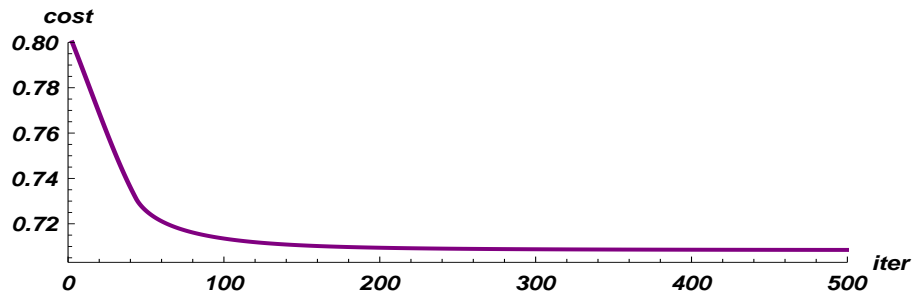


Figure 3.4: Cost functional with respect to the number of iteration.

### 3.7.2 Case 2: $t_f = 1$

In this case the time interval is assumed to be  $[0, t_f] = [0, 1]$ . It captures three switchings in the optimal control function, which is exposed in the Figure 3.5.

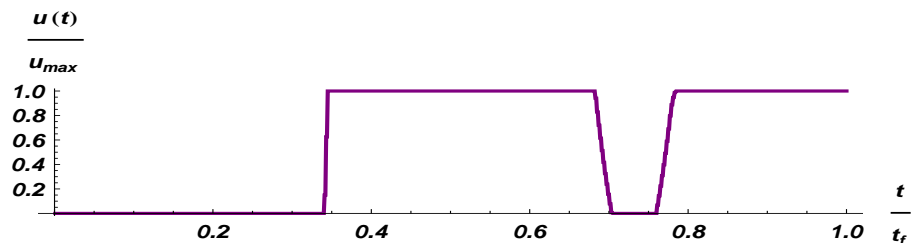


Figure 3.5: Optimized control function – the gradient method.

The first and the third switchings are caused by changing the sign of velocity  $y_2$  (Figure 3.6), while the second one results from the crossing the abscissa by trajectory  $p_2$  (Figure 3.7).

In the Figure 3.8 the objective functional with respect to number of iteration is presented. The rate of convergence in the presented cases is very satisfactory, even if the line search method is not applied. The computations were performed on the standard PC (Intel Pentium Core 2) and it took less then 180 seconds for any of presented examples.

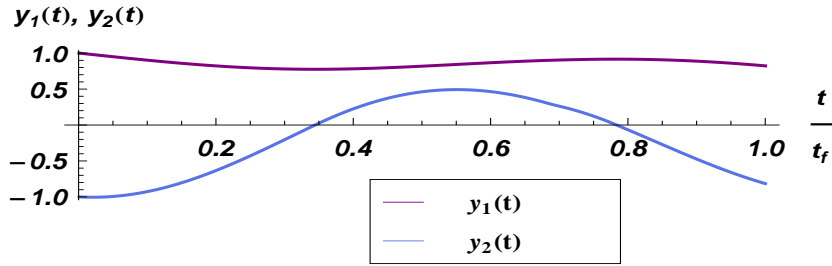


Figure 3.6: Trajectories of the optimized state.

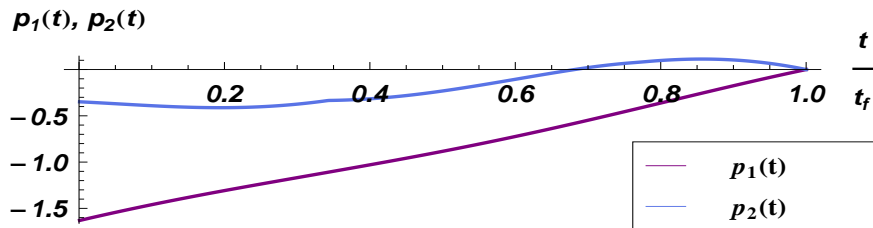


Figure 3.7: Trajectories of the optimized adjoint state.

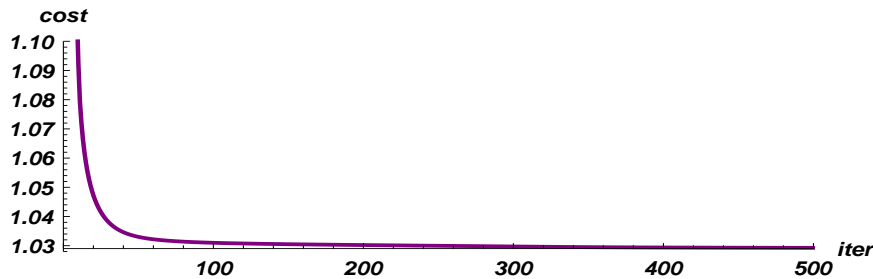


Figure 3.8: Cost functional with respect to the number of iteration.

For convenience we call the presented method as *the gradient method* in contrast to the method presented in the following section, which is called *the switching times method*.

### 3.8 The method of parameterized switching times

In the example presented in the previous section we observe that the numerical results coincide with the theoretical predictions. The postulated switching nature of optimized control is confirmed. In the case of more complex systems we expect difficulties in obtaining

so accurate, switching shaped, numerical solutions. Increasing precision of calculations is associated with higher dimensional optimization problem, which turns in the rapid extension of time required for computations. There is a need to use more efficient numerical algorithm for computing the optimal switching control solutions. For this purpose it is very intuitive to parameterize the switching times and reformulate the minimization problem. The objective functional is now optimized with respect to new parameters - the switching times. So, in fact, the optimal control problem becomes a nonlinear programming problem, where gradient and non-gradient optimization methods can be applied.

In this section we develop the method of parameterized switching times which is based on the derivative of objective functional with respect to these times. In calculations we use the fundamental facts from the calculus of variations as well as the property of Dirac delta function. After derivation, the complete numerical algorithm is given.

We again investigate the bilinear control systems given in autonomous form (the last term of state vector stands for time)

$$\dot{\mathbf{y}} = \mathbf{A}\mathbf{y} + \sum_{i=1}^m u_i \mathbf{B}_i \mathbf{y} + \tilde{\mathbf{f}}(\mathbf{y}). \quad (3.47)$$

For simplicity let us consider system driven by only one switching control

$$u = u_{max} \mathcal{U}(t - \tau), \quad \tau \in [0, t_f]. \quad (3.48)$$

Here,  $\mathcal{U}$  stands for the unit step function. Thus, system 3.47 can be rewritten as follows

$$\dot{\mathbf{y}} = \mathbf{f}(\mathbf{y}, \tau) = \mathbf{A}\mathbf{y} + u_{max} \mathcal{U}(t - \tau) \mathbf{B}\mathbf{y} + \tilde{\mathbf{f}}(\mathbf{y}). \quad (3.49)$$

Here, again  $\mathbf{y} = \mathbf{y}(t) : [0, t_f] \rightarrow \mathbb{R}^n$ ,  $y_n(t) = t$ ,  $f = f(\mathbf{y}, \tau) : \mathbb{R}^n \times [0, t_f] \rightarrow \mathbb{R}^n$ . Next, we introduce the cost functional to be minimized

$$J = \int_0^{t_f} f_0 dt, \quad (3.50)$$

where  $f_0 = f_0(\mathbf{y}) : \mathbb{R}^n \rightarrow \mathbb{R}$  and  $t_f$  is fixed. The cost functional subjected to system governed by 3.49 can be rewritten as follows

$$J = \int_0^{t_f} [f_0 + \mathbf{p}^T (\dot{\mathbf{y}} - \mathbf{f})] dt. \quad (3.51)$$

where  $\mathbf{p} = \mathbf{p}(t) : [0, t_f] \rightarrow \mathbb{R}^n$  is the adjoint state. The Hamiltonian for the considered problem is of the form

$$H : \mathbb{R}^n \times \mathbb{R}^n \times [0, t_f] \rightarrow \mathbb{R}, \quad H(\mathbf{y}, \mathbf{p}, \tau) = \mathbf{p}^T \mathbf{f} - f_0. \quad (3.52)$$

Inserting the Hamiltonian into the formula for the objective functional we get

$$J = \int_0^{t_f} (\mathbf{p}^T \dot{\mathbf{y}} - H) dt. \quad (3.53)$$

Infinitesimal change  $d\tau$  causes variations of the functions  $\delta\mathbf{y}(t)$ ,  $\delta\dot{\mathbf{y}}(t)$ ,  $\delta\mathbf{p}(t)$ . This results in the following variation of the cost functional

$$\delta J = \int_0^{t_f} \left\{ -\frac{\partial H}{\partial \tau} d\tau - \left( \frac{\partial H}{\partial \mathbf{y}} \right)^T \delta\mathbf{y} + \mathbf{p}^T \delta\dot{\mathbf{y}} + \left( \dot{\mathbf{y}} - \frac{\partial H}{\partial \mathbf{p}} \right)^T \delta\mathbf{p} \right\} dt. \quad (3.54)$$

To fulfill Eq. 3.49 the last term must be equal to zero  $(\dot{\mathbf{y}} - \mathbf{f}) \delta\mathbf{p} = \mathbf{0}$ . Now, under the assumption  $\delta\dot{\mathbf{y}} = \frac{d}{dt}(\delta\mathbf{y})$ , the integration by parts yields

$$\delta J = \int_0^{t_f} -\frac{\partial H}{\partial \tau} d\tau dt - \int_0^{t_f} \left( \dot{\mathbf{p}} + \frac{\partial H}{\partial \mathbf{y}} \right)^T \delta\mathbf{y} dt + [\mathbf{p}^T \delta\mathbf{y}]_0^{t_f}. \quad (3.55)$$

The second and last terms in 3.55 vanish by using the definition for adjoint state, respecting its final condition

$$\dot{\mathbf{p}} = -\frac{\partial H}{\partial \mathbf{y}}, \quad \mathbf{p}(t_f) = \mathbf{0} \quad (3.56)$$

and also regarding the initial boundary condition  $\delta\mathbf{y}(0) = \mathbf{0}$ . For small  $d\tau$  we can now use the approximation

$$\Delta J \approx \delta J = - \int_0^{t_f} \frac{\partial H}{\partial \tau} d\tau dt = \left( - \int_0^{t_f} \frac{\partial H}{\partial \tau} dt \right) d\tau. \quad (3.57)$$

This implies that the total derivative of the objective functional with respect to switching time fulfills the following equation

$$\frac{\partial J}{\partial \tau} = - \int_0^{t_f} \frac{\partial H}{\partial \tau} dt. \quad (3.58)$$

Hamiltonian for the system 3.49 takes the following form

$$H = \mathbf{p}^T \left( \mathbf{A}\mathbf{y} + u_{max} \mathcal{U}(y_n - \tau) \mathbf{B}\mathbf{y} + \tilde{\mathbf{f}}(\mathbf{y}) \right) - f_0. \quad (3.59)$$

Then, the approximated gradient of the cost functional is

$$\frac{\partial J}{\partial \tau} = - \int_0^{t_f} \mathbf{p}^T(t) \mathbf{B}\mathbf{y}(t) \frac{\partial [u_{max} \mathcal{U}(t - \tau)]}{\partial \tau} dt. \quad (3.60)$$

Finally we get

$$\frac{\partial J}{\partial \tau} = u_{max} \int_0^{t_f} \mathbf{p}^T(t) \mathbf{B}\mathbf{y}(t) \delta(t - \tau) dt = u_{max} \mathbf{p}^T(\tau) \mathbf{B}\mathbf{y}(\tau). \quad (3.61)$$

Now, we consider the next switching action defined by the control

$$\bar{u} = u_{max} \mathcal{U}(t) - u_{max} \mathcal{U}(t - \bar{\tau}), \quad \tau \in [0, t_f]. \quad (3.62)$$

Following the previous procedure we immediately get the gradient of the cost functional with respect to the switching time  $\bar{\tau}$

$$\frac{\partial J}{\partial \bar{\tau}} = -u_{max} \mathbf{p}^T(\bar{\tau}) \mathbf{B}\mathbf{y}(\bar{\tau}). \quad (3.63)$$

To summarize the obtained results, the switching actions and the appropriate gradients are listed below:

$$\begin{aligned} \text{Switching action}(t = \tau) : \quad & [\text{off}] \longrightarrow [\text{on}], \quad \frac{\partial J}{\partial \tau} = u_{max} \mathbf{p}^T(\tau) \mathbf{B} \mathbf{y}(\tau), \\ \text{Switching action}(t = \bar{\tau}) : \quad & [\text{on}] \longrightarrow [\text{off}], \quad \frac{\partial J}{\partial \bar{\tau}} = -u_{max} \mathbf{p}^T(\bar{\tau}) \mathbf{B} \mathbf{y}(\bar{\tau}). \end{aligned} \quad (3.64)$$

Alternate methods for computation of switching times were presented by R. Mohler [Mohler 1973] and C.Y. Kaya together with J.L. Noakes [Kaya 1996].

Before the computational algorithm is developed, the number of controls  $m$  is presumed. Next, for such controls we assume  $n$  to be the number of switching actions  $[\text{off}] \rightarrow [\text{on}]$  or  $[\text{on}] \rightarrow [\text{off}]$ . Therefore, we can collect the switching times into two matrices:  $\tau = [\tau_{i,j}]_{m \times n}$ ,  $\bar{\tau} = [\bar{\tau}_{i,j}]_{m \times n}$ , where  $\{\tau_{i,j}\}$  and  $\{\bar{\tau}_{i,j}\}$  are increasing sequences with respect to  $j$ , where for every pair  $(i, j)$  we have  $\tau_{i,j} \in [0, t_f]$ ,  $\bar{\tau}_{i,j} \in (0, t_f]$ . Moreover we assume that  $\tau_{i,j} < \bar{\tau}_{i,j}$  for all  $i, j$ . The state equation is then of the form

$$\dot{y} = Ay + u_{max} \sum_{i=1}^m \sum_{j=1}^n [\mathcal{U}(t - \tau_{i,j}) - \mathcal{U}(t - \bar{\tau}_{i,j})] B_i y + \tilde{f}(y). \quad (3.65)$$

The computational algorithm based on the predefined gradient method compounds of the following steps:

- Step 1.** Guess initial matrices  $[\tau_{i,j}]$  and  $[\bar{\tau}_{i,j}]$ .
- Step 2.** Solve the state equation 3.65 by substituting  $[\tau_{i,j}]$  and  $[\bar{\tau}_{i,j}]$ .
- Step 3.** Calculate Hamiltonian 3.52, then solve the adjoint state 3.56 by backward integration.
- Step 4.** Compute the derivatives 3.67 for all components of switching time matrices.
- Step 5\*.** Modify time switching matrices by using first-order optimization algorithm.
- Step 6.** Check whether switching times  $\tau_{i,j}$  or  $\bar{\tau}_{i,j}$  extend their limited values 0 or  $t_f$ , respectively. If so, then set these switchings to appropriate infimum or supremum of the set  $[0, t_f]$  and then go to the Step 2.
- Step 7.** Check if length of any of interval  $[\tau_{i,j}, \bar{\tau}_{i,j}]$  approaches zero. If so, discard those switching time, resize the matrices  $[\tau_{i,j}]$ ,  $[\bar{\tau}_{i,j}]$  and go back to the Step 2.
- Step 8.** Repeat the Steps 2-7 until the defined stop condition is fulfilled.

**Remark:** The Step 5\* can be proceed in analogy to Step 5 in the algorithm presented in the section 3.6, where the control vector is now replaced by the components of matrices  $[\tau_{i,j}]$  and  $[\bar{\tau}_{i,j}]$ .

The approach presented in this section is not limited to the bilinear systems only. As soon as the controls are assumed to be bang - bang or the bang - bang type resulting from the PMP, the problem of finding the required controls becomes one of finding switching times.

### 3.9 Switching times method - numerical examples

In this section the method of parameterized switching times is applied to the optimal control problem formulated in the section 3.7. The goal is to examine the performance of the switching method as well as to provide the comparative results to these obtained by using previously investigated gradient method.

Assuming  $[\tau_{1,j}]$  and  $[\bar{\tau}_{1,j}]$  as the switching time matrices, the Hamiltonian for the system described in 3.42 can be written in the form

$$\begin{aligned}
 H(\mathbf{y}, \mathbf{p}, \boldsymbol{\tau}, \bar{\boldsymbol{\tau}}) = & \begin{bmatrix} p_1 \\ p_2 \\ p_3 \end{bmatrix}^T \begin{bmatrix} y_2 \\ -ky_1 + P \sin(\omega y_3) \\ 1 \end{bmatrix} + \\
 & + \begin{bmatrix} p_1 \\ p_2 \\ p_3 \end{bmatrix}^T \begin{bmatrix} 0 \\ -y_2 \\ 0 \end{bmatrix} u_{max} \sum_{j=1}^n [\mathcal{U}(t - \tau_j) - \mathcal{U}(t - \bar{\tau}_j)] - (y_1)^2 - (y_2)^2.
 \end{aligned} \tag{3.66}$$

Thus, the derivatives of cost functional with respect to switching times are

$$\begin{aligned}
 \text{Switching action}(t = \tau) : \quad & [\text{off}] \longrightarrow [\text{on}], \quad \frac{\partial J}{\partial \tau} = -u_{max} p_2(\tau) y_2(\tau), \\
 \text{Switching action}(t = \bar{\tau}) : \quad & [\text{on}] \longrightarrow [\text{off}], \quad \frac{\partial J}{\partial \bar{\tau}} = u_{max} p_2(\bar{\tau}) y_2(\bar{\tau}).
 \end{aligned} \tag{3.67}$$

Numerical computations are performed on the discretized time interval  $[0, t_f]$ , that is split into 1000 equal subintervals. As the first order optimization method, used in Step 5\* in algorithm 3.8, the gradient descent is applied. The stepsize  $\lambda_k$  is chosen in such a way, that for every iteration the inequality holds  $\lambda_k d_k \geq [0, t_f]/1000$ . This condition provides modification of elements of  $\boldsymbol{\tau}$  and  $\bar{\boldsymbol{\tau}}$  in every iteration. The computation stops when all components of  $\boldsymbol{\tau}$  and  $\bar{\boldsymbol{\tau}}$  oscillate between two nearest values of the discretized time domain.

#### 3.9.1 Case 1: $t_f = 0.67$

Likewise in the section 3.7 we first consider the problem in the time interval  $[0, t_f] = [0, 0.67]$ . The computations are performed for two cases, each with the different initial

matrices: (case A)  $\tau = 0.1 t_f$ ,  $\bar{\tau} = 0.9 t_f$ , (case B)  $\tau = 0.7 t_f$ ,  $\bar{\tau} = 0.8 t_f$ . The length of matrices is assumed on the basis of results obtained by gradient method.

The Figure 3.9 displays switching times convergence. The point of convergence is the same for both cases A and B.

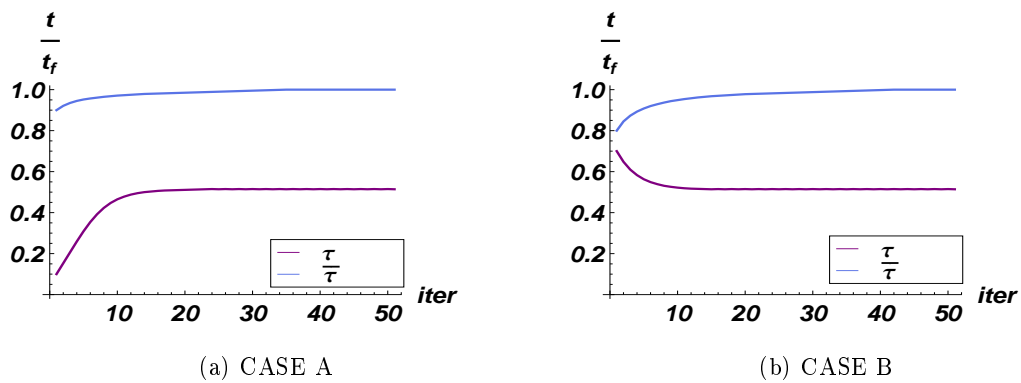


Figure 3.9: Switching time values with respect to the number of iteration.

The optimized control trajectory is show in the Figure 3.10.

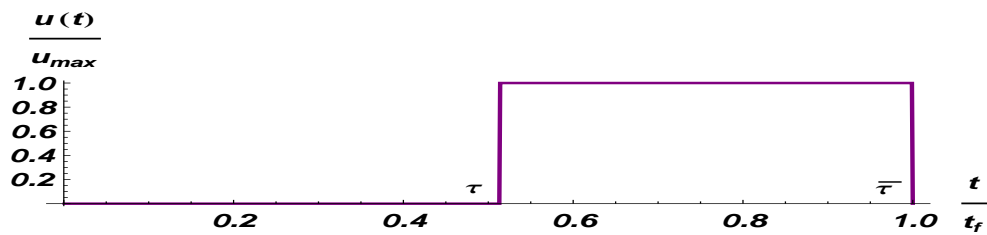


Figure 3.10: Optimized control function – the switching times method.

Comparing the solution obtained by the gradient method 3.1, we observe, that the instant of switching denoted as  $\tau$  is equal to the coordinate of the middle point of the slope in 3.1. Thus, the coincidence of the results is very high.

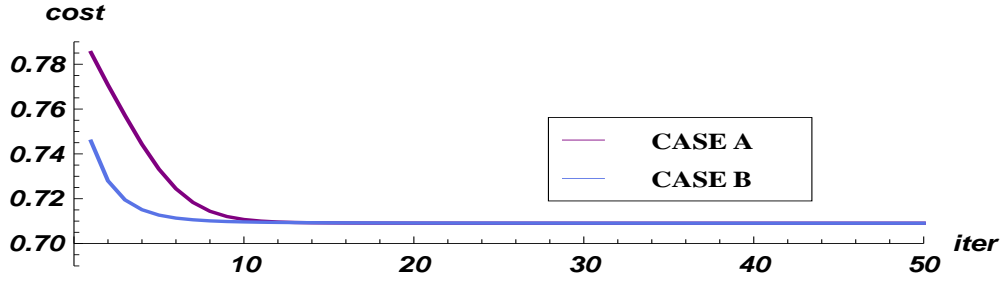


Figure 3.11: Cost functional with respect to the number of iteration.

In the Figure 3.11 we present the evolution of the objective functional in the iterative process. Finally, the Figure 3.12 demonstrates the optimized state and adjoint trajectories:  $y_1(t)$ ,  $y_2(t)$  and  $p_1(t)$ ,  $p_2(t)$ , respectively.

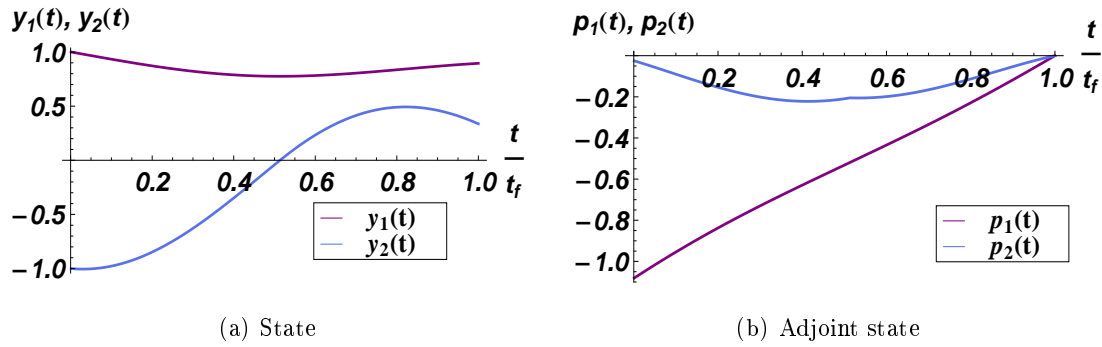


Figure 3.12: Optimized state and adjoint state trajectories.

### 3.9.2 Case 2: $t_f = 1$

In the second case, the initial switching matrices are assumed to be  $\tau = [0.4t_f, 0.8t_f]$ ,  $\bar{\tau} = [0.6t_f, 0.9t_f]$ . The evolution of the switching times and objective functional in the iterative process is exposed in the Figure 3.9.2.

In the Figure 3.14 the trajectory of optimized switching control is depicted. The coincidence with 3.5 is clearly visible.

In order to check the correctness of the algorithm 3.8 computations were also performed with larger size of initial matrices  $\tau$ ,  $\bar{\tau}$ . In each of presented cases the algorithm forced discarding of extra switchings. While the proper sizes of initial matrices are assumed, the time required for computation is reduced more then five times in comparison to the gradient method.

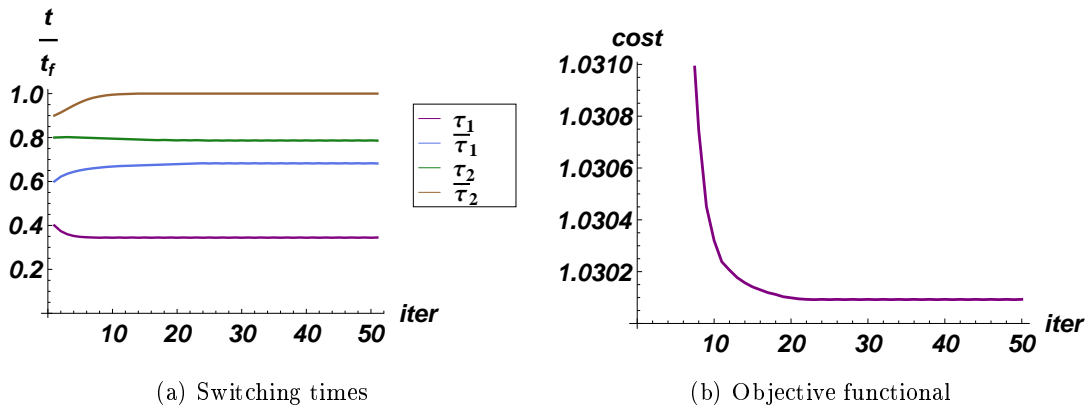


Figure 3.13: Switching times and cost functional with respect to the number of iteration.

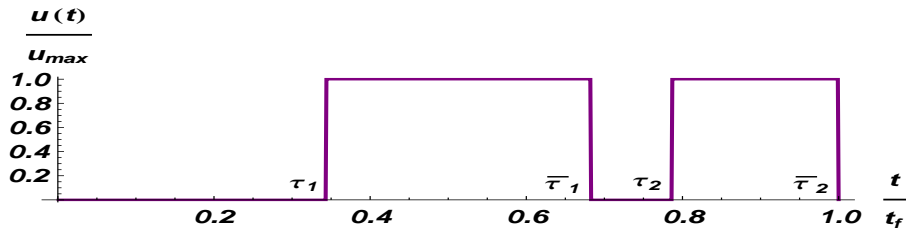


Figure 3.14: Optimized control function – the switching times method.

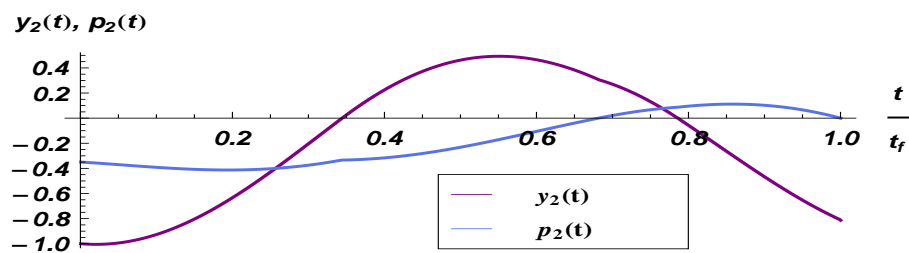


Figure 3.15: Optimized state and adjoint state trajectories.

For comparison the state and adjoint trajectories are presented in the Figure 3.15.

---

In this chapter the problem of optimal control of bilinear systems has been considered. Application of the first order necessary optimality condition has enabled us to characterize the general structure of optimal solutions. The optimal controls are bang-bang type. To obtain the optimal solutions one has to solve the difficult multidimensional TPBVP. Thus, the problem has to be treated numerically. Two different methods based on the gradients has been applied to the simple oscillator problem. The numerical results show that the switching times methods can be very efficient if the proper number of switchings is assumed.

---

## Optimization of moving load trajectories via semi-active control method

### Contents

- 4.1 Optimal control problem formulation**
- 4.2 Numerical optimization methods in the semi-active controlled elastic systems**
- 4.3 The total number of semi-active dampers**
- 4.4 The placement of semi-active dampers**
- 4.5 The velocity of a travelling load**
- 4.6 Initially deflected beam**
- 4.7 Double beam system**

This chapter is devoted to optimization problems in the semi-active controlled elastic systems. The aim is to provide shapes of the optimal control functions as well as quantitative results that may be directly used in further design of control systems. The investigations are based on the models and computational tools presented during two previous chapters. The control method that is proposed has to meet the two following important conditions: it has to be safety and the resulting control system has to outperform the passive system. Typically, the optimal switching pattern results in a large number of switching events. If an error occurs and the switching pattern is shifted in the time domain, then such a complicated control may immediately drive the system to an undesired or even unstable state. Therefore, it is desirable to reduce the number of switching events.

The chapter is organized as follows: In the first section the optimal control problem for the straight line passage of a moving load is formulated. Then, the gradient method

and the switching times method is applied to solve the posed problem. A short divagation on the relevant number of switchings is also provided. Next, in order to demonstrate how different parameters of the system effect the quality of the proposed control methods, a number of numerical examples is given. Finally, the two particular cases are considered.

## 4.1 Optimal control problem formulation

In this section we formulate the optimal control problem which corresponds to the problem of finding the straight line passage of a moving load upon an elastic one-dimensional body. The form of the cost functional is assumed. Then, in order to derive the optimal controls the Pontryagin Maximum Principle is applied. Finally, the adjoint system is written.

As the representative example of elastic one-dimensional body we consider the Euler-Bernoulli beam. The objective is to reduce the total deflection of a travelling load. The cost functional can be written as the  $L^2$  norm of the deflection function i. e. of the form

$$J = \langle w(vt, t) | w(vt, t) \rangle = \int_0^{t_f} [w(vt, t)]^2 dt. \quad (4.1)$$

Thus, the optimal control problem can be written as the following:

$$\begin{aligned} \text{Minimize } & J = \int_0^{t_f} [w(vt, t)]^2 dt, \\ \text{subject to } & \begin{cases} EI \frac{\partial^4 w(x, t)}{\partial x^4} + \mu \frac{\partial^2 w(x, t)}{\partial t^2} = - \sum_{i=1}^m u_i(t) \frac{\partial w(x, t)}{\partial t} \delta(x - a_i) + P \delta(x - vt), \\ w(x = 0, t) = 0, \quad w(x = l, t) = 0, \quad \left( \frac{\partial^2 w(x, t)}{\partial x^2} \right)_{|x=0}, \quad \left( \frac{\partial^2 w(x, t)}{\partial x^2} \right)_{|x=l}, \\ w(x, t = 0) = 0, \quad \dot{w}(x, t = 0) = 0, \end{cases} \\ \mathbf{u}(t) \in \Omega & = [u_{min}, u_{max}]^m. \end{aligned} \quad (4.2)$$

The equivalent optimization problem, but given in the state space representation (as reported in Section 2.7), can be rewritten in the form:

$$\begin{aligned} \text{Minimize } & J = \int_0^{t_f} \left[ \frac{l}{2} \sum_{k=1}^{n/2} y_{2k-1}(t) \sin \left( \frac{k\pi v y_{n+1}(t)}{l} \right) \right]^2 dt, \\ \text{subject to } & \dot{\mathbf{y}}(t) = \mathbf{A}\mathbf{y}(t) + \sum_{i=1}^m u_i \mathbf{B}_i \mathbf{y}(t) + \mathbf{f}(\mathbf{y}), \\ \mathbf{u}(t) \in \Omega & = [u_{min}, u_{max}]^m. \end{aligned} \quad (4.3)$$

For such a problem we write the Hamiltonian as the following

$$H(\mathbf{y}, \mathbf{p}, \mathbf{u}) = \mathbf{p}^T \left( \mathbf{A}\mathbf{y}(t) + \sum_{i=1}^m u_i \mathbf{B}_i \mathbf{y}(t) + \mathbf{f}(\mathbf{y}) \right) - \left[ \frac{l}{2} \sum_{k=1}^{n/2} y_{2k-1}(t) \sin \left( \frac{k\pi v y_{n+1}(t)}{l} \right) \right]^2. \quad (4.4)$$

The problem 4.3 is analogous with the one presented in the Chapter 3. The application of PMP yields the optimal control functions of the bang-bang type

$$u_i^*(t) = \begin{cases} u_{max}, & \mathbf{p}^T(t) \mathbf{B}_i \mathbf{y}(t) > 0 \\ u_{min}, & \mathbf{p}^T(t) \mathbf{B}_i \mathbf{y}(t) < 0 \end{cases}. \quad (4.5)$$

Here the adjoint system is given in the following form

$$\dot{\mathbf{p}} = -\frac{\partial H}{\partial \mathbf{y}} = -\mathbf{p}^T \left( \mathbf{A} + \sum_{i=1}^m u_i \mathbf{B}_i + \frac{\partial \mathbf{f}}{\partial \mathbf{y}} \right) + \frac{\partial \left\{ \left[ \frac{l}{2} \sum_{k=1}^{n/2} y_{2k-1}(t) \sin \left( \frac{k\pi v y_{n+1}(t)}{l} \right) \right]^2 \right\}}{\partial \mathbf{y}} \quad (4.6)$$

and it fulfils the terminal condition:  $\mathbf{p}(t_f) = 0$ . The adjoint state is a necessary component for numerical procedures used for solving the optimal control problems presented later in the work.

## 4.2 Numerical optimization methods in the semi-active controlled elastic systems

In this section we apply the numerical optimization methods (presented in the Chapter 3) to the elastic semi-active controlled system. We define the Euler-Bernoulli beam as the representative elastic body for numerical investigations. Next we solve the optimal control problem 4.3 by using both the gradient method and the switching times method (for Matlab code see the Appendix B). The goal is to establish the relevant number of switching actions to achieve good performance of resulting control system. Reduction in the number of switchings is beneficial for two reasons: the system is less sensitive for errors and the time required for computations is significantly shortened. The comparison of cost values obtained by different methods is presented in the end of the section.

It must be mentioned here that the gradient method used in this work leads to a local optima that refer to sub-optimal solutions. The assumption that has to be made is that the objective functional is locally convex with respect to control functions. By the optimization we mean the process of searching for the solution that for some objective is better than one taken as initial value in the optimization process. In fact, in this work we look for the solutions that outperform the passive cases. Thus, it is reasonable to assume the passive cases as the initial values in the optimization procedures.

We consider the system as showed in the Figure 2.1. We assume the following elastic body: HE - A 300A steel beam (according to DIN 1025 and Euronorm 53 – 62). The constants for the beam are as follows: the length  $l = 24$  m, the mass density  $\mu = 88.3$  kg/m, the bending stiffness  $EI = 38.3 \cdot 10^6$  Nm<sup>2</sup> ( $E = 210 \cdot 10^9$  Pa). The force  $P = 10^4$  N travels with the velocity  $v = 0.7c$ , where  $c = (\pi/l)\sqrt{EI/\mu}$  is the critical speed (In this case  $c = 86.2$  m/s). In the computations the following placements of the two active dampers are established:  $0.33l, 0.66l$ . For every damper the value of variable damping coefficient belongs to the set:  $[u_{min}, u_{max}] = [10^3, 5 \cdot 10^5]$  Ns/m. 10 first modes are taken into account in computations.

### 4.2.1 The passive cases

In this section we execute the simulations of the system 2.1 in the case of constant controls. The purpose is to show that among the passive cases the control functions which values are set to  $u_{max}$  exhibit the best efficiency for the straight line passage of a moving load. Thus, in further investigations it is reasonable to compare the trajectories driven by these best passive controls with the variable control functions obtained by optimization. For simplicity we assume here that all controls are set to the same value. The simulation are performed for the following cases:  $u_1 = u_2 = 0.25u_{max}, u_1 = u_2 = 0.5u_{max}, u_1 = u_2 = 0.75u_{max}, u_1 = u_2 = u_{max}$ . The results are presented in the Figure 4.1.

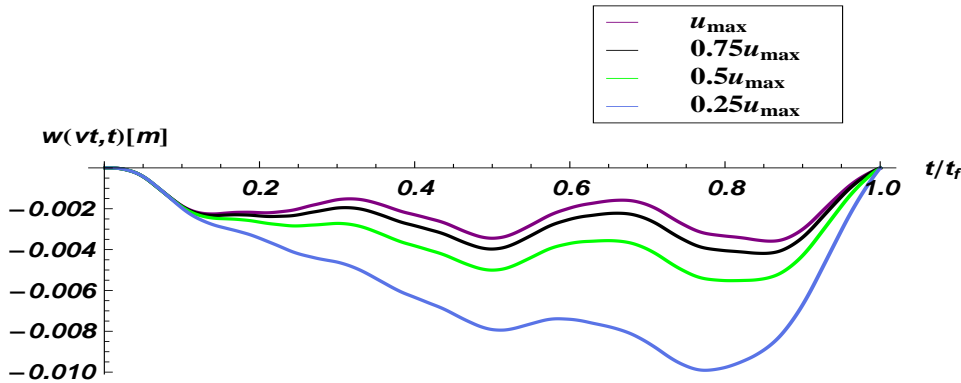


Figure 4.1: Comparison of moving load trajectories driven by constant controls.

### 4.2.2 The gradient method

In this part the problem 4.3 is solved by using the gradient method (Procedure 3.6 presented in the Chapter 3). In the computation we assume a constant value for  $\lambda_k$  for every iteration. The discrete time interval  $[0, t_f]$  is split into 1000 equal subintervals. We assume the constant control for any of these subintervals. The initial controls are set to the

maximum values for all subintervals  $u_i^{initial}(t) = u_{max}$  ( $i = 1, 2$ ),  $\forall t \in [0, t_f]$ . This refers to the passive case. The computations are terminated after performing  $k = 200$  iterations.

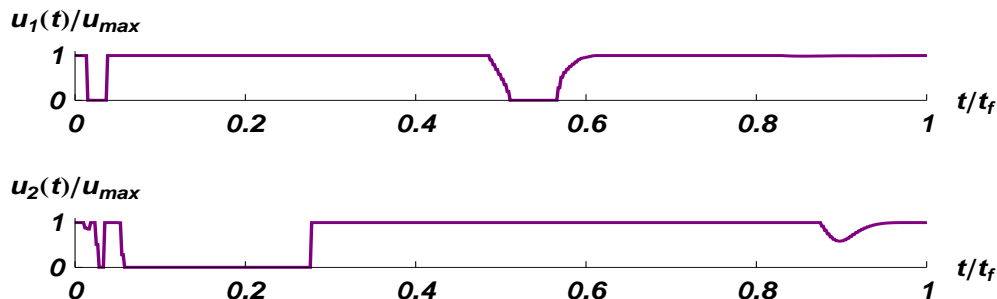


Figure 4.2: Control functions - optimized by using the gradient method.

The optimized controls are demonstrated in the Figure 4.2. Some minor numerical errors occur. However, the switching shapes of the control functions can be clearly noticed. For more precise results one should incorporate the line search method for optimization of values  $\lambda_k$ .

When observing the optimized controls one can distinguish four switchings for control  $u_1$  and two major switching actions for control  $u_2$ . This information is crucial when the switching times method is applied.

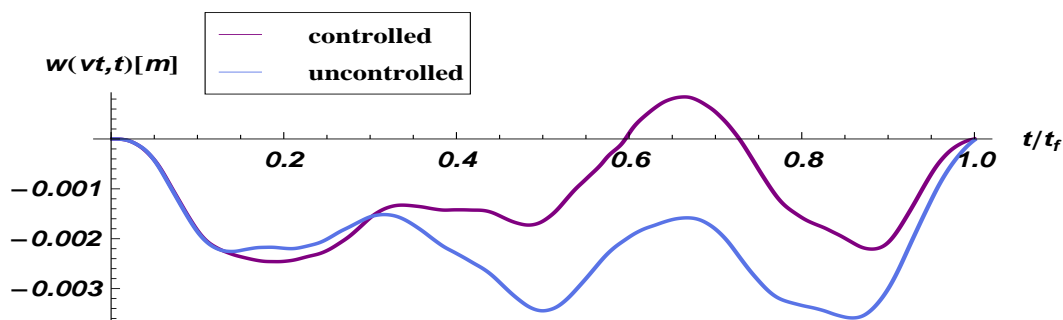


Figure 4.3: Moving load trajectories—optimized by using the gradient method.

In the Figure 4.3 we demonstrate the optimized moving load trajectory (*controlled*). It is compared with the *uncontrolled* case i. e. when the system is driven by constant controls  $u_i(t) = u_{max}$  ( $i = 1, 2$ ),  $\forall t \in [0, t_f]$ . The *uncontrolled* trajectory is typical for the moving load when transversing the span supported with passive dampers. The clearly visible local maximas, that occur near the following instants:  $t = 0.33t_f$  and  $t = 0.66t_f$ , are the evidence of presence of supports. In the *controlled* case these maximas are shifted

toward the line  $w = 0$  along with the whole trajectory.

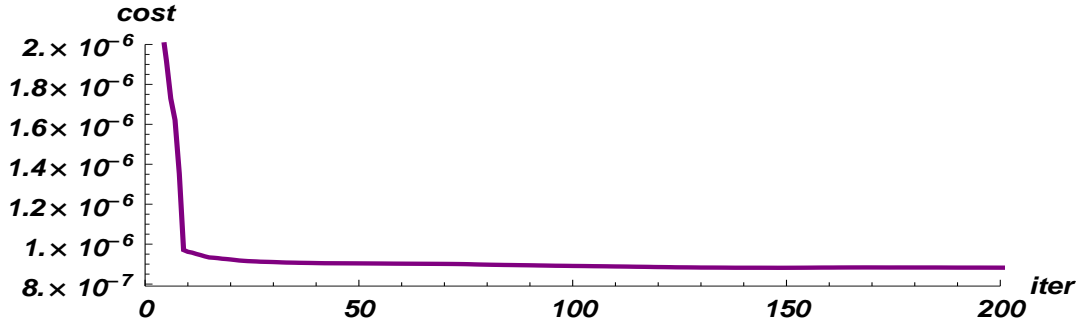


Figure 4.4: The cost functional values versus iteration in the case of the gradient method.

The values of the cost functional are presented in the Figure 4.4. The *controlled* case clearly outperforms the *uncontrolled* one (*uncontrolled* state is set for the first iteration in the optimizing operation). The time required for computation did not extend 500 seconds (PC, Intel Pentium Core 2).

### 4.2.3 The switching times method

The optimal control problem 4.3 is now solved by using the switching times method. We assume four switching actions for every control and then apply the Procedure 3.8 presented in the Chapter 3. As in the case of the gradient method the discrete time interval  $[0, t_f]$  is split into 1000 equal subinterval and the computations are terminated after performing  $k = 200$  iterations. The initial values for switching times matrices are assumed as follows:

$$[\tau_{i,j}] = t_f \cdot \begin{bmatrix} 0.01 & 0.5 \\ 0.1 & 0.7 \end{bmatrix}, \quad [\bar{\tau}_{i,j}] = t_f \cdot \begin{bmatrix} 0.2 & 0.8 \\ 0.5 & 0.9 \end{bmatrix}. \quad (4.7)$$

The Figures 4.5, 4.6 show the switching times as a function of iteration.

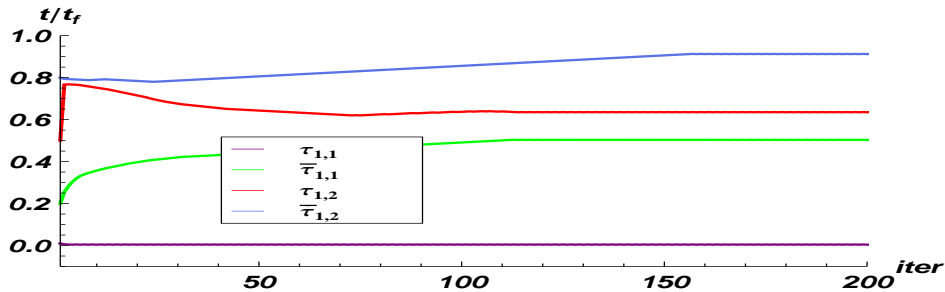


Figure 4.5: Switching times versus iteration for the control function  $u_1$ .

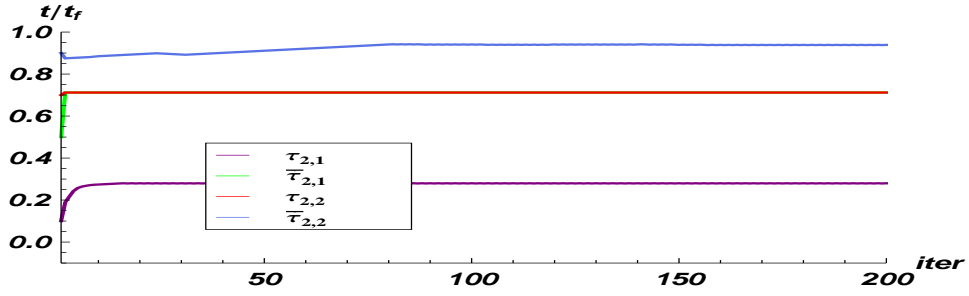


Figure 4.6: Switching times versus iteration for the control function  $u_2$ .

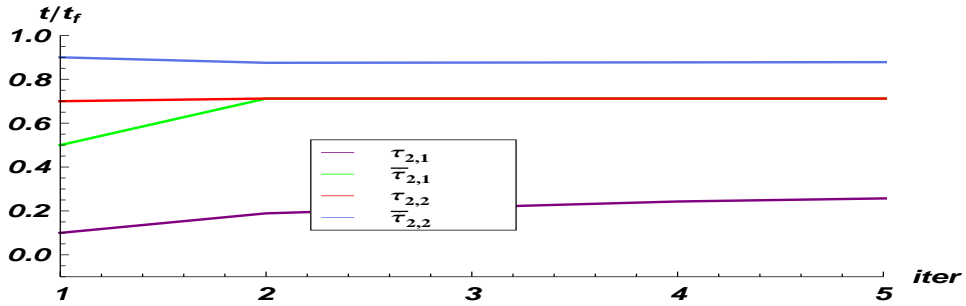


Figure 4.7: Switching times versus iteration for the control function  $u_2$  (zoomed version).

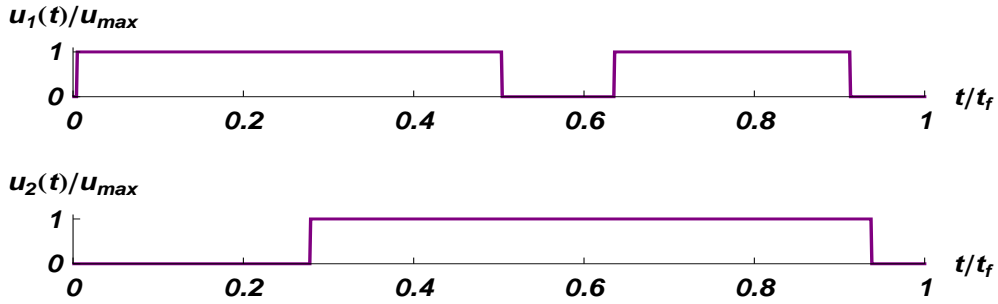


Figure 4.8: Control functions—optimized by using the switching times method.

In order to highlight how  $\bar{\tau}_{2,1}$  coincide with  $\tau_{2,2}$  below we plot (Figure 4.7) the zoomed version of the Figure 4.6. As a result of this coincidence the switchings are discarded. Finally, it is found approximately that  $\mathbf{u}^T = [u_{min}, u_{min}]$  on  $[0, 0.001)t_f$ ,  $\mathbf{u}^T = [u_{max}, u_{min}]$  on  $[0.001, 0.28)t_f$ ,  $\mathbf{u}^T = [u_{max}, u_{max}]$  on  $[0.28, 0.51)t_f$ ,  $\mathbf{u}^T = [u_{min}, u_{max}]$  on  $[0.51, 0.63)t_f$ ,  $\mathbf{u}^T = [u_{max}, u_{max}]$  on  $[0.63, 0.91)t_f$ ,  $\mathbf{u}^T = [u_{min}, u_{max}]$  on  $[0.91, 0.94)t_f$ ,  $\mathbf{u}^T = [u_{min}, u_{min}]$

on  $[0.94, 1)t_f$ . This is depicted in the Figure 4.8. When omitting narrow strips in the controls obtained by using the gradient methods one can find that the shapes of 4.2 and 4.8 concur.

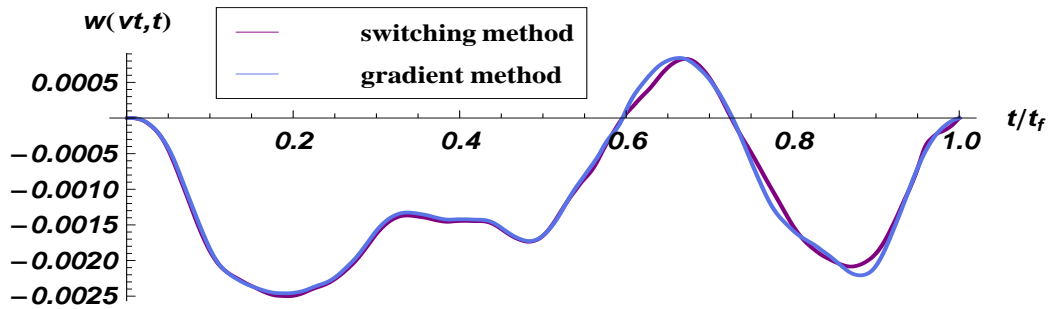


Figure 4.9: Optimized moving load trajectories. Gradient method versus switching times method.

The Figure 4.9 displays a comparison of two optimized moving load trajectories. The coincidence of the results is very high.

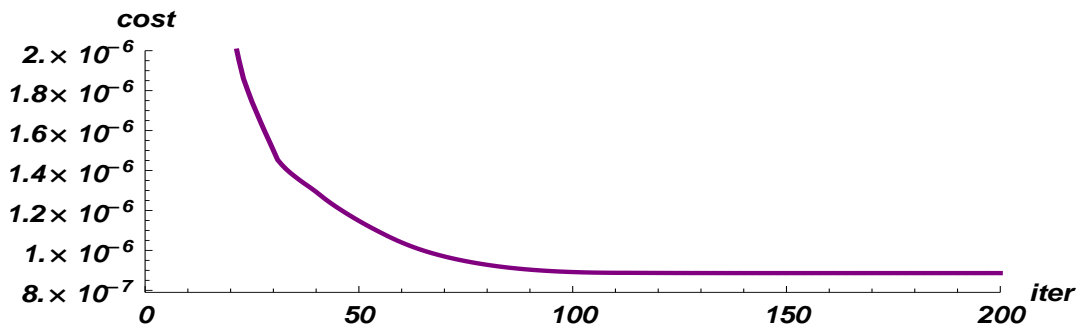


Figure 4.10: The cost functional values versus iteration in the case of the switching times method.

In the Figure 4.10 we present the evolution of the objective functional in the iterative process. The time required for computations is approximately five to twenty times shorter than in case of the gradient method. This is an obvious result of the size of the optimization problem. In the case of the switching times method the size was equal to 8 in contrast to the gradient method where the size was equal to 1000 for the same optimal control problem.

Now we can pose the following question: what is the impact of further limitation in switching actions on the performance of the control system? To answer to this question let us consider the same optimal control problem 4.3, however this time any of the control

function switches only twice. We assume the following initial values for switching times vectors:

$$[\tau_{i,j}] = t_f \cdot \begin{bmatrix} 0.1 \\ 0.5 \end{bmatrix}, \quad [\bar{\tau}_{i,j}] = t_f \cdot \begin{bmatrix} 0.8 \\ 0.9 \end{bmatrix}. \quad (4.8)$$

The evolution of the switching times in the iterative process is demonstrated in the Figures 4.11, 4.12.

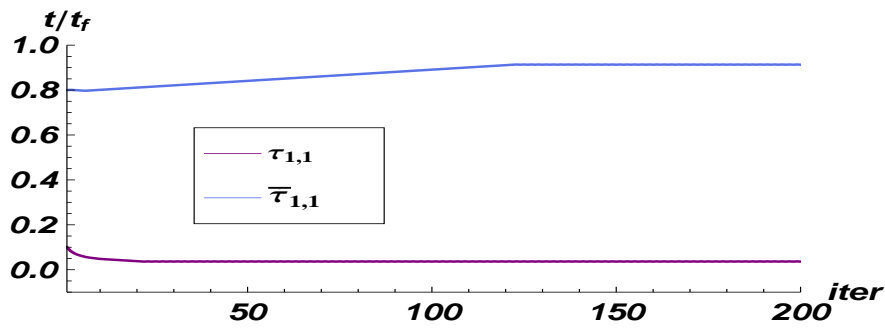


Figure 4.11: Switching times versus iteration for the control function  $u_1$ .

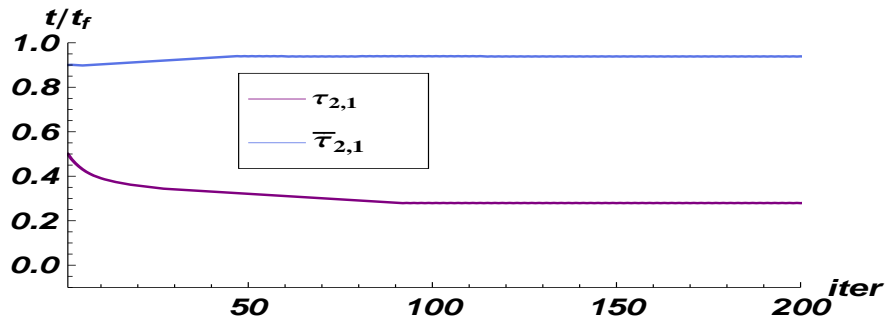


Figure 4.12: Switching times versus iteration for the control function  $u_2$ .

In this case no switching is discarded. The controls and resulting trajectory are presented in the Figures 4.13 and 4.14, respectively. In comparison with the previous example now the control  $u_1$  is simplified while the shape of  $u_2$  is retained with the high accuracy.



Figure 4.13: Control functions—optimized by using the switching times method.

The most important thing in this result is that the intuitive prediction of the shapes of controls, as presented in the first Chapter (please see the Figure 1.1(b)), are now confirmed by the numerical solution. The left damper is activated as the first, then it is also turned off before the right damper.

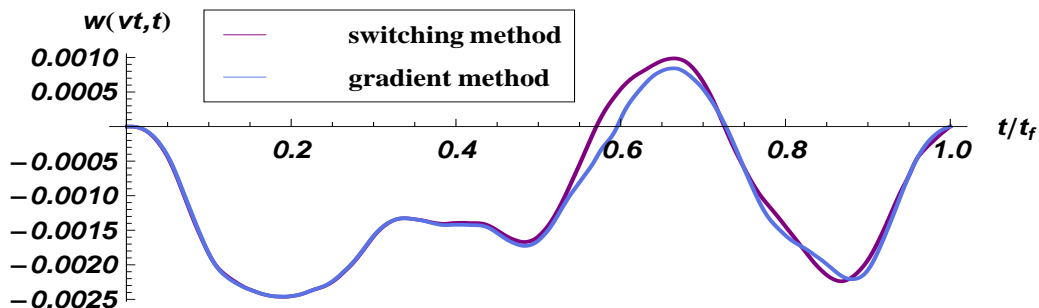


Figure 4.14: The cost functional values versus iteration in case of the switching times method.

To summarize the results we list the final cost values obtained by every of the methods in the Table 4.2.3. The best efficiency, measured as the cost value for optimized trajectory, is performed for the control computed by the gradient method. The system steered by the switching controls where the number of switchings is equal to 2 (SW. T. METHOD (2)) exhibits comparable result with the variant of four switching actions (SW. T. METHOD (4)). Any of the presented control methods outperforms the uncontrolled case. From now, if this is not specified, all of the examples are computed by using the switching times method where two switchings for every control are assumed.

Table 4.1: Cost values comparison.

uncontrolled	controlled	controlled	controlled
	Gr. Method	Sw. T. Method (4)	Sw. T. Method (2)
$0.2167 \cdot 10^{-5}$	$0.0875 \cdot 10^{-5}$	$0.0883 \cdot 10^{-5}$	$0.0886 \cdot 10^{-5}$

Base on the presented numerical results we can conclude this section with the following statement:

*Let us consider the problem of straight line passage of the moving load upon the elastic beam. Then the following statement is true: For a wide range of system parameters there exists at least one semi-active switching control method such that it outperforms the best passive case. The near optimal solution requires a finite number of switchings for every control.*

### 4.3 The total number of semi-active dampers

In this section we try to answer to the following question: how the number of semi-active dampers effects on quality of the proposed control method? We assume the speed of a moving load then we solve the optimal control problem 4.3 in four different cases, where the number of semi-active dampers is set to 3, 5, 7 and 12, respectively. The measure of the quality of the proposed switching control method is the fraction of cost values computed for two cases: *controlled/uncontrolled*. All parameters are adopted as in the previous example. Positions of  $m$  dampers are assumed according the following formula:  $a_i = i l / (m + 1)$ .

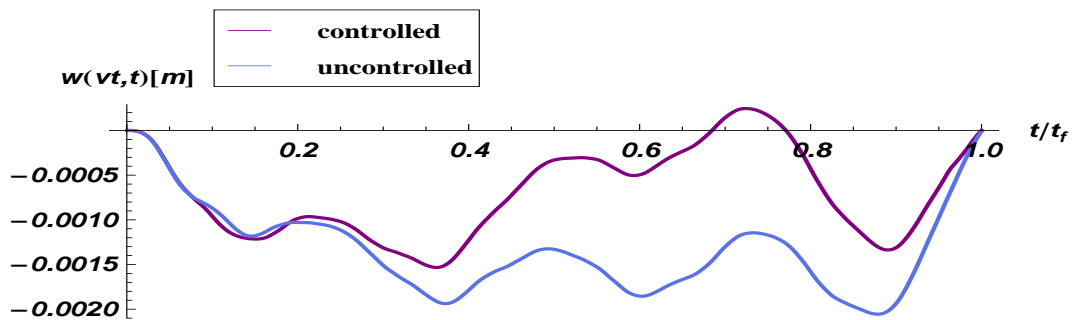


Figure 4.15: Moving load trajectories in the case of 3 semi-active dampers.

The optimized (*controlled*) and *uncontrolled* trajectories for the case of 3, 5, 7 and 12 dampers are demonstrated in the Figures 4.15, 4.16, 4.17 and 4.18, respectively. For optimized control functions please see the Appendix A.

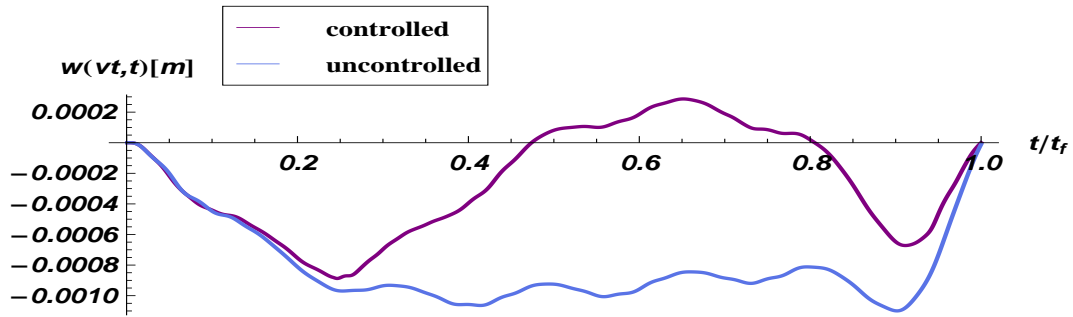


Figure 4.16: Moving load trajectories in the case of 5 semi-active dampers.

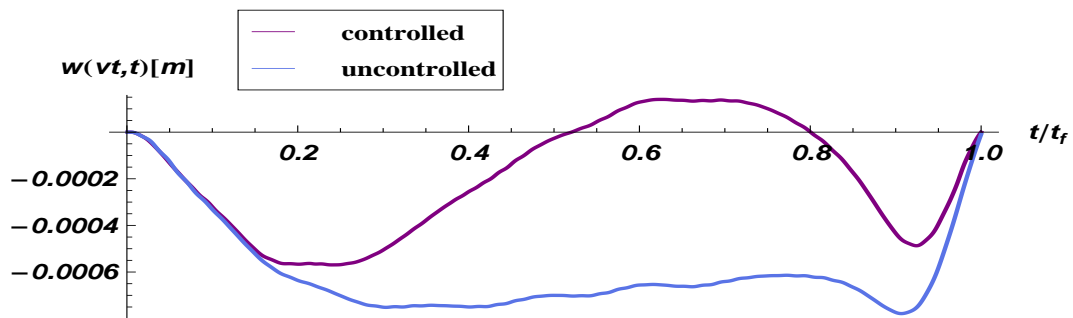


Figure 4.17: Moving load trajectories in the case of 7 semi-active dampers.

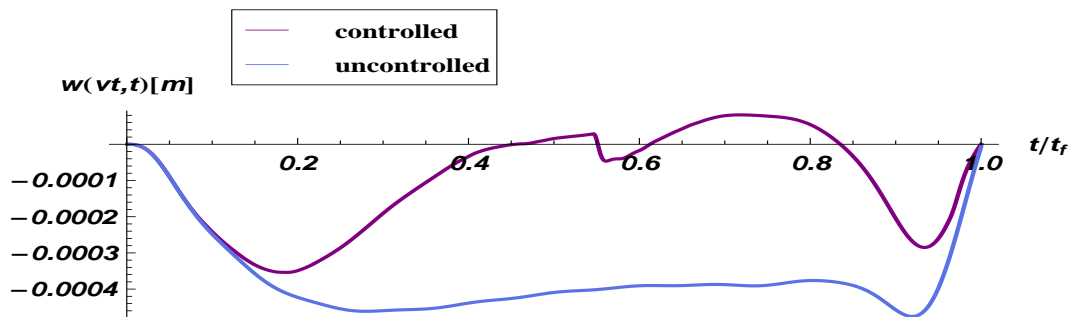


Figure 4.18: Moving load trajectories in the case of 12 semi-active dampers.

Table 4.2: Cost values comparison.

total nr. of dampers	uncontrolled	controlled	c/uc
3	$0.0795 \cdot 10^{-5}$	$0.0291 \cdot 10^{-5}$	0.36
5	$0.2851 \cdot 10^{-6}$	$0.0740 \cdot 10^{-6}$	0.26
7	$0.1556 \cdot 10^{-6}$	$0.0385 \cdot 10^{-6}$	0.24
12	$0.5848 \cdot 10^{-7}$	$0.1106 \cdot 10^{-7}$	0.19

The cost values are summarized in the Table 4.2. The best value of the assumed measure of control quality (*controlled/uncontrolled* denoted by  $c/uc$ ) is exhibited in the case of 12 semi-active dampers. This conclusion suggests that a dense distribution of dissipators may result in precisely straight passage of a moving load. In practical design such a system could be represented as so called sandwich beam-two parallel beams filled with magneto-rheological (MR) fluid. Sandwich beams have been previously investigated by some authors. In the paper [V. Rajamohan 2010] an optimal control strategy based on linear quadratic regulator is formulated to suppress the vibrations of the beam. Further investigation of the switching control method in application to sandwich beam systems seems to be very valuable and it is dedicated to future works.

The following statement concludes this section:

*Total number of semi-active dampers significantly affects the quality of the switching control method. Dense distribution of controlled dampers gives an excellent opportunity to realize precisely straight passage of a moving load.*

#### 4.4 The placement of semi-active dampers

To demonstrate how the placement of dampers affects the control efficiency, we assume two controlled dampers and then compare the following three cases:  $[0.3333l, 0.6666l]$ ,  $[0.31l, 0.69l]$ ,  $[0.36l, 0.64l]$ , where the values in parenthesis indicate the placements of dampers. The results are summarized in the Table 4.3. The comparison of optimized (*controlled*) trajectories for the considered cases are presented in the Figure 4.19. There is no control action on the third mode in the first case (for the explanation please see the Equation 2.14).

It seems intuitive that the best control capability is achieved when  $\sin \frac{k\pi a_i}{l} \neq 0$  for the first few modes i.e.  $k = 1, 2, 3$ . However, in some cases the better effect could be obtained by letting a certain mode to stay out of the suspension to increase its velocity. Then it might beneficially affect other modes by the higher rate of damping force. This phenomenon is confirmed by numerical results.

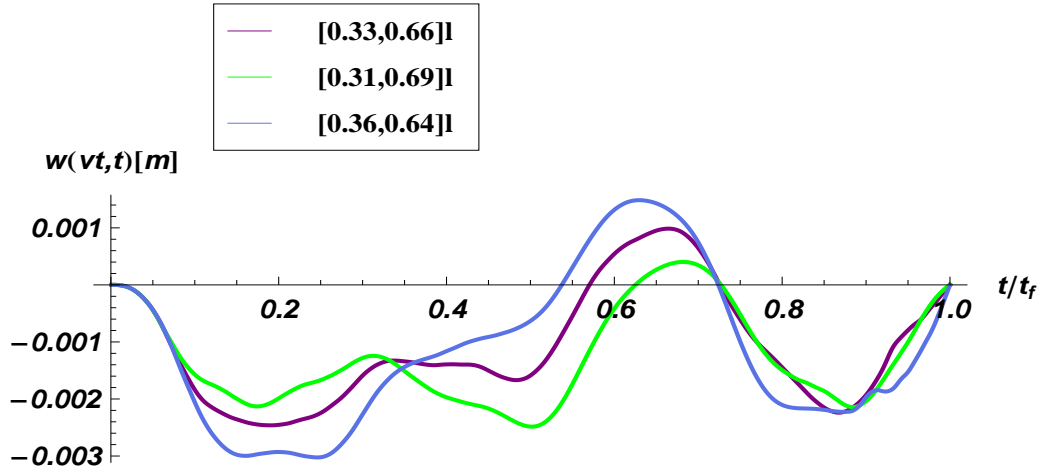


Figure 4.19: Deflection trajectories for different placement of dampers for the case  $v=0.7c$  with two active dampers

Table 4.3: Cost values comparison.

position vector	uncontrolled	controlled	$c/uc$
$[0.3333, 0.6666]l$	$0.2287 \cdot 10^{-5}$	$0.0883 \cdot 10^{-5}$	0.38
$[0.31, 0.69]l$	$0.2372 \cdot 10^{-5}$	$0.0926 \cdot 10^{-5}$	0.39
$[0.36, 0.64]l$	$0.2268 \cdot 10^{-5}$	$0.1229 \cdot 10^{-5}$	0.54

In the Table 4.3 one can find that the best efficiency of control method is exhibited for the case where  $\sin \frac{k\pi a_i}{l} = 0$  for  $k=3$ . The complete analysis how the placement of dampers affects the control efficiency needs further detailed study. Its high complication rate is associated with conjugate structure of ODEs that describe the physical system. More extensive investigation is addressed in future research.

## 4.5 The velocity of a travelling load

The velocity of a moving load significantly affects the dynamics of the whole system. The effect of turning the beam around its center of gravity (please see the Figure 1.1(b)) is clearly observable when the speed of moving load is high enough. In most cases this speed should satisfy the following inequality:  $v > 0.3c$  ( $c$  denotes the critical speed). For such a travel at the first stage we are able to produce the temporal increment of displacements on the right hand part of the beam. This increment provides the straight line passage at the second stage.

The purpose of this section is to answer to the following question: What is the travel speed that allows us to efficiently control the passage trajectory? We consider the following velocity range:  $v \in [0.1c, 0.99c]$ . For such a range we proceed the optimization of the passage trajectories. The measure used to assess the performance of the control method is the same as used in the previous examples (The fraction of cost values computed for two cases: *controlled/uncontrolled*).

In the computations five semi-active dampers are assumed. The numerical results are presented for the three cases  $v = 0.1c$ ,  $v = 0.5c$  and  $v = 0.9c$ , respectively. The cost values comparison, extended by three additional cases, is presented in the Table A.1. The discussion is provided in the end of the section.

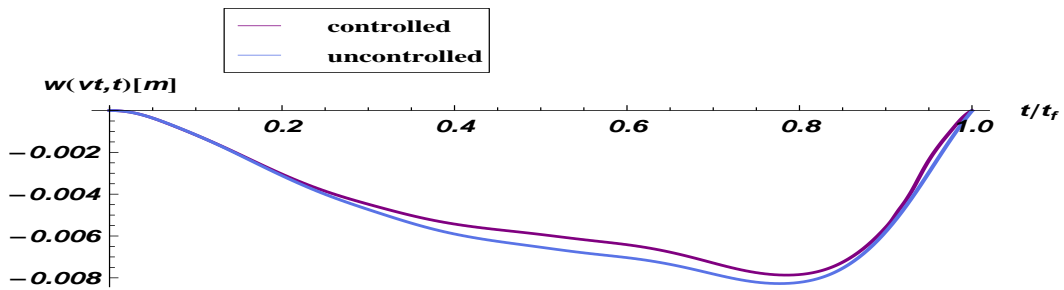


Figure 4.20: Moving load trajectories in the case of  $v = 0.1c$ .

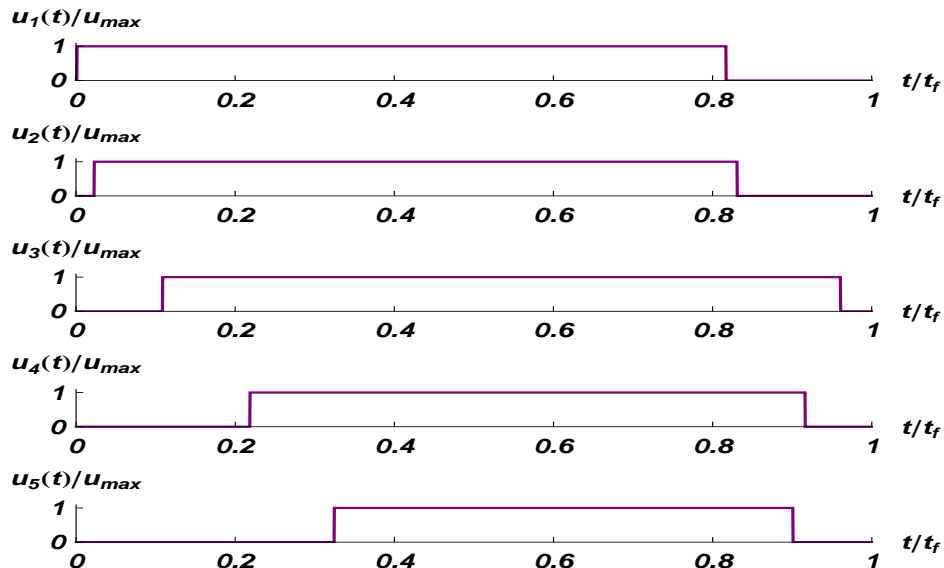


Figure 4.21: Control functions in the case of  $v = 0.1c$ .

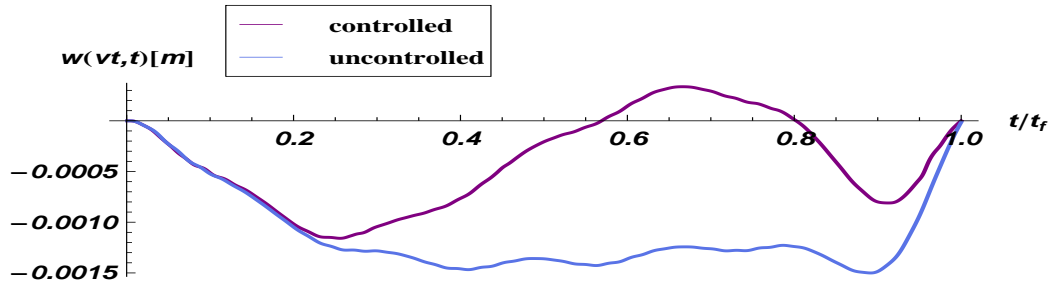


Figure 4.22: Moving load trajectories in the case of  $v = 0.5c$ .

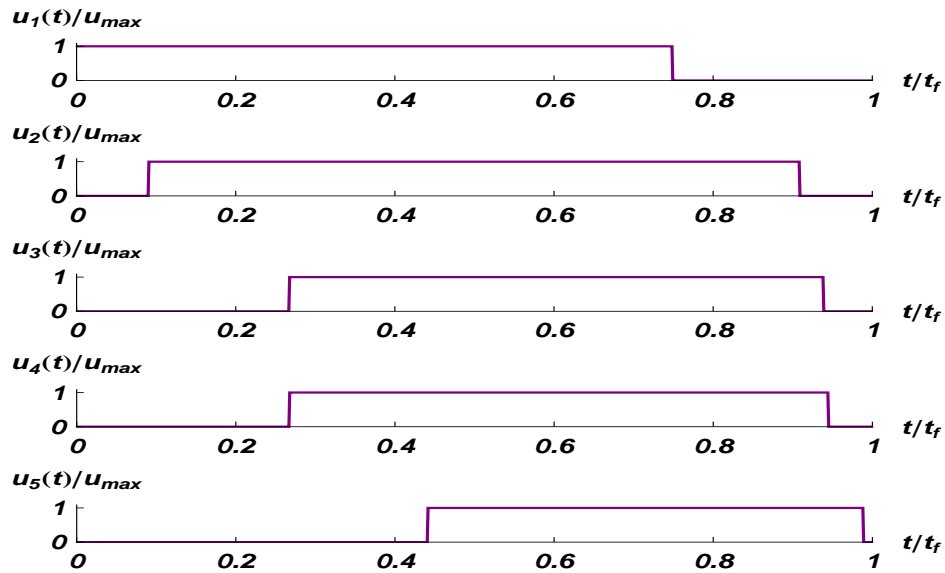


Figure 4.23: Control functions in the case of  $v = 0.5c$ .

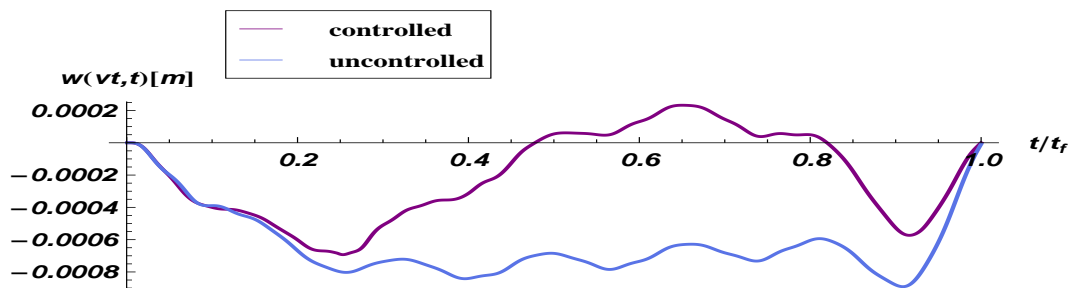


Figure 4.24: Moving load trajectories in the case of  $v = 0.9c$ .

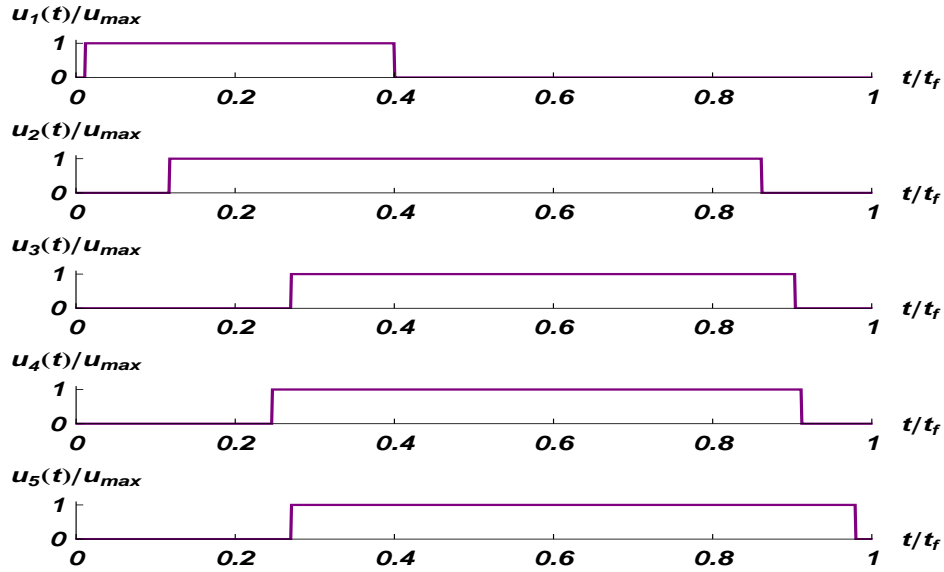
Figure 4.25: Control functions in the case of  $v = 0.9c$ .

Table 4.4: Cost values comparison.

velocity	uncontrolled	controlled	$c/uc$
$v = 0.1c$	$0.8972 \cdot 10^{-4}$	$0.7819 \cdot 10^{-4}$	0.87
$v = 0.3c$	$0.3630 \cdot 10^{-5}$	$0.1545 \cdot 10^{-5}$	0.42
$v = 0.5c$	$0.7812 \cdot 10^{-6}$	$0.2343 \cdot 10^{-6}$	0.30
$v = 0.75c$	$0.2323 \cdot 10^{-6}$	$0.0680 \cdot 10^{-6}$	0.29
$v = 0.9c$	$0.1369 \cdot 10^{-6}$	$0.0383 \cdot 10^{-6}$	0.28
$v = 0.99c$	$0.1031 \cdot 10^{-6}$	$0.0271 \cdot 10^{-6}$	0.26

For more comparative results please see the Appendix A.

The main corollary which arises from the analysis of the numerical results is that the efficiency of the control methods strictly increases while increasing the velocity of the passage. This confirms the previous statement that the dynamical effects, that enable us to design an effective control method, rise together with the speed of the travel. The optimized trajectory for the case of  $v = 0.1c$  (please see the Figure 4.20) poorly outperforms the uncontrolled case while in the case of high speed travel  $v = 0.9c$  the cost value is reduced nearly four times (please see the Figure 4.24).

It is interesting to observe the shapes of the optimized control functions when increasing the travel velocity. This is more noticeable in the case of multiple dampers (please see the Appendix A) that the width of the rectangles decreases. This fact may be very important for the practical reason. For more please see the Chapter 5.

The conclusion for this section is as follows:

*The velocity of a moving load significantly affects the behaviour of the semi-active control system. The proposed switching control method exhibits the best efficiency in the case of high speed passage. The regularity in the structure of control functions may have a very important practical aspect.*

## 4.6 Initially deflected beam

In this section we consider the system with initially deflected Euler-Bernoulli beam as demonstrated in the Chapter 2. The optimal control problem is solved for two cases, each with different shape of the initial deflection. The comparison of the cost values, presented at the end of the section, manifest the high efficiency of the method.

In this thesis the shapes of the initial curves are adopted intuitively. The goal is to enhance the straight line passage. However, it must be noticed here, that the moving load trajectories strictly depends on the velocity of the passage. Thus, the initial shape should be selected individually for every case. Further optimization of the shapes is not of the scope of this dissertation and it is dedicated to future works.

We consider the following optimal control problem:

$$\begin{aligned}
 \text{Minimize } J &= \int_0^{t_f} [w(vt, t)]^2 dt = \int_0^{t_f} [\bar{w}(vt, t) + w_0(vt)]^2 dt, \\
 \text{subject to } &\begin{cases} EI \frac{\partial^4 \bar{w}(x, t)}{\partial x^4} + \mu \frac{\partial^2 \bar{w}(x, t)}{\partial t^2} = - \sum_{i=1}^m u_i(t) \frac{\partial \bar{w}(x, t)}{\partial t} \delta(x - a_i) + P \delta(x - vt), \\ \bar{w}(x = 0, t) = 0, \quad \bar{w}(x = l, t) = 0, \quad \left( \frac{\partial^2 \bar{w}(x, t)}{\partial x^2} \right)_{|x=0}, \quad \left( \frac{\partial^2 \bar{w}(x, t)}{\partial x^2} \right)_{|x=l}, \\ \bar{w}(x, t = 0) = 0, \quad \dot{\bar{w}}(x, t = 0) = 0. \end{cases} \\
 \mathbf{u}(t) \in \Omega &= [u_{min}, u_{max}]^m.
 \end{aligned} \tag{4.9}$$

The problem is analogous to the problem described by the Equation 4.2, but now the initial deflection, denoted by  $w_0$ , is taken into account.

### 4.6.1 Case 1: The first mode

In the first case we assume the following curve for the initial deflection:

$$w_0(x) = 0.0007 \sin \left( \frac{1\pi x}{l} \right). \tag{4.10}$$

The magnitude of the sine function is assumed so to shift the whole moving load trajectory near the abscissa. The optimized (*controlled*) moving load trajectories are depicted in the Figure 4.26.

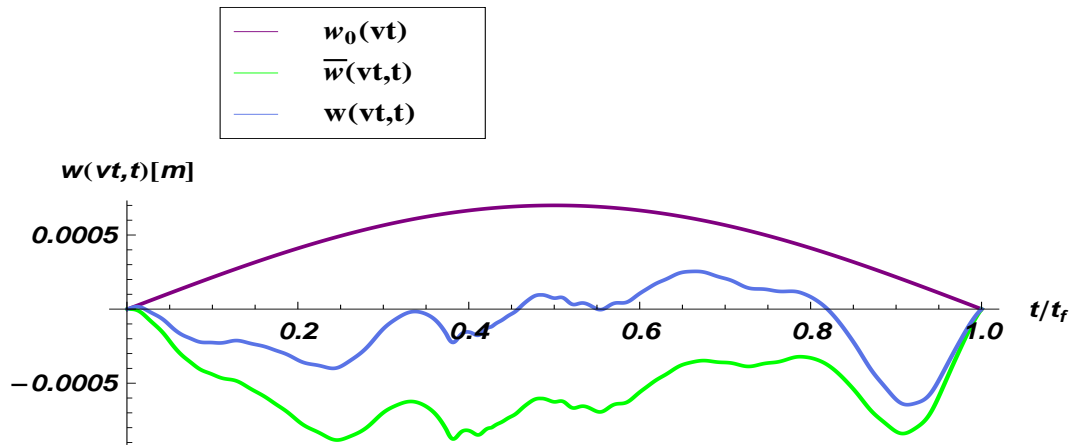


Figure 4.26: Deflection trajectories for the case  $v = 0.7c$  with five active dampers and the initial deflection.

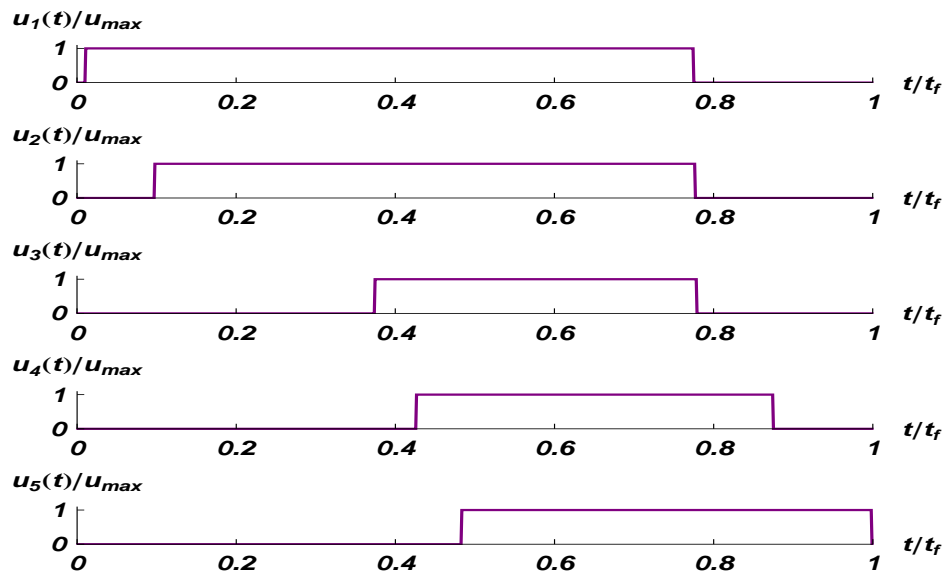


Figure 4.27: Control functions.

The presence of the initial deflection results in satisfactory straight moving load trajectory. However, clear visible extremes at the positions:  $0.21t/t_f$ ,  $0.9t/t_f$  are not significantly

shifted upwards. The introduction of the additional modes into the initial curve may efficiently reduce these extremes. The optimized controls are presented in the Figure 4.27. What is interesting, the general switching patten is preserved. The dampers placed on the left are set to maximum value as first.

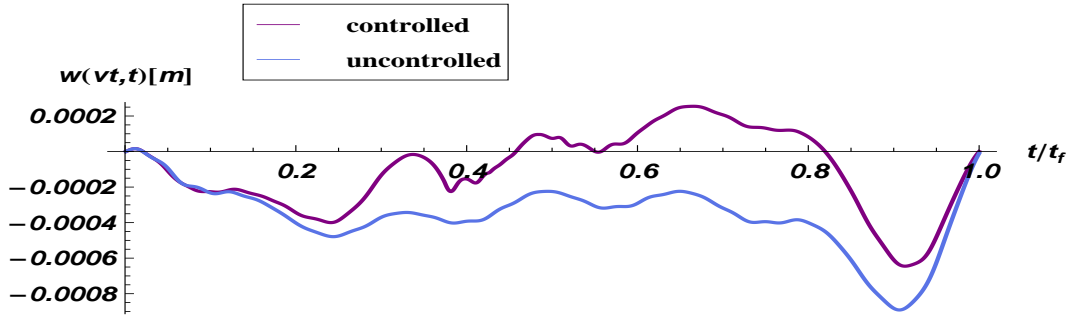


Figure 4.28: Deflection trajectories for the case  $v = 0.7c$  with five active dampers and the initial deflection.

The comparison of the cases *controlled* and *uncontrolled* is displayed in the Figure 4.28. We can easily observe the improvement by means of the semi-active control method. The values of the cost functional are listed below in the Table 4.5. We evidence that even in the case of relatively slow passage ( $v = 0.3c$ ) the initial deflection defined by the Equation 4.10 enable us to control the system efficiently. In this case we reduce the cost over three times.

Table 4.5: Cost values comparison.

velocity	uncontrolled	controlled	c/uc
$v = 0.3c$	$0.2115 \cdot 10^{-5}$	$0.0679 \cdot 10^{-5}$	0.32
$v = 0.5c$	$0.2904 \cdot 10^{-6}$	$0.0908 \cdot 10^{-6}$	0.31
$v = 0.7c$	$0.0638 \cdot 10^{-6}$	$0.0245 \cdot 10^{-6}$	0.38

#### 4.6.2 Case 2: The third mode added

In this case we improve the inial curve by adding the third mode as follows:

$$w_0(x) = 0.0007 \sin\left(\frac{1\pi x}{l}\right) + 0.0003 \sin\left(\frac{3\pi x}{l}\right). \quad (4.11)$$

The optimized trajectories and controls are depicted in the Figures 4.29, 4.30, 4.31.

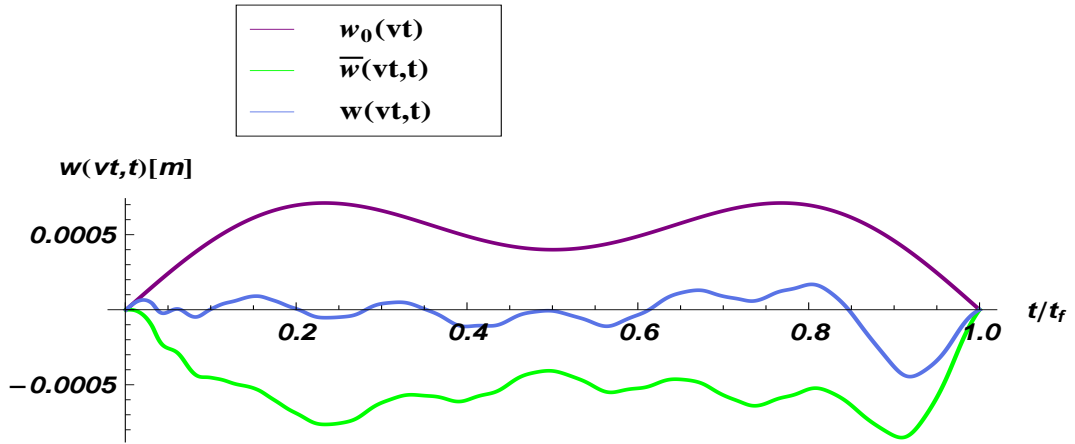


Figure 4.29: Deflection trajectories for the case  $v = 0.9c$  with five active dampers and the initial deflection.

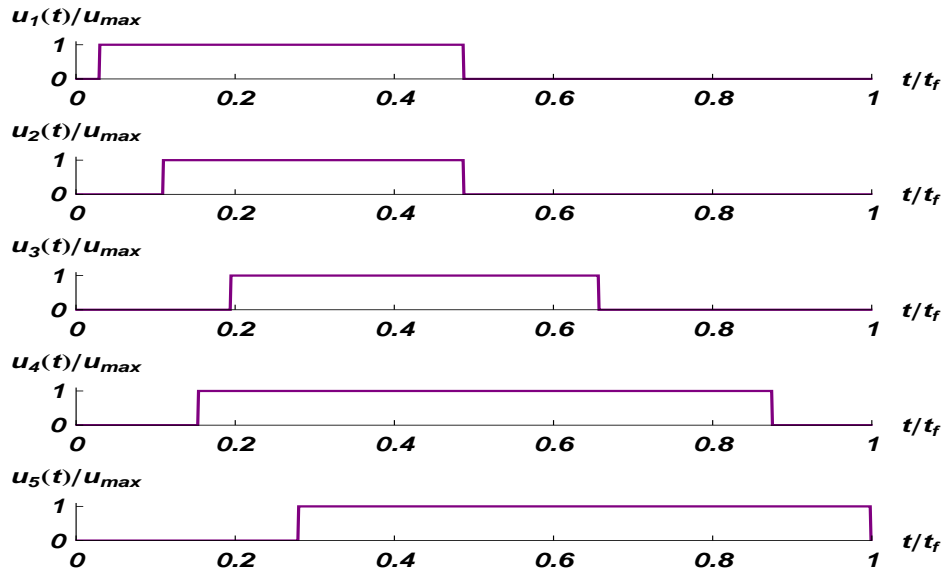


Figure 4.30: Control functions.

In the Table 4.6 the cost values for different speed of passage are summarized. We observe the best efficiency of the control method in case of  $v = 0.7c$ . That confirms the previous statement that the specific initial deflection curve should be apply to the specific travel only. The optimization of the initial deflection shape is an attractive topic for further investigations.

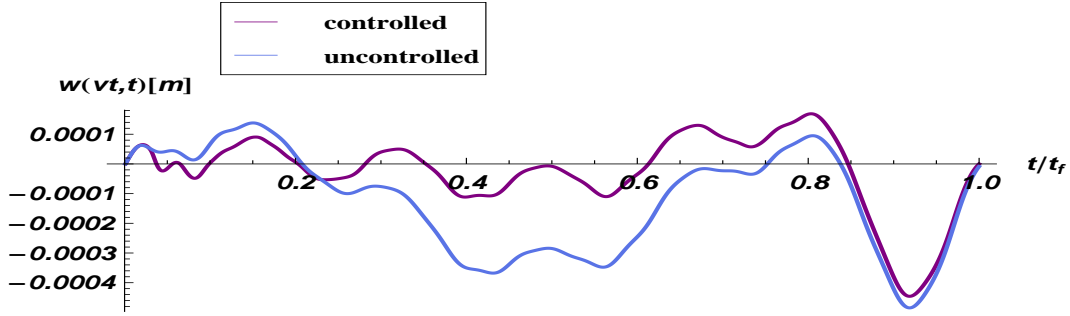


Figure 4.31: Deflection trajectories for the case  $v = 0.9c$  with five active dampers and the initial deflection.

Table 4.6: Cost values comparison.

velocity	uncontrolled	controlled	$c/uc$
$v = 0.5c$	$0.2645 \cdot 10^{-6}$	$0.0635 \cdot 10^{-6}$	0.24
$v = 0.7c$	$0.0529 \cdot 10^{-6}$	$0.0114 \cdot 10^{-6}$	0.21
$v = 0.9c$	$0.0136 \cdot 10^{-6}$	$0.0055 \cdot 10^{-6}$	0.40

## 4.7 Double beam system

This section is devoted to double beam system introduced in the Chapter 2. The lower beam is rigid and is considered to be the main span while the upper beam is added to increase the total load carrying capacity and is relatively soft (Figure 2.8). As before the magnitude of the moving force is taken as constant by neglecting the inertial forces.

For double beam system the different control strategy is proposed. We assume one switching action for every control. The dampers placed on the left-hand side are first set *on*, then after a certain time they are switched into the *off* state. The situation for the rest of the dampers is reversed. Formally, this can be written as follows:

$$\begin{aligned}
 u_i(t) &= u_{max}\mathcal{U}(t) - u_{max}\mathcal{U}(t - \tau_i), & i = 1, 2, \dots, m', \\
 u_i(t) &= u_{max}\mathcal{U}(t - \tau_i), & i = m' + 1, m' + 2, \dots, m,
 \end{aligned}
 \tag{4.12}$$

where  $\tau_i$  is the switching time of the  $i$ -th damper and  $\mathcal{U}(t)$  is a unit step function. The position of the damper with index  $m'$  can be assumed after preliminary numerical simulations. The optimal switching times are the solutions of the following problem:

$$(\tau_1, \tau_2, \dots, \tau_m) = \arg \min_{\tau_1, \tau_2, \dots, \tau_m \in (0, t_f]} J(\mathbf{y}(t)), \tag{4.13}$$

where  $\mathbf{y}(t)$  is the resulting trajectory under controls 4.12.

To obtain the trajectories  $\mathbf{y}(t)$  (used in the non-gradient optimising method), the solution of the system of ODEs 2.22 by using power expansions is proposed (the method is presented in details in Chapter 2) for  $V_1(k, t)$  and  $V_2(k, t)$  calculated in the time domain split into intervals that are bounded by every pair of switching events:

$$\begin{aligned} V_1(k, t) &= \sum_{n=0}^s d_n(1, k)(t - \hat{\tau})^n, \\ V_2(k, t) &= \sum_{n=0}^s d_n(2, k)(t - \hat{\tau})^n. \end{aligned} \quad (4.14)$$

Here,  $\hat{\tau}$  is first equal to zero, and then  $\hat{\tau} \in (0, t_f]$  are the times of successive switching events. The time marching scheme allows us to proceed to successive layers with initial conditions taken from the end of previous stages. The number  $s$  stands for the length of power series

Substitution of 4.14 into 2.22, after some simple algebraic transformations, yields the system of recurrence equations for sequences  $d_n(1, k)$  and  $d_n(2, k)$ :

$$\begin{aligned} \mu_1(2n+1)(2n+2)d_{2n+2}(1, k) &= -EI_1 \frac{k^4 \pi^4}{l^4} d_{2n}(1, k) + \\ &- \frac{2}{l} \sum_{i=1}^m \sum_{j=1}^s u_i(t) \alpha_{ijk} (2n+1) [d_{2n+1}(1, j) - d_{2n+1}(2, j)] + P \sin(k\omega\hat{\tau}) \frac{(-1)^n (k\omega)^{2n}}{(2n)!}, \\ \mu_2(2n+1)(2n+2)d_{2n+2}(2, k) &= -EI_2 \frac{k^4 \pi^4}{l^4} d_{2n}(2, k) + \\ &- \frac{2}{l} \sum_{i=1}^m \sum_{j=1}^s u_i(t) \alpha_{ijk} (2n+1) [d_{2n+1}(2, j) - d_{2n+1}(1, j)], \end{aligned} \quad (4.15)$$

$$\begin{aligned} \mu_1(2n+2)(2n+3)d_{2n+3}(1, k) &= -EI_1 \frac{k^4 \pi^4}{l^4} d_{2n+1}(1, k) + \\ &- \frac{2}{l} \sum_{i=1}^m \sum_{j=1}^s u_i(t) \alpha_{ijk} (2n+2) [d_{2n+2}(1, j) - d_{2n+2}(2, j)] + P \cos(k\omega\hat{\tau}) \frac{(-1)^n (k\omega)^{2n+1}}{(2n+1)!}, \\ \mu_2(2n+2)(2n+3)d_{2n+3}(2, k) &= -EI_2 \frac{k^4 \pi^4}{l^4} d_{2n+1}(2, k) + \\ &- \frac{2}{l} \sum_{i=1}^m \sum_{j=1}^s u_i(t) \alpha_{ijk} (2n+2) [d_{2n+2}(2, j) - d_{2n+2}(1, j)], \end{aligned} \quad (4.16)$$

where the following notation is introduced:  $\pi v/l = \omega$ ,  $\sin(j\pi a_i/l) \sin(k\pi a_i/l) = \alpha_{ijk}$ . The controls  $u_i(t)$  are constant in every time interval as stated in 4.12. The first few terms of the sequences appear directly as initial conditions  $d_0(1, j) = V_1(j, \hat{\tau})$ ,  $d_1(1, j) = \dot{V}_1(j, \hat{\tau})$ ,  $d_0(2, j) = V_2(j, \hat{\tau})$ ,  $d_1(2, j) = \dot{V}_2(j, \hat{\tau})$ .

Now, the efficiency of the designed control method is verified by means of numerical simulations. Comparisons with uncontrolled cases are presented and discussed for a wide range of velocities of the moving load. Three cases are evaluated for different numbers of active dampers.

Constants for the lower beam in the system are assumed as follows:  $l = 5$  m,  $\mu_2 = 16.8$  kg/m,  $EI_2 = 2 \cdot 10^5$  Nm<sup>2</sup> ( $E = 210 \cdot 10^9$  Pa). The upper beam, which carries the load, is treated with three different values of bending stiffness. These are given as fractions of  $EI_2$ , as follows:  $EI_1 = EI_2/20$ ,  $EI_1 = EI_2/5$ ,  $EI_1 = EI_2/2$ . The force  $P = 100$  N travels with velocity  $v = 0.1c$ ,  $v = 0.5c$ ,  $v = 0.9c$ , where  $c$  denotes the critical speed of the lower beam ( $c = (\pi/l)\sqrt{EI_2/\mu_2}$ ). In the computations, the following placements of the dampers were established:  $[0.2l, 0.4, 0.6l, 0.8l]$ ;  $[0.2l, 0.5l, 0.8l]$ ;  $[0.25l, 0.75l]$  for the cases when the number of active dampers was four, three and two, respectively.

We assume controls as follows:

$$\begin{aligned} u_i(t) &= u_{max}\mathcal{U}(t) - u_{max}\mathcal{U}(t - \tau_i), & i = 1, \\ u_i(t) &= u_{max}\mathcal{U}(t - \tau_i), & i = 2, 3, 4. \end{aligned} \quad (4.17)$$

In every case, we set the value  $u_{max} = 5 \cdot 10^4$  Ns/m.

For optimization, we use the Hooke-Jeeves Direct Search Method [R. Hooke 1961]. In the computations, we consider at least 3 different starting points with 3 reducing step size schemes for each case. 10 modes and 40 terms in the power series were taken into account in computations. Optimal switching time vectors and related cost values are summarized in Tables 4.7-4.9. By the passive case, as before we mean a constant damping  $u_i(t) = u_{max}$ ,  $\forall t \in [0, t_f]$ .

Table 4.7: Cost values and optimal switching times for different speeds of the travelling load (active suspension/passive suspension), for the cases: (\*) $EI_1 = EI_2/20$ , (\*\*) $EI_1 = EI_2/5$ , (\*\*\*) $EI_1 = EI_2/2$  with four active dampers.

velocity	cost values (active/passive)·10 <sup>-5</sup>	$(\tau_1, \tau_2, \tau_3, \tau_4)/t_f$ (*)
$v = 0.1c$	31.079/61.886	(0.574, 0.137, 0.298, 0.580)
$v = 0.5c$	5.9379/13.492	(0.622, 0.185, 0.420, 0.553)
$v = 0.9c$	1.0308/4.7160	(0.220, 0.216, 0.464, 0.706)
velocity	cost values (active/passive)·10 <sup>-5</sup>	$(\tau_1, \tau_2, \tau_3, \tau_4)/t_f$ (**)
$v = 0.1c$	47.796/51.775	(0.797, 0.087, 0.292, 0.600)
$v = 0.5c$	9.2959/11.279	(0.837, 0.168, 0.338, 0.566)
$v = 0.9c$	2.6669/3.7560	(0.860, 0.203, 0.464, 0.533)
velocity	cost values (active/passive)·10 <sup>-5</sup>	$(\tau_1, \tau_2, \tau_3, \tau_4)/t_f$ (***)
$v = 0.1c$	38.659/39.748	(0.886, 0.069, 0.226, 0.400)
$v = 0.5c$	8.5706/9.0609	(0.854, 0.140, 0.293, 0.466)
$v = 0.9c$	2.8183/3.1338	(0.724, 0.202, 0.401, 0.466)

Table 4.8: Cost values and optimal switching times for different speeds of the travelling load (active suspension/passive suspension), for the cases: (\*) $EI_1 = EI_2/20$ , (\*\*) $EI_1 = EI_2/5$ , (\*\*\*) $EI_1 = EI_2/2$  with three active dampers.

velocity	cost values (active/passive)·10 <sup>-5</sup>	( $\tau_1, \tau_2, \tau_3$ )/ $t_f$ (*)
$v = 0.1c$	43.395/70.854	(0.802, 0.137, 0.382)
$v = 0.5c$	8.1419/14.899	(0.746, 0.241, 0.474)
$v = 0.9c$	2.1244/5.8716	(0.565, 0.276, 0.618)
velocity	cost values (active/passive)·10 <sup>-5</sup>	( $\tau_1, \tau_2, \tau_3$ )/ $t_f$ (**)
$v = 0.1c$	50.831/55.766	(0.729, 0.256, 0.498)
$v = 0.5c$	10.273/11.630	(0.918, 0.226, 0.304)
$v = 0.9c$	2.9417/3.9570	(0.860, 0.203, 0.464)
velocity	cost values (active/passive)·10 <sup>-5</sup>	( $\tau_1, \tau_2, \tau_3$ )/ $t_f$ (***)
$v = 0.1c$	40.886/41.970	(0.442, 0.072, 0.270)
$v = 0.5c$	8.8617/9.2059	(0.788, 0.252, 0.452)
$v = 0.9c$	2.9621/3.2004	(0.892, 0.209, 0.416)

Table 4.9: Cost values and optimal switching times for different speeds of the travelling load (active suspension/passive suspension), for the cases: (\*) $EI_1 = EI_2/20$ , (\*\*) $EI_1 = EI_2/5$ , (\*\*\*) $EI_1 = EI_2/2$  with two active dampers.

velocity	cost values (active/passive)·10 <sup>-5</sup>	( $\tau_1, \tau_2$ )/ $t_f$ (*)
$v = 0.1c$	80.687/99.486	(0.683, 0.147)
$v = 0.5c$	12.583/20.997	(0.488, 0.383)
$v = 0.9c$	4.5709/7.3663	(0.372, 0.547)
velocity	cost values (active/passive)·10 <sup>-5</sup>	( $\tau_1, \tau_2$ )/ $t_f$ (**)
$v = 0.1c$	61.739/65.040	(0.680, 0.098)
$v = 0.5c$	10.877/12.855	(0.562, 0.317)
$v = 0.9c$	3.5002/4.7080	(0.446, 0.434)
velocity	cost values (active/passive)·10 <sup>-5</sup>	( $\tau_1, \tau_2$ )/ $t_f$ (***)
$v = 0.1c$	45.447/46.139	(0.672, 0.076)
$v = 0.5c$	9.1654/9.6521	(1.000, 0.286)
$v = 0.9c$	3.1412/3.4141	(0.518, 0.366)

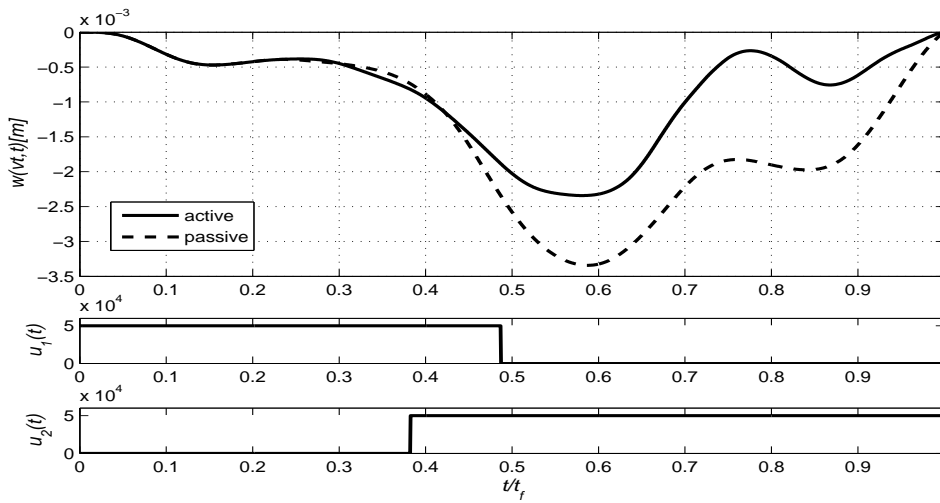


Figure 4.32: Extremal deflection trajectory and controls in the case  $EI_1/EI_2 = 1/20$ ,  $v = 0.5c$  with two active dampers.

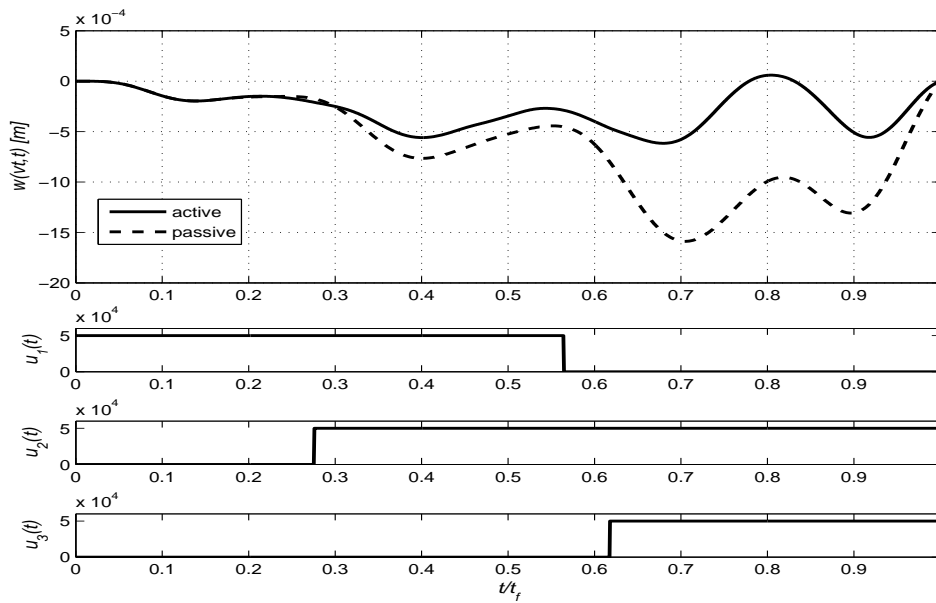


Figure 4.33: Extremal deflection trajectory and controls in the case  $EI_1/EI_2 = 1/20$ ,  $v = 0.9c$  with three active dampers.

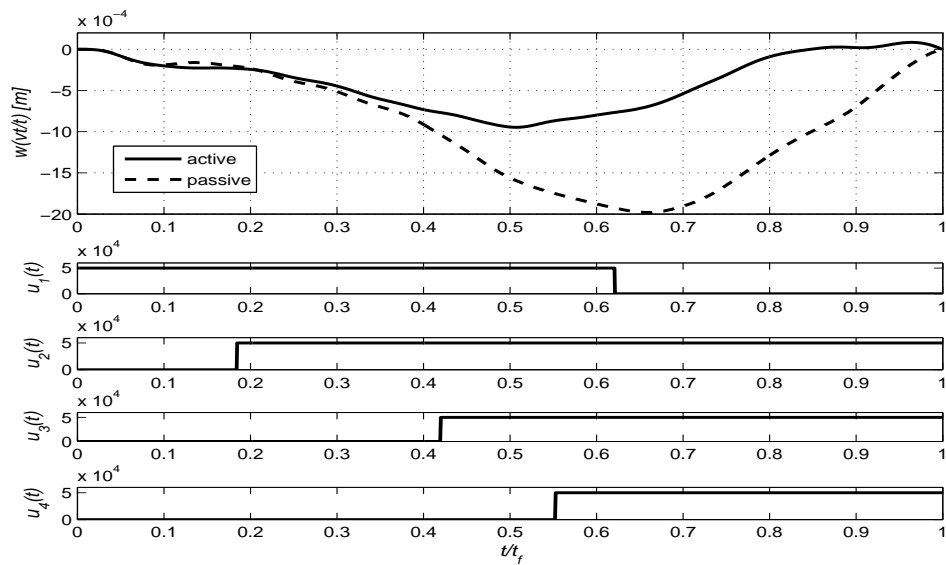


Figure 4.34: Extremal deflection trajectory and controls in the case  $EI_1/EI_2 = 1/20$ ,  $v = 0.5c$  with four active dampers.

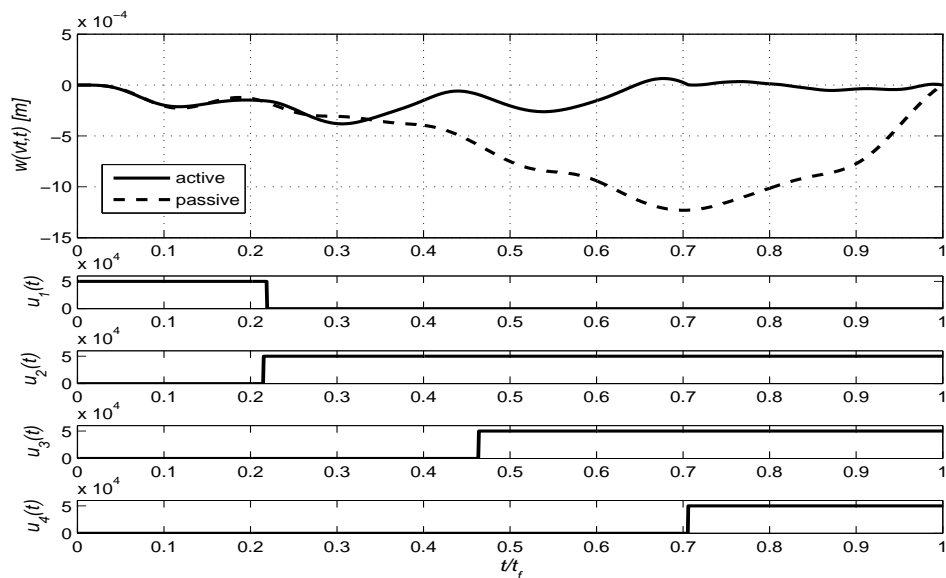


Figure 4.35: Extremal deflection trajectory and controls in the case  $EI_1/EI_2 = 1/20$ ,  $v = 0.9c$  with four active dampers.

The best efficiency of the proposed strategy, measured as the fraction of cost values, active/passive, is obtained in the cases where  $EI_1 = EI_2/20$ . In case of four active dampers, for the carriage travelling at high speed  $v = 0.5c$ ,  $v = 0.9c$  the maximum deflection was reduced by a factor of almost two (Figure 4.34) and three (Figure 4.35), respectively. The latter trajectory is almost flat for more than half of the travel time. For carriage movement at low speed, the dynamic effects are observed to be weak and the controls cannot change the process efficiently. For a lower number of active dampers, we observe an increasing deflection near the position of the absent damper (Figure 4.32). To provide a flat trajectory in the second stage of the passage, at least two active dampers have to be placed on the right-hand part of the beam to support the travelling load (Figure 4.33).

To show how the proposed system corresponds to a simple guideway, represented by a traditional single-beam span, we compare the trajectories of a carriage travelling along the controlled system and along a single beam with increased bending stiffness  $EI_2$ ,  $2 \cdot EI_2$ ,  $4 \cdot EI_2$ ,  $8 \cdot EI_2$  (Figure 4.36). In this case, we obtain a relatively flat trajectory if we increase the stiffness parameter by more than 8 times. At the same time, it requires an increased mass for the guideway and directly affects the static deflection curve.

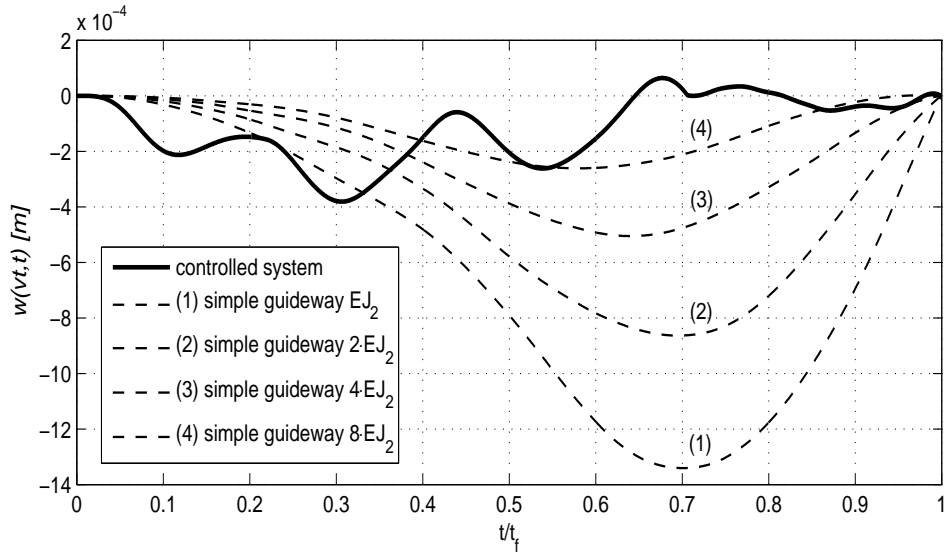


Figure 4.36: Carriage trajectories when travelling over controlled system and simple guideways,  $v = 0.9c$  with four active dampers.

---

This chapter has been devoted to the numerical optimization and analysis of trajectories of a moving load when transversing the semi-active controlled Euler-Bernoulli beam. The relevant number of switchings in control functions has been established. The numerical results have shown that the best efficiency of the proposed control method is exhibited for the cases of near critical value of velocity of a moving load. The optimization has been also performed for the two special extensions of the model: the initially deflected beam and double beam system. In the former extension the further optimization of the initial shape is required. However, the results presented in the chapter have shown that the idea is very attractive and it is worthy to special attention when designing the control systems for optimal passages. The second extension has been considered with different control method that requires only one switching action for every of the control functions. The system driven by such simple controls has exhibited very good performance.

---



## 5.1 Summary of the work

The aim of this work was to design a semi-active control method that provides the straight line passage of a moving object on an elastic body. The mathematical model was represented by multidimensional coupled bilinear system. For such a system no efficient optimal control methods have been developed so far. The original ideas had to be acquired and implemented. A brief summary of the work including the exposition of the the main results is given below.

The second chapter was devoted to the mathematical representation of one-dimensional semi-active controlled body. The approximated solutions were investigated and the relevant number of terms in the Fourier series was established. Model based on a string required at least  $N=50$  modes for good approximation. For the Euler-Bernoulli beam system the minimum number of terms in the Fourier series that one should take in to account is  $N=10$ . For the sake of control design the state space representation was introduced. The power series method for solving the bilinear PDE was proposed. The method enabled us to get an approximated solution as a function of time.

In the third chapter the problem of optimal control of bilinear systems was considered. Application of the first order necessary optimality condition enabled us to characterize the general structure of optimal solutions. The optimal controls derived by using the Maximum Pontryagin Principle were bang-bang type. Solving of difficult multidimensional TPBVP is necessary to find the optimal solutions. Thus, the problem had to be treated numerically. Two different methods based on the gradients were applied to the simple oscillator problem. The numerical results showed that the switching times methods can be very efficient if the proper number of switchings is presumed.

The fourth chapter was devoted to the numerical optimization and analysis of trajectories of a moving load when transversing the semi-active controlled Euler-Bernoulli beam.

The relevant number of switchings in control functions was established. The numerical results demonstrated that the best efficiency of the proposed control method is exhibited for the cases of near critical value of velocity of a moving load. The optimization was also performed for the two special extensions of the model: the initially deflected beam and double beam system. In the former extension the further optimization of the initial shape is required. However, the results presented in the chapter showed that the idea is very promising and it is worthy to special attention when designing the control systems for optimal passages. The second extension was considered with different control method that requires only one switching action for every of the control functions. The system driven by such simple controls also exhibited very good efficiency.

## 5.2 The idea of a smart damping layer

The idea of a smart damping layer came together with the numerical results presented in the Chapter 4 (Section 4.5). It was mentioned before that in some cases the structure of control functions is very regular. This fact may have a very interesting application. The idea is in the very initial phase, however its potential seems to be very attractive and it deserves special attention.

Let us consider a moving load travelling with nearly critical speed. The exemplary structure of the control functions in this case is presented in the Figure 5.2. The solid circles in the graph indicate the positions of the dampers. One can easily deduct that every damper is activated for a brief moment before the load is approaching it. On the other hand the deactivation of a damper occurs some time after a load is leaving it. This fact suggests that the switching actions may be performed by a smart material that possesses the required damping characteristics.

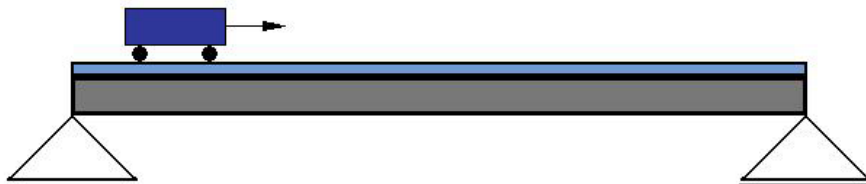


Figure 5.1: Semi-active span made of a smart damping layer.

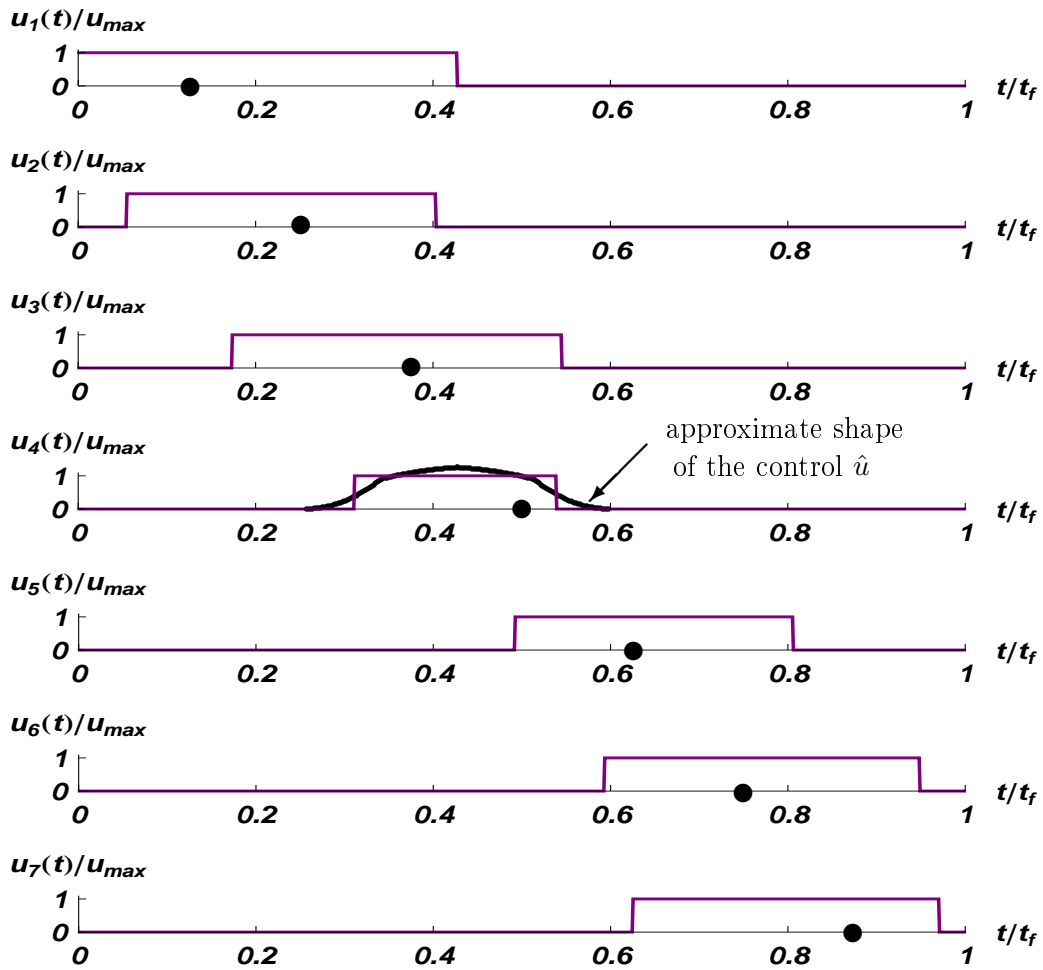


Figure 5.2: The example of control functions for the case  $v = 0.9c$ . Black marks indicate the instants in which a load meets the successive dampers.

The question is: what are these characteristics? One can imagine the damping layer (Figure 5.1) for which the distributed state is determined by the vectors:  $\mathbf{y}$ ,  $\dot{\mathbf{y}}$ . It might be expected that it is possible to find the controls  $\hat{\mathbf{u}}(\mathbf{y}, \dot{\mathbf{y}})$  that correspond to the functions  $\mathbf{u}(t)$  presented in the Figure 5.2. Perhaps we will not be able to obtain rectangular shapes but rather something like a bell shaped curves instead. The efficiency of the system driven by such non-switching controls needs to be verified first. We must recall that the structure of optimized switching controls strictly depends on the velocity of the travel. Besides the high speed passages the structures of optimized control are not so regular. Thus, it may be extremely difficult to find the feedback controls in the case of slow passages.

The approach opens a lot of new and interesting problems. Further research on the topic is highly recommended.

### 5.3 Future work

The work created a lot of important and previously unexplored problems. It provided the qualitative results that should be extended with more complex models to make the proposed ideas fully applicable. The purpose of this section is to indicate directions for further research.

A simplification of a moving vehicle to a single point load seems to be too far. In practice we require much more complex mathematical model to approach a real physical object. The inertial forces of the object should be included to the governing equation. In the case of a railway track the vibration of wheelsets should be taken into account. The interaction of a boggie with suspension model and complete body of the vehicle is relevant.

Further extensions in the span model also would be valuable. Imposing the different boundary conditions and incorporating internal damping of a beam could result in better efficiency of the proposed control method.

The objective of the control method was to provide the straight passage for a moving object. However, other objectives could also be considered. Among them we can distinguish the following: travel comfort, structural damage of the span, damage of the surrounding buildings. The computational methods demonstrated in the work enable one to obtain the suboptimal controls when another formula for the cost functional is assumed.

As mentioned in the Introduction the further optimization of initial curves should be proceeded. There are at least two ways to tackle this problem. The first one is more simple. It assumes the precise velocity of the passage. In this case the gradient method could be applied. The second way considers a wide range of a travel speed. In this case an integration of neural network controller would be convenient.

An interesting issue that rises from the work may be posed as the following: find a decentralized control method such that the desired global behaviour of the system is preserved. It might turn out that the optimal passage of a moving load can be achieved by using local interaction between some states and it is not necessary to use centralized computations. Those states (supplying the informations about displacements and velocities) could be related to beam modes or positions of semi-active dampers. By using consensus algorithms it might be possible to design a robust closed loop control system. For references on decentralized control methods and consensus algorithms please see for example [E. J. Davison 2011], [W. B. Dunbar 2006].

This appendix includes supplementary numerical results for the material presented in the Chapter 4.

## Appendix to the section: The total number of semi-active dampers

The optimized controls for the four cases presented in the Section 4.3 are depicted below in the Figures A.1, A.2, A.3, A.4, respectively.

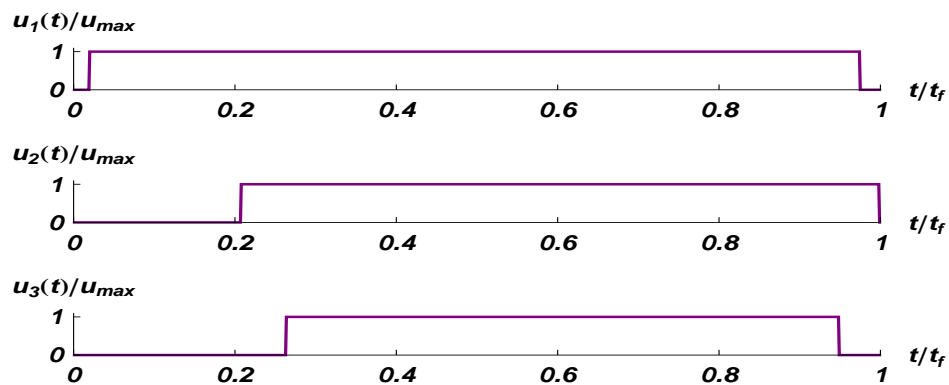


Figure A.1: Control functions in the case of 3 semi-active dampers.

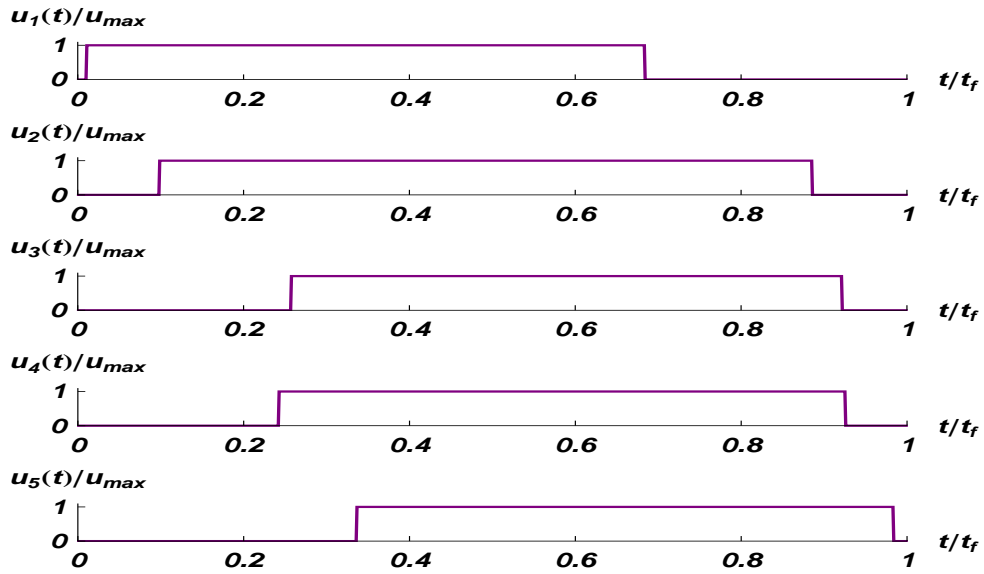


Figure A.2: Control functions in the case of 5 semi-active dampers.

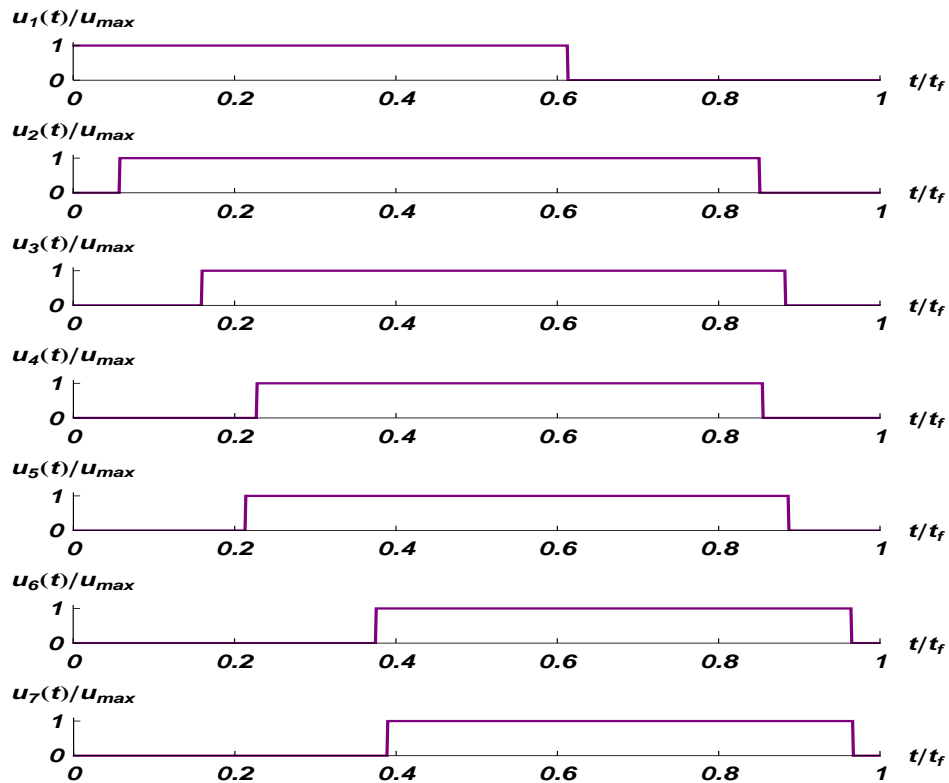


Figure A.3: Control functions in the case of 7 semi-active dampers.

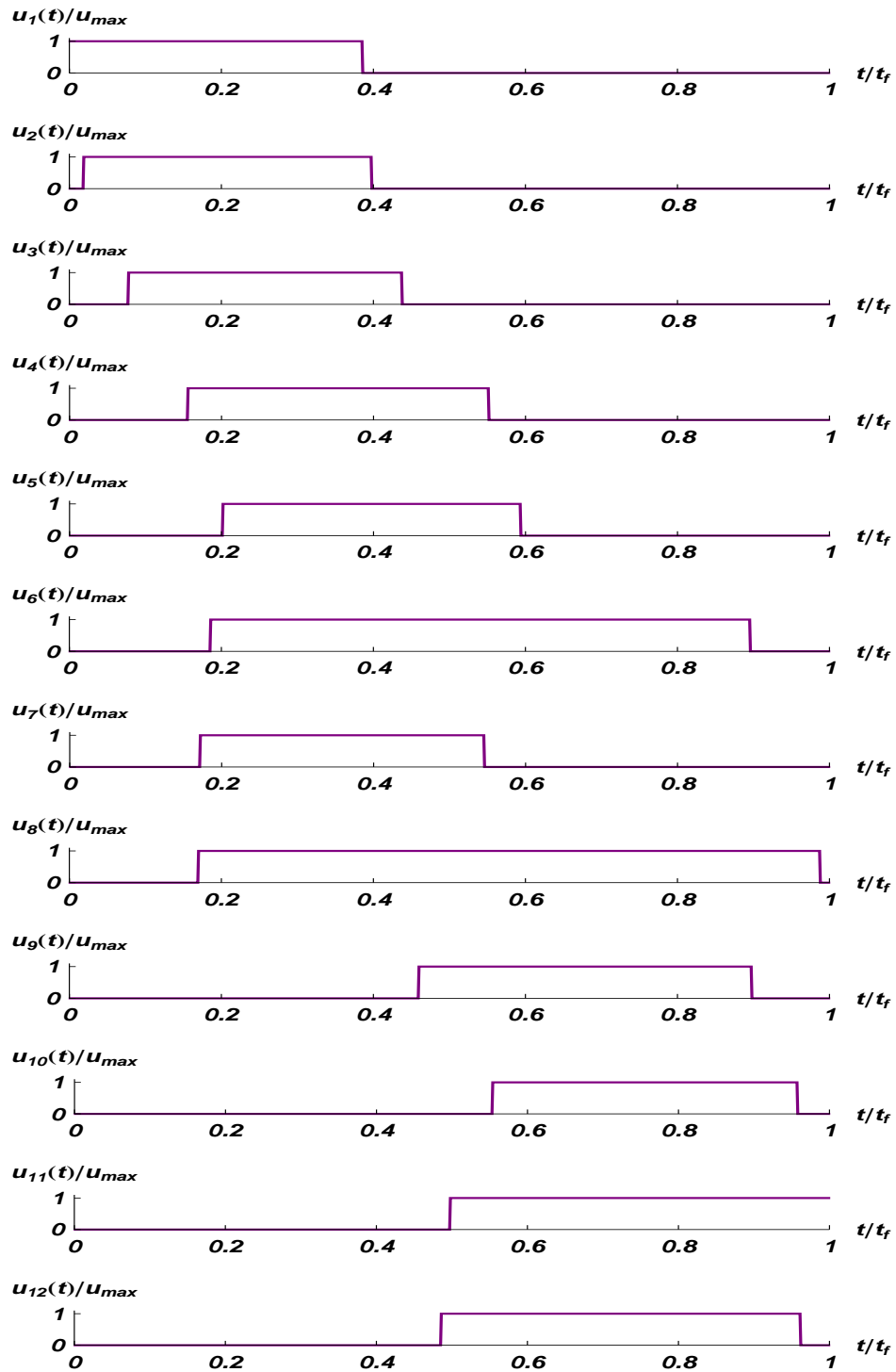


Figure A.4: Control functions in the case of 12 semi-active dampers.

## Appendix to the section: The velocity of a travelling load

We consider again the semi-active controlled Euler-Bernoulli beam system. In the computations the following placements of the seven dampers were established:  $0.125l$ ,  $0.25l$ ,  $0.375l$ ,  $0.5l$ ,  $0.625l$ ,  $0.750l$ ,  $0.875l$ . Constants for the beam are as follows:  $l = 10$  m,  $\mu = 69.8$  kg/m,  $EI = 290 \cdot 10^5$  Nm<sup>2</sup> ( $E = 210 \cdot 10^9$  Pa). The force  $P = 2 \cdot 10^4$  N travels with velocity  $v = 0.1c$ ,  $v = 0.3c$ ,  $v = 0.5c$ ,  $v = 0.7c$ ,  $v = 0.9c$ .

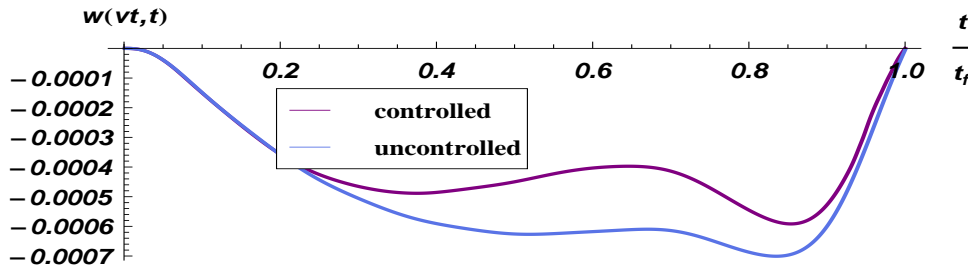


Figure A.5: Moving load trajectories in the case of  $v = 0.3c$ .

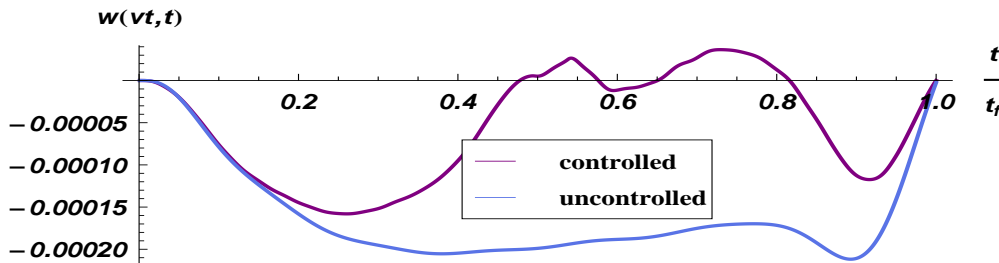
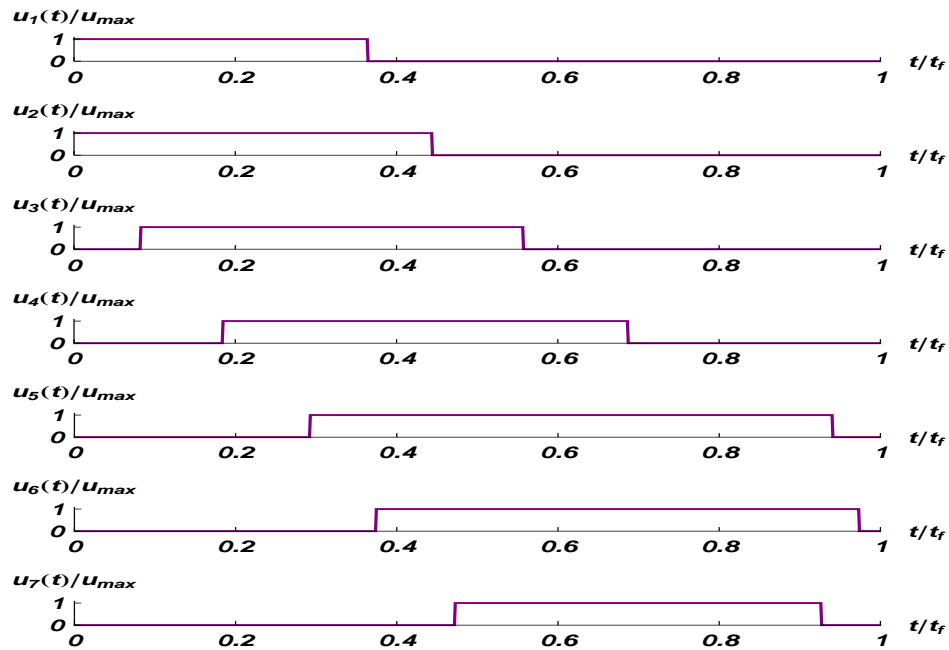
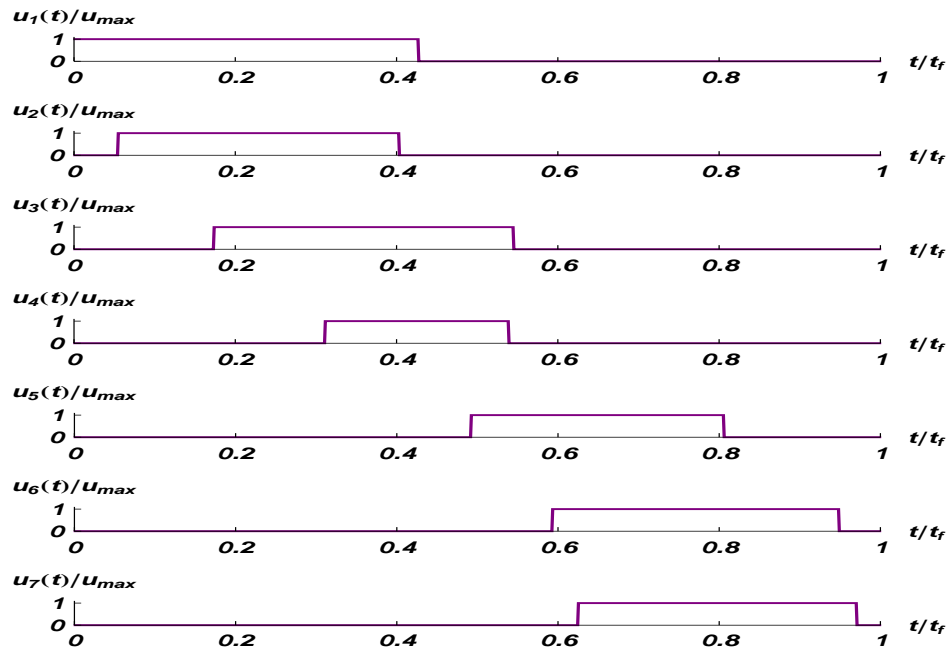


Figure A.6: Moving load trajectories in the case of  $v = 0.9c$ .

Table A.1: Cost values comparison.

VELOCITY	UNCONTROLLED	CONTROLLED	C/UC
$v = 0.1c$	$0.2590 \cdot 10^{-4}$	$0.2428 \cdot 10^{-4}$	0.93
$v = 0.3c$	$0.1119 \cdot 10^{-5}$	$0.0701 \cdot 10^{-5}$	0.62
$v = 0.5c$	$0.2420 \cdot 10^{-6}$	$0.0807 \cdot 10^{-6}$	0.33
$v = 0.7c$	$0.8574 \cdot 10^{-7}$	$0.2248 \cdot 10^{-7}$	0.26
$v = 0.9c$	$0.3944 \cdot 10^{-7}$	$0.0975 \cdot 10^{-7}$	0.24

Figure A.7: Control functions in the case of  $v = 0.3c$ .Figure A.8: Control functions in the case of  $v = 0.9c$ .





## Matlab codes

Most of numerical computations were performed by using Matlab computing language. In this appendix an exemplary code written for the switching times method is presented. The full program consist of the following codes:

**run.m**

```
clc; clear all;

wymiar_zadania=21; n=(wymiar_zadania-1)/2;
x0=zeros(wymiar_zadania,1); p0=zeros(wymiar_zadania,1);
wymiar_sterowania=5; a=zeros(wymiar_sterowania,1);

for i=1:wymiar_zadania
    x0(i)=0;
    p0(i)=0;
end

mi=88.3; l=24; EI=38346000; P=-10000; v=0.7*pi*sqrt(EI/mi)/l;

for i=1:wymiar_sterowania a(i,1)=i*l/(wymiar_sterowania+1); end
Tk=l/v; liczba_krokow=1000;
u=zeros(liczba_krokow,wymiar_sterowania); krok_u=4000;R=0;
delta_t=Tk/(liczba_krokow-1); iterator=0;
cost_int1=zeros(liczba_krokow,1);
ppomm=zeros(liczba_krokow+1,n,n,wymiar_sterowania);
ppom=zeros(liczba_krokow+1,n,wymiar_sterowania);
```

```

pom=zeros(liczba_krokow+1,wymiar_sterowania);
cost_pom=zeros(liczba_krokow,n);
tau_pom_on=zeros(wymiar_sterowania,1);
tau_pom_off=zeros(wymiar_sterowania,1);

nofiter=1;

u_max=500000;u_min=10; tau_start_on=[100,100,100,100,100];
tau_start_off=[900,900,900,900,900];
tau_on=zeros(nofiter,wymiar_sterowania);
tau_off=zeros(nofiter,wymiar_sterowania);
gradH_on=zeros(nofiter,wymiar_sterowania);
gradH_off=zeros(nofiter,wymiar_sterowania);

for i=1:wymiar_sterowania tau_on(1,i)=tau_start_on(i);
tau_off(1,i)=tau_start_off(i); end

for j=1:wymiar_sterowania for i=1:liczba_krokow
    u(i,j)=u_min;
    if i>=tau_start_on(j)
        u(i,j)=u_max;
    end if i>=tau_start_off(j)
        u(i,j)=u_min;
    end end end

stop_cond=0;

while stop_cond<3;

    iterator=iterator+1

x=rrk4prim(x0,u,Tk,liczba_krokow,wymiar_zadania);
p_pom=rrk4pprim(p0,x,u,Tk,liczba_krokow,wymiar_zadania);

for i=1:liczba_krokow for j=1:n
    cost_pom(i,j)=x(i,2*j-1)*sin(j*pi*v*x(i,2*n+1)/l);
end end

for i=1:liczba_krokow cost_int1(i)=((2/l)*sum(cost_pom(i,:)))^2; end

```

---

```
cost(iterator,1)=delta_t*sum(cost_int1);

for i=1:liczba_krokow+1
    p(i,:)=p_pom(liczba_krokow+2-i,:);
end

for i=1:n
    for j=1:n
        for k=1:liczba_krokow+1
            for m=1:wymiar_sterowania
                ppomm(k,i,j,m)=p(k,2*i)*x(k,2*j)*sin(j*pi*a(m)/l)*sin(i*pi*a(m)/l);
            end
        end
    end
end

    for i=1:n
        for k=1:liczba_krokow+1
            for j=1:wymiar_sterowania
                ppom(k,i,j)=sum(ppomm(k,i,:,j));
            end
        end
    end

        for k=1:liczba_krokow+1
            for j=1:wymiar_sterowania
                pom(k,j)=sum(ppom(k,:,j));
            end
        end

for j=1:wymiar_sterowania
gradH_on(iterator,j)=-(2/l)*(1/mi)*pom(tau_on(iterator,j),j);
gradH_off(iterator,j)=(2/l)*(1/mi)*pom(tau_off(iterator,j),j); end

for i=1:wymiar_sterowania
tau_pom_on(i,1)=krok_u*gradH_on(iterator,i);
tau_pom_off(i,1)=krok_u*gradH_off(iterator,i); end
```

```
for i=1:wymiar_sterowania if abs(tau_pom_on(i,1))<delta_t
    if gradH_on(iterator,i)<0
        tau_pom_on(i,1)=1.1*abs(delta_t/gradH_on(iterator,i))*gradH_on(iterator,i);
    else
        tau_pom_on(i,1)=0.9*abs(delta_t/gradH_on(iterator,i))*gradH_on(iterator,i);
    end
end end

for i=1:wymiar_sterowania if abs(tau_pom_off(i,1))<delta_t
    if gradH_off(iterator,i)<0
        tau_pom_off(i,1)=1.1*abs(delta_t/gradH_off(iterator,i))*gradH_off(iterator,i);
    else
        tau_pom_off(i,1)=0.9*abs(delta_t/gradH_off(iterator,i))*gradH_off(iterator,i);
    end
end end

for i=1:wymiar_sterowania
tau_t_on(i)=delta_t*tau_on(iterator,i)-tau_pom_on(i,1);
tau_t_off(i)=delta_t*tau_off(iterator,i)- tau_pom_off(i,1); end

for j=1:wymiar_sterowania if tau_t_on(j)>0 for i=1:liczba_krokow if
tau_t_on(j)>=delta_t*i
    tau_on(iterator+1,j)=i;
end end else
    tau_on(iterator+1,j)=1;
end end

for j=1:wymiar_sterowania for i=1:liczba_krokow if
tau_t_off(j)>=delta_t*i
    tau_off(iterator+1,j)=i;
end end end

for j=1:wymiar_sterowania for i=1:liczba_krokow
    u(i,j)=u_min;
if i>=tau_on(iterator+1,j)
    u(i,j)=u_max;
end if i>=tau_off(iterator+1,j)
    u(i,j)=u_min;
end end end
```

```
if iterator>2 for j=1:wymiar_sterowania
    diff_var_on(j)=tau_on(iterator+1,j)-tau_on(iterator-1,j);
    diff_var_off(j)=tau_off(iterator+1,j)-tau_off(iterator-1,j);
end

licznik_stop=0;

for j=1:wymiar_sterowania if abs(diff_var_on(j))<1
    licznik_stop=licznik_stop+1;
end if abs(diff_var_off(j))<1
    licznik_stop=licznik_stop+1;
end end

licznik_stop

if licznik_stop>=2*wymiar_sterowania
    stop_cond=stop_cond+1;
end

end

end
```

### **fdiff.m**

```
function [dx]=fdiff(x,u,t)

mi=88.3; l=24; EI=38346000; P=-10000; v=0.7*pi*sqrt(EI/mi)/l;

[liczba_krokow,wymiar_zadania]=size(x);
[liczba_krokow2,wymiar_sterowania]=size(u); n=(wymiar_zadania-1)/2;
dx = zeros(wymiar_zadania,1);
xppom=zeros(n,n,wymiar_zadania);xpom=zeros(n,wymiar_sterowania);

for i=1:wymiar_sterowania a(i,1)=i*l/(wymiar_sterowania+1); end

mnoznik_u=1;
```

```

for i=1:n for j=1:n for k=1:wymiar_sterowania
    xppom(i,j,k)=x(2*i)*sin(i*pi*a(k)/l)*sin(j*pi*a(k)/l);
end end end

for j=1:n for k=1:wymiar_sterowania
    xpom(j,k)=u(k)*sum(xppom(:,j,k));
end end

for k=1:n
    dx(2*k-1)=x(2*k);
    dx(2*k)= (1/mi)*((-2/l)*(mnozник_u*(sum(xpom(k,:))))-...
    EI*(k^4*pi^4/l^4)*x(2*k-1)+P*sin(k*pi*v*x(2*n+1)/l) );
end dx(2*n+1)=1;

end

```

### fdiffp.m

```

function[dp]=fdiffp(p,x,u,t)

mi=88.3; l=24; EI=38346000; P=-10000; v=0.7*pi*sqrt(EI/mi)/l;

[liczba_krokw2,wymiar_sterowania]=size(u);
[liczba_krokw,wymiar_zadania]=size(x); n=(wymiar_zadania-1)/2; dp =
zeros(wymiar_zadania,1); ppom1=zeros(n,1);
ppom2=zeros(n,1); pom_p=zeros(n,wymiar_sterowania);

for i=1:wymiar_sterowania a(i,1)=i*l/(wymiar_sterowania+1); end

mnozник_u=1;

for k=1:n for i=1:wymiar_sterowania
    pom_p(k,i)=mnozник_u*u(i)*(sin(k*pi*a(i)/l))^2;
end end

dppom=0;dppom2=0; for k=1:n
    dppom=dppom+x(2*k-1)*sin(k*pi*v*x(2*n+1)/l);
    dppom2=dppom2+x(2*k-1)*cos(k*pi*v*x(2*n+1)/l)*(k*pi*v/l);
end

```

```

end

for k=1:n
    dp(2*k-1)= (1/mi)*p(2*k)*EI*(k^4*pi^4/l^4)+2*(sin(k*pi*v*x(2*n+1)/l))*dppom;
    dp(2*k)= -p(2*k-1)+ (1/mi)*p(2*k)*(2/l)*(sum(pom_p(k,:)));
end

for i=1:n ppom1(i)=p(2*i)*(i*pi*v/l)*cos(i*pi*v*x(2*n+1)/l); end

pom1=sum(ppom1(:));

dp(2*n+1)= -(1/mi)*P*pom1 + 2*dppom*dppom2;

end

```

### rrk4pprim.m

```

function [p]=rrk4pprim(p0,x,u,Tk,liczba_krokow,wymiar_zadania)

dt=-Tk/liczba_krokow; p=zeros(liczba_krokow+1,wymiar_zadania);
k1=zeros(1,wymiar_zadania);k2=zeros(1,wymiar_zadania);
k3=zeros(1,wymiar_zadania);k4=zeros(1,wymiar_zadania);

for j=1:wymiar_zadania p(1,j)=p0(j); end

for i=1:liczba_krokow

k1(:)=dt*fdiffp(p(i,:),x(liczba_krokow+1-i,:),...
u(liczba_krokow+1-i,:));
k2(:)=dt*fdiffp(p(i,.)+k1(1,.) /2,x(liczba_krokow+1-i,:),...
u(liczba_krokow+1-i,),(i+0.5)*dt);
k3(:)=dt*fdiffp(p(i,.)+k2(1,.) /2,x(liczba_krokow+1-i,:),...
u(liczba_krokow+1-i,),(i+0.5)*dt);
k4(:)=dt*fdiffp(p(i,.)+k3(1,.) ,x(liczba_krokow+1-i,:),...
u(liczba_krokow+1-i,),(i+1)*dt);

for j=1:wymiar_zadania
p(i+1,j)=p(i,j)+(k1(j)+2*k2(j)+2*k3(j)+k4(j))/6; end end

```

end

### rrk4prim.m

```
function[x]=rrk4prim(x0,u,Tk,liczba_krokow,wymiar_zadania)

dt=Tk/liczba_krokow; x=zeros(liczba_krokow+1,wymiar_zadania);
k1=zeros(1,wymiar_zadania);k2=zeros(1,wymiar_zadania);
k3=zeros(1,wymiar_zadania);k4=zeros(1,wymiar_zadania);

for j=1:wymiar_zadania x(1,j)=x0(j); end

for i=1:liczba_krokow

k1(:)=dt*fdiff(x(i,:),u(i,:),i*dt);
k2(:)=dt*fdiff(x(i,)+k1(1,)/2,u(i,),(i+0.5)*dt);
k3(:)=dt*fdiff(x(i,)+k2(1,)/2,u(i,),(i+0.5)*dt);
k4(:)=dt*fdiff(x(i,)+k3(1,),u(i,),(i+1)*dt);

for j=1:wymiar_zadania
x(i+1,j)=x(i,j)+(k1(j)+2*k2(j)+2*k3(j)+k4(j))/6; end

end

end
```

## Bibliography

- [A. E. Bryson 1962] Jr. Yu-Chi Ho A. E. Bryson. *Applied optimal control*. Hemisphere, Washington, 1962. (Cited on page 35.)
- [A. Myslinski 2011] A. Chudzikiewicz A. Myslinski. *Thermoelastic Wheel-Rail Contact Problem With Elastic Graded Materials*. Proceedings of the 8th International Conference on Contact Mechanics and Wear of Rail / Wheel Systems, Florence, 2009, vol. 271, pages 417–425, 2011. (Cited on page 6.)
- [A. Ruangrassamee 2003] K. Kawashima A. Ruangrassamee. *Control of Nonlinear Bridge Response With Pounding Effect by Variable Dampers*. Engineering Structures, vol. 25, pages 593–606, 2003. (Cited on page 6.)
- [Abu-Hilal 2006] M. Abu-Hilal. *Dynamic Response of a Double Euler-Bernoulli Beam due to a Moving Constant Load*. Journal of Sound and Vibration, vol. 297, pages 477–491, 2006. (Cited on page 9.)
- [B. Dyniewicz 2009] C. I. Bajer B. Dyniewicz. *Paradox of the Particle's Trajectory Moving on a String*. Archive of Applied Mechanics, vol. 79, no. 3, pages 213–223, 2009. (Cited on page 5.)
- [B. Kang 2005] J. K. Mills B. Kang. *Vibration Control of a Planar Parallel Manipulator Using Piezoelectric Actuators*. Journal of Intelligent and Robotic Systems, vol. 42, pages 51–70, 2005. (Cited on page 7.)
- [Balas 1978] M. J. Balas. *Modal Control of Certain Flexible Dynamic Systems*. Siam Journal of Control and Optimization, vol. 16, no. 3, pages 450–462, 1978. (Cited on page 19.)

- [Baz 1997] A. Baz. *Dynamic Boundary Control of Beams Using Active Constrained Layer Damping*. Mechanical Systems and Signal Processing, vol. 11, pages 811–825, 1997. (Cited on page 6.)
- [Bellman 1957] R. Bellman. Dynamic programming. Princeton Univ. Pr., New Jersey, 1957. (Cited on page 35.)
- [Bergman 1997] A. V. Pesterev L. A. Bergman. *Response of Elastic Continuum Carrying Moving Linear Oscillator*. ASCE Journal of Engineering Mechanics, vol. 123, pages 878–884, 1997. (Cited on page 5.)
- [Bernoulli 1696] J. Bernoulli. *Acta Eruditorum*. 1696. (Cited on page 5.)
- [Bolotin 1950] W. W. Bolotin. *On the Influence of Moving Load on Bridges*. ASCE Journal of Engineering Mechanics (in Russian), vol. 74, pages 269–296, 1950. (Cited on page 5.)
- [C. A. Tan 2000] S. Ying C. A. Tan. *Active Wave Control of the Axially Moving String*. Journal of Sound and Vibration, vol. 236, pages 861–880, 2000. (Cited on page 7.)
- [C.I. Bajer 2008] B. Dyniewicz C.I. Bajer. *Space-Time Approach to Numerical Analysis of a String With a Moving Mass*. International Journal of Numerical Methods in Engineering, vol. 76, no. 10, pages 1528–1543, 2008. (Cited on page 5.)
- [C.I. Bajer 2009a] B. Dyniewicz C.I. Bajer. *Numerical Modelling of Structure Vibrations Under Inertial Moving Load*. Archives of Applied Mechanics, vol. 79, pages 499–508, 2009. (Cited on page 5.)
- [C.I. Bajer 2009b] B. Dyniewicz C.I. Bajer. *Virtual Functions of the Space-Time Finite Element Method in Moving Mass Problems*. Computers and Structures, vol. 87, pages 444–455, 2009. (Cited on page 5.)
- [Coddington 1955] E. A. Coddington. Theory of ordinary differential equations. McGraw-Hill, New York, 1955. (Cited on page 36.)
- [D. Bojczuk 2005] Z. Mroz D. Bojczuk. *Determination of Optimal Actuator Forces and Positions in Smart Structures Using Adjoint Method*. Structural and Multidisciplinary Optimization, vol. 30, pages 308–319, 2005. (Cited on page 7.)
- [D. Giraldo 2002] Sh. J. Dyke D. Giraldo. *Control of an Elastic Continuum When Traversed by a Moving Oscillator*. Journal of Structural Control and Health Monitoring, vol. 14, pages 197–217, 2002. (Cited on page 6.)

- [D. Karnopp 1974] R. Harwood D. Karnopp M. Crosby. *Vibration Control Using Semi-Active Force Generators*. ASME Journal of Engineering for Industry, vol. 96, pages 619–626, 1974. (Cited on page 6.)
- [D. Kincaid 2002] W. Cheney D. Kincaid. *Numerical analysis: Mathematics of scientific computing*. American Mathematical Society, Providence, 2002. (Cited on page 20.)
- [D. Liberzon 1999] A. S. Morse D. Liberzon J. P. Hespanha. *Stability of Switched Systems: a Lie-Algebraic Condition*. Systems and Control Letters., vol. 37, pages 117–122, 1999. (Cited on page 8.)
- [D. Liberzon 2006] A. S. Morse D. Liberzon J. P. Hespanha. *Lie-Algebraic Stability Conditions for Nonlinear Switched Systems and Differential Inclusions*. Systems and Control Letters, vol. 55, pages 8–16, 2006. (Cited on page 8.)
- [D. Pisarski 2009a] C. Bajer D. Pisarski. *Active Suspension Control of 1D Continuum Under Travelling Load*. Theoretical Foundations of Civil Engineering, vol. 17, pages 273–278, 2009. (Cited on page 9.)
- [D. Pisarski 2009b] C. Bajer D. Pisarski. *Aktywne Tlumienie Drgan Jednowymiarowego Osrodka Ciaglego pod Obciazeniem Ruchomym*. Drogi i Mosty, vol. 8, no. 4, pages 71–87, 2009. (Cited on page 9.)
- [D. Pisarski 2010a] C. Bajer D. Pisarski. *On the Semi-Active Control of Carrying Structures Under a Travelling Load*. Vibrations in Physical Systems, vol. 24, pages 325–330, 2010. (Cited on page 9.)
- [D. Pisarski 2010b] C. Bajer D. Pisarski. *Semi-active Control of 1D Continuum Vibrations Under a Travelling Load*. Journal of Sound and Vibration, vol. 329, no. 2, pages 140–149, 2010. (Cited on pages 8 and 9.)
- [D. Pisarski 2011a] C. Bajer D. Pisarski. *Moving Load Passage Optimization via Semi-Active Control System*. 19th International Conference on Computer Methods in Mechanics, pages 411–412, 2011. (Cited on page 9.)
- [D. Pisarski 2011b] C. Bajer D. Pisarski. *Smart Suspension System for Linear Guideways*. Journal of Intelligent and Robotic Systems, vol. 62, no. 3-4, pages 451–466, 2011. (Cited on page 8.)
- [Dirac 1958] P. Dirac. *Principles of quantum mechanics*. Oxford at the Clarendon Press, 1958. (Cited on page 15.)
- [E. J. Davison 2011] A. G. Aghdam E. J. Davison. *Decentralized control of large-scale systems*. Springer-Verlag, New York, 2011. (Cited on page 90.)

- [Elliott 2009] D. L. Elliott. Bilinear control systems: Matrices in action. Springer-Heidelberg, New York, 2009. (Cited on page 37.)
- [Evans 1998] L. C. Evans. Partial differential equations. American Mathematical Society, 1998. (Cited on page 16.)
- [Evans 2000] L.C. Evans. An introduction to mathematical optimal control theory. University of California, Berkeley, 2000. (Cited on page 40.)
- [Fryba 1972] L. Fryba. Vibration of solids and structures under moving loads. American Society Of Civil Engineers, 1972. (Cited on pages 5, 15 and 17.)
- [Fryba 1993] L. Fryba. Dynamics of railway bridges. Ellis Horwood, 1993. (Cited on page 15.)
- [H. V. Vu 2000] B. H. Karnopp H. V. Vu A. M. Ordonez. *Vibration of a Double-Beam System*. Journal of Sound and Vibration, vol. 229, no. 4, pages 807–822, 2000. (Cited on page 17.)
- [H. W. Park 1999] Y. P. Park S. H. Kim H. W. Park H. S. Yang. *Position and Vibration Control of a Flexible Robot Manipulator Using Hybrid Controller*. Robotics and Autonomous Systems, vol. 28, pages 31–41, 1999. (Cited on page 7.)
- [Hilal 2006] M. Abu Hilal. *Dynamic Response of a Double Euler-Bernoulli Beam Due to a Moving Constant Load*. Journal of Sound and Vibration, vol. 297, pages 477–491, 2006. (Cited on page 17.)
- [Hofer 1988] E. P. Hofer and B. Tibken. *An Iterative Method for the Finite Time Bilinear Quadratic Control Problem*. Journal of Optimization Theory and Applications, vol. 57, no. 3, pages 411–427, 1988. (Cited on page 38.)
- [J. L. Junkis 1993] Y. Kim J. L. Junkis. Introduction to dynamics and control of flexible structures. AIAA, Washington, 1993. (Cited on page 19.)
- [J. Macki 1982] A. Strauss J. Macki. Introduction to optimal control theory. Springer-Verlag, New York, 1982. (Cited on pages 39 and 40.)
- [K. Yoshida 2000] T. Fujio K. Yoshida. *Semi-Active Base Isolation for a Building Structure*. International Journal of Computer Applications in Technology, vol. 13, pages 52–58, 2000. (Cited on pages 6 and 7.)
- [Kaya 1996] C.Y. Kaya and J.L. Noakes. *Computations and Time-Optimal Controls*. Optimal Control Applications and Methods, vol. 17, pages 171–185, 1996. (Cited on page 51.)

- [Komkov 1972] V. Komkov. Optimal control theory for the damping vibrations of a simple elastic systems. Springer-Verlag, New York, 1972. (Cited on page 5.)
- [L. S. Pontryagin 1962] R. V. Gamkrelidze L. S. Pontryagin V. G. Boltyanskii. The mathematical theory of optimal processes. Wiley, New York, 1962. (Cited on page 35.)
- [Lee 1978] K. Y. Lee. Optimal bilinear control theory applied to pest management in recent developments in variable structure systems, economics and biology. Springer-Verlag, Berlin, 1978. (Cited on pages 37 and 39.)
- [M. Athans 2007] P. Falb M. Athans. Optimal control: An introduction to the theory and its applications. Dover Publications, Inc., New York, 2007. (Cited on page 40.)
- [Mohler 1970] R. R. Mohler. Controllability and optimal control of bilinear systems. Prentice-Hall, New York, 1970. (Cited on page 37.)
- [Mohler 1973] R. R. Mohler. Bilinear control processes. Academic Press, New York, 1973. (Cited on pages 7, 37 and 51.)
- [Mohler 1991] R. R. Mohler. Nonlinear systems: volume ii, applications to bilinear control. Prentice-Hall, New York, 1991. (Cited on page 37.)
- [Myslinski 2008] A. Myslinski. *Level Set Method for Optimization of Contact Problems*. Engineering Analysis With Boundary Elements, vol. 32, pages 986–994, 2008. (Cited on page 6.)
- [Olsson 1991] M. Olsson. *On the Fundamental Moving Load Problem*. Journal of Sound and Vibration, vol. 154, no. 2, pages 299–307, 1991. (Cited on page 5.)
- [Ossowski 2003] A. Ossowski. *Semi-active Control of Free Beam Vibration*. Theoretical Foundations of Civil Engineering, vol. 11, pages 557–566, 2003. (Cited on page 7.)
- [P. Flont 1997] J. Holnicki-Szulc P. Flont. *Adaptive Railway Truck with Improved Dynamic Response*. 2nd World Congress of Structural and Multidisciplinary Optimization, Zakopane 97, vol. 4, 1997. (Cited on page 6.)
- [Pietrzakowski 2001] M. Pietrzakowski. *Active Damping of Beams by Piezoelectric System Effects of Bonding Layer Properties*. International Journal of Solids and Structures, vol. 38, pages 7885–7897, 2001. (Cited on page 6.)
- [R. Bogacz 2000] C. Bajer R. Bogacz. *Active Control of Beams Under Moving Load*. Journal of Theoretical and Applied Mechanics, vol. 38, no. 3, pages 523–530, 2000. (Cited on page 8.)

- [R. F. Curtain 1995] H. J. Zwart R. F. Curtain. An introduction to infinite-dimensional linear systems theory. Springer-Verlag, New York, 1995. (Cited on page 19.)
- [R. Hooke 1961] T. A. Jeeves R. Hooke. *Direct Search Solution of Numerical and Statistical Problems*. Journal of the ACM, vol. 8, pages 212–229, 1961. (Cited on page 80.)
- [Rahn 2001] Ch. D. Rahn. Mechatronic control of distributed noise and vibration. Springer-Verlag, Berlin, Heidelberg, New York, 2001. (Cited on pages 5 and 19.)
- [Rudin 1987] W. Rudin. Real and complex analysis. McGraw-Hill, New York, 1987. (Cited on page 36.)
- [S. Choura 2001] A. S. Yigit S. Choura. *Control of a Two-Link Rigid Flexible Manipulator With a Moving Payload Mass*. Journal of Sound and Vibration, vol. 243, pages 883–890, 2001. (Cited on page 7.)
- [Snyman 2005] J. A. Snyman. Practical mathematical optimization: An introduction to basic optimization theory and classical and new gradient-based algorithms. Springer, Cambridge, 2005. (Cited on page 43.)
- [Soong 2005] T. Soong. Active hybrid and semi-active structural control. John Wiley and Sons, 2005. (Cited on page 7.)
- [Stokes 1883] G. G. Stokes. *Discussion of a Differential Equation Relating to the Breaking Railway Bridges*. Mathematical and Physical Papers (Reprint), vol. 2, pages 179–220, 1883. (Cited on page 5.)
- [Symon 1971] K. R. Symon. Mechanics. Addison-Wesley, Reading, MA, 1971. (Cited on page 14.)
- [T. Das 2006] R. Mukherjee T. Das. *Optimally Switched Linear Systems*. Automatica, vol. 44, pages 1437–1441, 2006. (Cited on page 8.)
- [T. Frischgesel 1998] H. Reckmann O. Schütte T. Frischgesel K. Popp. *Regelung Eines Elastischen Fahrwegs Inter Verwendung Eines Variablen Beobachters*. Technische Mechanik, vol. 18, pages 44–55, 1998. (Cited on page 6.)
- [Timoshenko 1954] S. P. Timoshenko. History of strength materials. McGraw-Hill, New York, 1954. (Cited on pages 5 and 14.)
- [V. Rajamohan 2010] R. Sedaghati V. Rajamohan S. Rakheja. *Semi-Active Vibration Control of Magnetorheological Fluid Sandwich Beam*. CSME Forum 2010, Victoria, British Columbia, Canada, 2010. (Cited on page 69.)

- [Vinter 2000] R. Vinter. *Optimal control*. Birkhauser, Boston, 2000. (Cited on page 35.)
- [W. B. Dunbar 2006] R. M. Murray W. B. Dunbar. *Distributed Receding Horizon Control for Multi-Vehicle Formation Stabilization*. *Automatica*, vol. 42, pages 549–558, 2006. (Cited on page 90.)
- [W. H. Press 1992] W. T. Vetterling B. P. Flannery W. H. Press S. A. Teukolsky. *Numerical recipes in c: The art of scientific computing*. Cambridge University Press, Cambridge, 1992. (Cited on page 41.)
- [Y. B. Yang 2004] Y. S. Wu Y. B. Yang J. D. Yau. *Vehicle-bridge interaction dynamics*. World Scientific, New Jersey, 2004. (Cited on page 5.)
- [Y. Chen 2002] L. A. Bergman T. C. Tsao Y. Chen C. A. Tan. *Smart Suspension Systems for Bridge-Friendly Vehicles*. *SPIE Proceedings Series*, vol. 4696, pages 52–61, 2002. (Cited on page 6.)
- [Z. Fulin 2002] Y. Weiming W. Lushun Z. Fulin T. Ping. *Theoretical and Experimental Research on a New System of Semi-Active Structural Control With Variable Stiffness and Damping*. *Earthquake Engineering and Engineering Vibration*, vol. 1, pages 130–135, 2002. (Cited on page 6.)